NECESSITY AND SUFFICIENCY OF MITOGEN-ACTIVATED PROTEIN KINASE KINASE SIGNALING PATHWAYS FOR MELANOMA CELL PROLIFERATION

By

CHIH-SHIA LEE

A DISSERTATION

Submitted to
Michigan State University
in partial fulfillment of the requirements
for the degree of

DOCTOR OF PHILSOPHY

Biochemistry and Molecular Biology

2010

ABSTRACT

NECESSITY AND SUFFICIENCY OF MITOGEN-ACTIVATED PROTEIN KINASE KINASE SIGNALING PATHWAYS FOR MELANOMA CELL PROLIFERATION

By

CHIH-SHIA LEE

The mitogen activated protein kinase kinases (MKK or MEK) signaling pathways are critical for melanoma survival. Although MEK1 and MEK2 generally are considered functionally redundant, a few studies have indicated that they may have distinct biological functions. However, in assessing the relative contribution of MEK1 and MEK2 towards extracellular signal-regulated kinase (ERK)-mediated biologic response, investigators have relied on tests of necessity, not sufficiency. Dissecting both necessity and sufficiency of MEK signaling pathways is important to understand the interplay of the signaling network. To do so, I used two complementary approaches to determine the necessity and sufficiency of MEK1 and MEK2 signaling pathways for melanoma cell proliferation. To determine the necessity, I used isoform-specific siRNA to knock down either MEK1 or MEK2 in human melanoma SK-MEL-28 cells. An effect on proliferation was observed only when both MEK1 and MEK2 were knocked down, indicating that neither of the individual isoforms is necessary for SK-MEL-28 cell proliferation. To determine the sufficiency, I have developed a novel experimental system that allows only one MEK/MKK signaling pathway to be present in cells. In this system, anthrax lethal toxin (LeTx), a pan-MEK/MKK protease, is used to inhibit multiple endogenous MEK/MKKs in cells, and either MEK1 or MEK2 signaling pathway is simultaneously rescued by the cleavage-resistant form of MEK (MEKcr). Surprisingly,

ERK activity persisted in LeTx-treated cells expressing MEK2cr but not MEK1cr. Microarray analysis revealed groups of non-overlapping downstream transcriptional targets of MEK1 and MEK2, and indicated a substantial rescue effect of MEK2cr on proliferation pathways. Furthermore, LeTx efficiently inhibited the cell proliferation and anchorage-independent growth of SK-MEL-28 cells expressing MEK1cr but not MEK2cr. These results indicate MEK2 signaling is sufficient for ERK activation, melanoma cell proliferation, and anchorage-independent growth, and demonstrate that in SK-MEL-28 cells MEK1 and MEK2 signaling pathways are not redundant and interchangeable for cell proliferation. I conclude that in the absence of other MKK, MEK2 is sufficient for SK-MEL-28 cell proliferation. MEK1 can conditionally compensate for MEK2 only in the presence of other MKK.

Acknowledgments

Nothing is sufficient to express how grateful I am for the experience of being a graduate student and to be trained in the Duesbery Lab. I am everlastingly indebted to Dr. Duesbery for his guidance and inexhaustible patience over the past several years. The debt of gratitude that I owe Dr. Duesbery is so deep that I can only repay it by keeping Dr. Duesbery's words in mind. In an E-mail Dr. Duesbery wrote to me: "*Yoshio Masui, my PhD supervisor, told me that my training was conditional on my agreement to do the same with my students. In turn, this obligation will pass to you.*"

I would to thank Drs. Justin McCormick, Lee Kroos, Gregg Howe, and Kathy Gallo for agreeing to serve as my Guidance Committee members, and for their invaluable advice throughout my graduate school career. Many thanks are also necessary to Drs. Art Alberts, Jeff MacKeigan, Cindy Miranti, and Kyle Furge (Investigators at the Van Andel Research Institute) for their helpful advice and suggestions. I would like to thank Ms. Elissa Boguslawski for her professional assistance with xenograft experiments, as well as Mr. Karl Dykema for his help with microarray data analysis. I would also like to thank the current and former members in the Duesbery Lab for their help, especially to Dr. Jenn Bromberg-White for her invaluable advice, discussion, and encouragement. Finally, I would like to thank the Core Services at the Van Andel Research Institute for their technical help, Mr. David Nadziejka for his professional comments on scientific writing, and Ms. Laura Holman and Laura Round for their administration support during the past five years. This research would not be possible without their supportive help.

This dissertation is dedicated to my best-loved family members: my grandmother, parents, aunt, brother and sister-in-law as well as the expected nephew.

Table of Contents

List of Tables

List of Figures

Images in this thesis/dissertation are presented in color.

List of Abbreviations

B-Raf, *v-raf* murine sarcoma viral oncogene homolog B1

CDKN2A, cyclin-dependent kinase inhibitor 2A

cDNA, complementary DNA

CHO K1, Chinese hamster ovary K1

DMSO, dimethyl sulfoxide

DNA, deoxyribonucleic acid

EDTA, ethylenediaminetetraacetic acid

EGF, epidermal growth factor

EGTA, ethylene glycol-bis(2-aminoethylether)-*N,N,N',N'*-tetraacetic acid

ERK, extracellular signal-regulated kinase

GST, glutathione S-transferase

JNK, c-Jun N-terminal kinase

LeTx, lethal toxin (anthrax lethal toxin)

LF, lethal factor (anthrax lethal factor

MAP, mitogen-activated protein

MAPK, mitogen-activated protein kinase

MAPKK, mitogen-activated protein kinase kinase

MEK, mitogen-activated protein kinase/extracellular signal-regulated kinase kinase

MEKcr, cleavage-resistant form of MEK

MKK, mitogen-activated protein kinase kinase

mRNA, messenger RNA

PA, protective antigen

PMA, phorbol 12-myristate 13-acetate

PTEN, phosphatase and tensin homolog

Ras, rat sarcoma viral oncogene homolog

RNA, ribonucleic acid

SDS, sodium dodecyl sulfate

shRNA, small hairpin RNA

siRNA, small interfering RNA

SV40, simian virus 40

TPA, 12-O-tetradecanoylphorbol-13-acetate

UV, ultraviolet

YopJ, *Yersinia* outer protein J

Chapter I. General introduction: MEK signaling pathway and cancer

1.1. Introduction to MEK signaling pathway

1.1.1. Exploring the Raf-MEK-ERK signaling pathway

In late 1980s, Ray and Sturgill (1987; 1988a) observed that soluble fractions of cell extracts prepared from insulin-treated 3T3-L1 adipocytes were capable of phosphorylating the microtubule-associated protein 2 (MAP-2) protein. Initially this protein kinase was termed microtubule-associated protein (MAP) kinase, as it catalyzed the phosphorylation of MAP-2 on serine and threonine residues (Sturgill & Ray, 1986). Later, MAP kinase activity was shown to be stimulated not only by insulin but also by other mitogenic factors such as serum, insulin-like growth factors, epidermal growth factor (EGF), and phorbol 12-myristate 13-acetate (PMA; also called TPA) (Rossomando *et al.*, 1989; Erickson *et al.*, 1990). Therefore, this enzyme was also named mitogen-activated protein (MAP) kinase (Rossomando *et al.*, 1989) or extracellular signal–regulated kinase (ERK) (Boulton *et al.*, 1990). Since growth factor–stimulated MAP-2 phosphorylation was accompanied by DNA synthesis and cell cycle progression (Sato *et al.*, 1985; Sato *et al.*, 1986), Ray and Sturgill's seminal discovery opened the way to exploring the MAP kinase signal transduction pathway through which these cellular events were regulated.

Ray and Sturgill (1988b) also showed that ERK was phosphorylated at threonine and tyrosine residues upon stimulation, and serine/threonine phosphatase as well as tyrosine phosphatase could completely deactivate ERK (Anderson *et al.*, 1990). These findings indicated that ERK itself was a phosphoprotein and that activation of ERK

involved phosphorylation by another protein kinase having threonine and tyrosine specificity. Soon after, the activator for ERK was identified and purified from EGF-stimulated cells by Ahn (1991) and colleagues (Seger *et al.*, 1992). This dual-specificity protein kinase (both serine/threonine and tyrosine specificity) (Gomez & Cohen, 1991; Nakielny *et al.*, 1992; Seger *et al.*, 1992) was called MAP kinase kinase (MAPKK, MAP2K or MKK) (Gomez & Cohen, 1991) or MAPK/ERK kinase (MEK) (Crews & Erikson, 1992). Similarly, MEK was characterized as a phosphoprotein that required serine/threonine phosphorylation for its own kinase activity (Gomez & Cohen, 1991). Serine/threonine protein phosphatase 2 (PP2A) — but not tyrosine phosphatases — was shown to inactivate MEK activity (Gomez & Cohen, 1991; Nakielny *et al.*, 1992). This indicated that downstream of the growth factor receptors (which were tyrosine kinases) there must be at least one serine/threonine protein kinase that functioned as the MEK activator. Subsequent to this, the Raf family of protein kinases, cellular homologues of the acutely transforming viral oncogene v-*raf* (Rapp *et al.*, 1983), were identified as direct activators of MEK (Dent *et al.*, 1992; Kyriakis *et al.*, 1992). c-Mos has also been identified as a kinase that activates MEK, though its normal expression is limited to oocytes (Sagata *et al.*, 1988).

1.1.2. Activation mechanism of the MAP kinase cascade

MAP kinase pathways are evolutionarily conserved signaling pathways that transduce signals from the cell membrane to the nucleus in eukaryotic cells (reviewed by English *et al.*, 1999; Chen *et al.*, 2001; Pearson *et al.*, 2001; Johnson & Lapadat, 2002; Roux & Blenis, 2004). Signal transduction through the Raf-MEK-ERK pathway (Figure

1) begins with the binding of extracellular growth factors to specific transmembrane receptors. This results in dimerization and/or conformational changes in the receptors, leading to a series of cytoplasmic protein recruitment/activation steps that include the Raf family of proteins. Raf then activates MEK1 and MEK2, the only known MEK isoforms, by phosphorylating them on the conserved serine residues in the activation loop (Ser218/Ser222 of human MEK1 and Ser222/Ser226 of human MEK2) (Alessi *et al.*, 1994; Zheng & Guan, 1994). Active MEK1 and MEK2 then in turn activate ERK1 and ERK2, the only known substrates of MEK, by phosphorylating the threonine and tyrosine residues in the conserved T-E-Y motif (Thr202/Tyr204 of human ERK1 and Thr185/Tyr187 of human ERK2) (Payne *et al.*, 1991). After activation, ERK phosphorylates and activates downstream effectors regulating a variety of cellular events at the transcriptional and posttranslational levels (reviewed by English *et al.*, 1999; Chen *et al.*, 2001; Pearson *et al.*, 2001; Johnson & Lapadat, 2002; Roux & Blenis, 2004).

Why does the MAP kinase pathway employ three tiers of protein kinases to transduce signals instead of one? To simulate MAPK phosphorylation and activation, Huang and Ferrell (1996) constructed an elegant mathematical model and then tested predictions of this model in cytoplasmic extracts of *Xenopus* oocytes. They found that whereas Raf behaved as a typical Michaelis-Menten enzyme, MEK and ERK behaved as "ultrasensitive" enzymes. In other words, MEK and ERK are relatively less sensitive to low concentrations of stimuli but above a threshold level stimuli evoke a strikingly rapid response. This makes MEK and ERK respond to stimuli in an all-or-none fashion, like a switch. Moreover, according to their model, the ultrasensitivity of this reaction is directly linked to the dual phosphorylation that is required to activate MEK and then ERK. This

observation has profound functional implications and should be an important consideration in designing strategies to inhibit this pathway.

1.2. Involvement of MEK signaling pathway in human cancers

The Raf-MEK-ERK pathway is an important signaling pathway that, in response to growth factor signals, promotes cell cycle progression and cell proliferation (reviewed by English *et al.*, 1999; Chen *et al.*, 2001; Pearson *et al.*, 2001; Johnson & Lapadat, 2002; Roux & Blenis, 2004). Therefore, it is not surprising that deregulated activities of the kinases in this pathway disrupt growth control, which can lead to cancers. The hypothesis that elevated activity of the Raf-MEK-ERK signaling pathway may lead to cancer was tested more than ten years ago when constitutively active MEK-ERK signaling was shown to be sufficient to transform mammalian cells (Mansour *et al.*, 1994a). In support of this, screening of somatic mutations in a panel of human cancer cell lines identified the presence of the constitutively active B-Raf mutant V600E, which results in a persistent activation of the downstream pathway, in 66% of human melanomas and in a lower percentage of other types of cancers (Davies *et al.*, 2002). Based on these findings, targeting the Raf-MEK-ERK signaling pathway became a prospective strategy for treating human cancers.

1.3. Targeting the Raf-MEK-ERK pathway as a strategy for treating cancers

In principle inhibitors can be designed that will block any step in this pathway (reviewed by Kohno & Pouyssegur, 2003; Sebolt-Leopold & Herrera, 2004; Kohno & Pouyssegur, 2006). However, because this is an amplifying signal cascade, it makes

most sense to block that signal as close to the stimulus (receptor tyrosine kinase) as possible. This is particularly true in this case as MEK and ERK respond to stimuli in an all-or-none fashion. Therefore, it might be argued that Raf kinases are the preferred point of intervention. However, in an unexpected twist several investigators now report that B-Raf inhibitors paradoxically can activate MEK-ERK signaling in cells that express wild-type B-Raf (Hatzivassiliou *et al.*, 2010; Heidorn *et al.*, 2010; Poulikakos *et al.*, 2010). It appears that the binding of ATP-competitive B-Raf inhibitors causes conformational changes in the kinase that promotes dimerization and transactivation of non–drug-bound C-Raf in an active Ras-dependent fashion. So, while it makes sense to target tumors harboring B-Raf mutations with B-Raf inhibitors, it may actually be disadvantageous to use these drugs to treat tumors with wild-type B-Raf since they may enhance proliferation of tumor cells and may have adverse effects on normal cells with active Ras. In this case MEK inhibitors may be the most appropriate therapeutic option.

A great deal of effort has gone into looking for highly selective MEK inhibitors. Many of these are commonly used in laboratories as powerful tools in the study of the MEK-ERK signaling pathway, and select inhibitors are currently in cancer clinical trials, having shown promising anti-cancer activity in preclinical studies. In the following sections, I will review the discoveries, properties, and clinical applications of two categories of highly selective MEK inhibitors: non–ATP-competitive small-molecule inhibitors and biological inhibitors. By focusing on their MEK selectivity and inhibition mechanisms, the following review will provide insights into the potential of these inhibitors as tools for studying the Raf-MEK-ERK pathway and as anti-tumor agents.

1.3.1. Small-molecule inhibitors

In this section, the best known and commonly used non–ATP-competitive MEK inhibitors will be reviewed. These inhibitors result in MEK-specific inhibition by an allosteric mechanism which contributes to highly selective inhibition of MEK without affecting other protein kinases that have structurally similar ATP binding pockets.

1.3.1.1. PD 098059

By screening a compound library using an *in vitro* kinase cascade phosphorylation assay, Dudley *et al.* (1995) identified PD 098059, 2-(2'-amino-3'-methoxyphenyl)-oxanaphthalen-4-one (Figure 2a), as a synthetic inhibitor of the MAPK pathway. PD 098059 inhibits MEK (IC_{50} = 10 μM, see Table I) but not other components of the MAPK pathway. In later studies, PD 098059 showed no significant effect on a spectrum of other protein kinases, including protein kinase A (PKA), protein kinase C (PKC), and other kinase members in the MAPK family pathways such as p38 MAP kinase, c-Jun NH_2-terminal kinase (JNK), p38 MAP kinase kinase, and MKK4 (Alessi *et al.*, 1995; Davies *et al.*, 2000). Kamakura *et al.* (1999) showed that PD 098059 had no effect on MEK5 (a MEK/MKK family member which is independent from the MEK1/2-ERK1/2 pathway) *in vitro*, but did have an inhibition effect on intracellular MEK5 activity. This was later confirmed by Mody *et al.* (2001), although a high concentration (100 μM) of PD 098059 was required. PD 098059 inhibits growth factor–stimulated MAPK activation and DNA synthesis in Swiss 3T3 cells (Dudley *et al.*, 1995), suggesting the membrane permeability and in-cell inhibitory activity of PD 098059. Initial observation showed that PD 098059 did not inhibit MEK1 that had been

maximally phosphorylated by c-Raf (Alessi *et al.*, 1995; Ahn *et al.*, 2001), raising a possibility that PD 098059 did not bind to the active site of MEK but instead bound to another allosteric pocket. The allosteric inhibition mechanism was later confirmed by using classical Michaelis-Menten methods (Favata *et al.*, 1998).

1.3.1.2. U0126

U0126, 1,4-diamino-2,3-dicyano-1,4-bis(2-aminophenylthio)butadiene (Figure 2b), was the second compound identified as an allosteric inhibitor of MEK. Favata *et al.* (1998) screened a total of 40,000 compounds for their ability to inhibit activator protein 1 (AP-1)–driven transcription using a luciferase reporter assay. They reported that U0126 inhibited both AP-1–driven gene expression and TPA-induced up-regulation of c-Jun and c-Fos at the protein and the mRNA levels, suggesting that U0126 targeted the upstream activators of c-Jun and c-Fos. Indeed, U0126 inhibits MEK (see Table I), but not other MKK members and MAP kinases (Davies *et al.*, 2000) except for MEK5 (Kamakura *et al.*, 1999; Mody *et al.*, 2001). In addition, U0126 showed a 100-fold greater potency than PD 098059 (Favata *et al.*, 1998). This was later confirmed by Davies *et al.* (2000). Consistent with PD 098059 studies, U0126 has a much lower effect on activated wild-type MEK than constitutively active MEK (Alessi *et al.*, 1995; Ahn *et al.*, 2001), suggesting that the conformational change in MEK upon activation interferes with the binding of these inhibitors. In addition, this implied that these two MEK inhibitors might not compete with the ATP binding pocket of MEK. Using classical Michaelis-Menten enzyme modeling, Favata *et al.* (1998), confirmed the non–ATP-competitive mechanism

of these MEK inhibitors the structural basis of which will be discussed in detail later in this section.

The results of *in vitro* kinase assays using purified proteins suggested that PD 098059 and U0126 inhibited the phosphorylation and activation of MEK but not the ability of MEK to phosphorylate ERK (Alessi *et al.*, 1995; Ahn *et al.*, 2001). However, in later studies, the inhibitory effect of PD 098059 and U0126 on MEK phosphorylation was not observed in intact cells when using antibodies specifically against phospho-MEK (Ahn *et al.*, 2001). A possible explanation for this controversy is that the action of these two inhibitors in intact cells is mediated by inhibition of MEK phosphoryl-transferase activity, and that both inhibitors may interfere with Raf-dependent MEK phosphorylation *in vitro*, only when other intracellular components are absent. This controversy was also pointed out and discussed by Kohno and Pouyssegur (2003).

PD 098059 and U0126 are widely used in laboratories as powerful tools for studying the MEK signaling pathway. Both molecules are commercially available and have thousands of entries in the PubMed database. However, neither of them has entered clinical trials due to their limited *in vivo* bioactivity.

1.3.1.3. PD 184352 (CI-1040)

PD 184352 (Figure 2c), also known as CI-1040, was identified by Sebolt-Leopold *et al.* (1999) as a potent MEK inhibitor (IC_{50} = 17 nM; see Table I) in an *in vitro* kinase cascade assay using GST-fusion proteins of MEK1 and MAPK. PD 184352 has a higher potency than PD 098059 and U0126 (Table I), and has no effect on other kinases tested (Sebolt-Leopold *et al.*, 1999; Davies *et al.*, 2000). Similar to PD 098059 and U0126, PD

184352 inhibits intracellular MEK5 activity at a much higher concentration than that required to inhibit the activation of ERK (Mody *et al.*, 2001). PD 184352 is not competitive with ATP or ERK (Sebolt-Leopold *et al.*, 1999), suggesting a similar allosteric inhibition mechanism for PD 184352 as for PD 098059 and U0126. The cellular consequences of MEK inhibition by PD 184352 include a complete suppression of platelet-derived growth factor (PDGF)-induced ERK activation, induction of G_1 cell cycle arrest, reversion to untransformed morphology, and inhibition of anchorage-independent growth in colon cancer cells as well as in other cancer cell lines (Table I) (Sebolt-Leopold *et al.*, 1999). Interestingly, PD 184352 showed a stronger effect on three colon cancer cell lines that had high ERK activity relative to cancer cell lines with low ERK activity, suggesting that the inhibitor is more potent for cancer cells that are addicted to MEK signaling. This was further confirmed by Solit *et al.* (2006), who showed that the B-Raf V600E oncogenic mutation in cancer cell lines was associated with enhanced and selective sensitivity to PD 184352 when compared with B-Raf wild-type cell lines. In addition to the *in vitro* effects, Sebolt-Leopold *et al.* (1999) successfully showed that PD 184352 actively suppressed ERK activation in colon cancer cell xenograft tumors in mice within one hour after oral administration. More importantly, this *in vivo* efficacy was achieved over a wide range of doses (48–200 mg/kg, two treatments per day for 14 days) without signs of toxicity. This was the first study demonstrating the *in vivo* efficacy of MEK inhibition by a small-molecule inhibitor.

A phase I study of PD 184352 was conducted to test the toxicity, pharmacokinetics, pharmacodynamics, maximum tolerated dose, food effect, and clinical activity in patients with advanced cancers, including colorectal, non-small cell lung,

pancreatic, and kidney cancers, as well as melanoma (Allen *et al.*, 2003; LoRusso *et al.*, 2005b). PD 184352 was administrated orally in single to multiple daily doses from 100 mg to 1,600 mg for 21 days, followed by 7 days off, for a total of three cycles. After the maximum tolerated dose profile was determined, the "holiday" week between treatment cycles was removed to test the safety profile of continuous dosing. Blood and urine samples were collected throughout the treatment for pharmacokinetics and biomarker assessments. Phospho-ERK levels were assessed in blood samples and tumor biopsies to determine the clinical targeting activity of PD 184352. The study results showed that PD 184352 was well tolerated at a treatment of 800 mg twice daily, with common grade 1 or 2 drug-related adverse events including diarrhea, asthenia, rash, nausea and vomiting. Although this was a phase I study initially designed only to assess toxicity, some patients showed promising signs of efficacy: one out of 66 patients had partial response lasting 355 days, and 19 patients (29%) achieved stable disease for 4-17 months with a median of 5.5 months.

Based on these results, a phase II trial was initiated to assess the antitumor activity and safety of PD 184352 in patients with advanced breast, colon, non-small-cell lung, and pancreatic cancers (Rinehart *et al.*, 2004). In this study, PD 184352 was given to patients at 800 mg twice daily and continuously, and was reduced later in 200-mg decrements for patients with grade 2 or greater adverse event severity. Continuous PD 184352 treatment exceeding one year was well tolerated without cumulative toxicities, and 81% of the patients experienced only grade 1 or 2 adverse events. However, PD 184352 was terminated in the phase II trial because no complete or partial responses were

observed, although eight patients (12%) achieved stable diseases lasting 4-18 months with a median of 4.4 months.

The change in ERK activity in the tumors after PD 184352 treatment was not available from the phase II study as the study was not designed to assess it in tumor biopsies. However, in the earlier phase I study, ERK activation was inhibited by 46% to 100%, with an average of 73% in tumor biopsies from ten out of ten (100%) patients (LoRusso *et al.*, 2005b). This suggests that the lack of response to PD 184352 in the phase II study might not be solely due to incomplete inhibition of ERK activity in the tumors. In addition, the authors of this study also attributed the lack of response to the poor metabolic stability of PD 184352. PD 0325901, a PD 184352 analog, was then developed as a second-generation MEK non–ATP-competitive inhibitor with improved potency and pharmaceutical properties, and it has since entered clinical trials (discussed immediately below).

1.3.1.4. Derivatives of PD 184352

PD 0325901 (Figure 2d), an analog of PD 184352, is also a non–ATP-competitive inhibitor and possesses high selectivity for MEK (Sebolt-Leopold *et al.*, 2004). PD 0325901 has a 500-fold higher cellular effect on ERK activation than does PD 184352 (see Table I). It is believed that this improvement is the result of several factors, including better solubility and higher metabolic stability. Similar to PD 184352, PD 0325901 has higher potency for xenograft tumors harboring the B-Raf V600E mutation than for tumors with wild-type B-Raf (Solit *et al.*, 2006). In recent studies, PD 0325901 showed *in vivo* potency for oncogenic B-Raf-induced lung adenocarcinoma and

melanoma (Dankort *et al.*, 2007; Dankort *et al.*, 2009a). More importantly, in preclinical studies, PD 0325901 suppressed ERK phosphorylation by more than 50% at a single oral dose of 25 mg/kg at 24 hours after treatment. In comparison, PD 184352 suppressed ERK phosphorylation at a much higher dose of 150 mg/kg for only eight hours, and the phospho-ERK level returned to the control level within 24 hours after treatment (Sebolt-Leopold *et al.*, 2004).

The improved biological profile and promising preclinical activity of PD 0325901 moved it into a phase 1-2 clinical study of patients with advanced cancers, including breast, colon, and non-small-cell lung cancers as well as melanoma (LoRusso *et al.*, 2005a; Menon *et al.*, 2005). Based on preclinical studies, cycles of PD 0325901 were administrated orally from 1 mg once daily to 1, 2, 4, 8, 15, 20 or 30 mg twice daily for 21 days and then repeated every four weeks. The study was designed to focus on pharmacokinetics, pharmacodynamics, and effectiveness. For this purpose, before and during treatment, tumors were biopsied to assess ERK activation and proliferation index, and blood samples were collected to measure the amount of circulating drug and its metabolite. The results showed that PD 0325901 was well tolerated. In addition to common toxicities (including rash, diarrhea, nausea, and vomiting), some patients had visual effects including blurred vision and halos. Strong inhibitory effects of PD 0325901 treatment on phospho-ERK and proliferation marker Ki67 were observed at a minimum dose of 2 mg twice daily: ERK phosphorylation was consistently suppressed by an average of 84%, while cell proliferation (measured by Ki67 immunostaining) declined by an average of 60%. Although one partial response (melanoma) and five stable disease cases (four melanoma and one non-small-cell lung carcinoma) were observed, this study

was terminated prematurely in 2007 mainly due to the safety concerns about the ocular and neurological toxicity that presented at 10 mg twice daily and higher (ClinicalTrials.gov Identifier: NCT00147550).

As both PD 184352 and PD 0325901 have failed in clinical trials, Pfizer recently has developed and investigated a series of PD 184352 derivatives, among which one compound has showed relatively superior ERK inhibition and better solubility then PD 184352 [compound 12a reported by Warmus *et al.* (2008)]. More importantly, the metabolic stability of this compound is much better than that of PD 184352.

1.3.1.5. ARRY-142886 (AZD6244)

ARRY-142886, or 6-(4-bromo-2-chloro-phenylamino)-7-fluoro-3-methyl-3*H*-benzoimidazole-5-carboxylic acid (2-hydroxy-ethoxy)-amide (Figure 2g), also called AZD6244, was disclosed in 2004 as another second-generation MEK small molecular inhibitor (Wallace *et al.*, 2004). Like PD 0325901, ARRY-142886 was developed based on the PD 184352 structure, and therefore was highly selective for MEK and noncompetitive with ATP (Lyssikatos *et al.*, 2004; Yeh *et al.*, 2007). In an *in vitro* assay, ARRY-142886 inhibited the activity of purified MEK with an IC_{50} of 14.1 nM (Table I), but had no effect on more than 40 other kinases and a minimal inhibitory effect on MEK5 (Yeh *et al.*, 2007). Similar to other MEK noncompetitive inhibitors, ARRY-142886 inhibits MEK activity but not the phosphorylation and activation of MEK in intact cells (Yeh *et al.*, 2004; Yeh *et al.*, 2007). ARRY-142886 has been shown to inhibit intracellular phosphorylation of ERK1/2 in several cancer cell lines including melanoma, colon, and pancreatic cancer lines, with an IC_{50} below 40 nM (Table I), but has no effect

on MEK5 (Yeh *et al.*, 2007; Haass *et al.*, 2008). Cellular responses to ARRY-142886 include an inhibition in proliferation and cell cycle arrest at the G_1/S transition (Yeh *et al.*, 2004; Yeh *et al.*, 2007; Haass *et al.*, 2008), whereas prolonged treatment (72 h) results in only limited apoptosis in some cell lines (Haass *et al.*, 2008). The cytostatic inhibitory effect of ARRY-142886 was also observed in a three-dimensional culture model of melanoma (Haass *et al.*, 2008).

Like an earlier study of PD 184352 (Solit *et al.*, 2006), ARRY-142886 had a much stronger inhibitory effect on cancer cells harboring Ras or Raf oncogenic mutations than on those without the mutations or on normal fibroblast cells (Yeh *et al.*, 2004; Yeh *et al.*, 2007; Haass *et al.*, 2008). Moreover, ARRY-142886 is active when given orally and shows *in vivo* efficacy. In mouse xenograft models, ARRY-142886 not only inhibits the growth of colon cancer and melanoma in a dose-dependent manner, but also induces pancreatic xenograft tumor regression (Lee *et al.*, 2004; Yeh *et al.*, 2007; Haass *et al.*, 2008). Although ARRY-142886 effectively inhibits melanoma xenograft tumor growth, it does not induce apoptosis in the tumor cells unless combined with microtubule-stabilizing agents (Haass *et al.*, 2008). Interestingly, xenograft tumor growth recovers after cessation of ARRY-142886 administration, and the tumors regress again upon re-administration (Yeh *et al.*, 2007). This supports the idea that the effect of ARRY-142886 is cytostatic as opposed to cytotoxic and that continuous treatment may be necessary to maintain the inhibitory effect.

With its promising *in vivo* antitumor activity, ARRY-142886 entered phase I clinical trial in 2004, which was initiated to assess the maximum-tolerated dose, pharmacokinetics, and pharmacodynamics in patients with advanced cancers, including

breast cancer, colorectal cancer, and melanoma (Adjei *et al.*, 2008). This study had two parts. Part A was to determine the maximum-tolerated dose. Patients were orally given ARRY-142886 at doses of 50, 100, 200, or 300 mg twice daily for 28-day cycles. Although the maximum-tolerated dose obtained from part A was 200 mg twice daily, this dose was discontinued in the second part of the study (Part B) because a substantial number of patients in Part A required dose reductions, treatment holidays, or even termination due to drug-related toxicities including rash, diarrhea, nausea, fatigue, and blurred vision. Therefore, a dose of 100 mg twice daily was recommended for the Part B study. The results showed that ARRY-142886 was well tolerated at 100 mg twice daily with grade 1 or 2 adverse events. Promising targeting effects of ARRY-142886 were observed in post-treatment tumor samples: ERK phosphorylation was strongly inhibited by an average of 79%, while greater than 50% inhibition of cell proliferation (measured by Ki67 immunostaining) was seen in 25% of the patients. One patient enrolled in this study with malignant melanoma had a 70% reduction of tumor size after three cycles of treatment but eventually developed brain metastases. Although no objective response was achieved in the phase I study, nine patients (16%) had stable disease for more than five months. Based on the promising targeting effect and recommended dosage obtained from the phase I study, ARRY-142886 is now in several phase II studies, including studies involving combination therapies.

1.3.2. Mechanism of allosteric inhibition

Initially both PD 098059 and U0126 were found to have a stronger effect on less active MEK than highly active MEK (Alessi *et al.*, 1995; Favata *et al.*, 1998), suggesting

that these kinase inhibitors do not bind to the enzyme active site of MEK. In addition, Favata *et al.* (1998) also confirmed the non–ATP-competitive mechanism of these MEK inhibitors by using classical Michaelis-Menten methods. While these inhibitors do not compete with ATP or ERK, they do compete with each other, indicating that the inhibitors share a common binding site independent of the ATP or ERK binding sites (Favata *et al.*, 1998). Ohren *et al.* (2004) identified the binding pocket of non–ATP-competitive MEK inhibitors by co-crystallizing MEK with MgATP and two PD 184352 derivatives [PD 318088 (Figure 2e) for MEK1 and PD 334581 (Figure 2f) for MEK2] as ternary complexes with satisfactory resolutions. The crystal structures indicate that the MEK inhibitors bind to MEK in a pocket adjacent to the MgATP binding site. The inhibitor binding pocket and the MgATP binding pocket are physically separated by the side chains of Lys97 and Met143, which are conserved in the MEK active site. This was the first structural study directly revealing the allosteric binding pocket of these MEK inhibitors.

Ohren *et al.* (2004) also showed that the diaryl amine (A ring and B ring, Figure 2c-g) structure of PD 184352 and its derivatives — including PD 0325901, PD 318088, PD 334581, and ARRY-142886 — was the key to stabilizing the inhibitors in the allosteric binding site. The A ring and the B ring form a crucial hydrogen-bond interaction and numerous non-covalent interactions, respectively, with the hydrophobic pocket formed by several residues. The binding of the inhibitors results in a series of conformational changes in MEK, leading to interference with the catalytic residue Lys97 (MEK1) and thus inactivation of MEK activity. In other words, upon inhibitor binding, MEK adopts a "closed" conformation of an active protein kinase, and the phosphoryl-

transferase activity of MEK is inhibited. This is supported by a fact that PD 184352 treatment inhibits ERK activation in human melanoma SK-MEL-28 cells without affecting the activation of MEK1 (Figure 3). The structures of MEK1 and MEK2, co-crystallized with MgATP plus the inhibitor, share high homology (Ohren *et al.*, 2004), indicating that the same mechanism of inhibition is involved in both. Most recently, it was shown that U0126 binds to MEK in the same pocket as PD 0325901 (Fischmann *et al.*, 2009). Since the two earliest non–ATP-competitive MEK inhibitors, PD 098059 and U0126, compete with each other (Favata *et al.*, 1998), it is very likely that all of the MEK inhibitors discussed above bind to the same pocket and use the same mechanism to inhibit MEK.

The high selectivity of these allosteric inhibitors for MEK can be explained on the basis of structure. First, these inhibitors do not compete with ATP, the major intracellular energy source for all protein kinases; this decreases the binding affinity of the inhibitors to other kinases. Second, these inhibitors bind to MEK in a unique binding pocket, which is formed by several residues of MEK and stabilizes the inhibitor binding. This pocket increases the MEK:inhibitor binding affinity as well as the complexity of the binding, resulting in a high selectivity for MEK. Since the diaryl amines of these MEK inhibitors are such a crucial structure for this MEK-specific inhibition mechanism, all the second-generation MEK allosteric inhibitors have been developed based on this structure in order to maintain the mechanism (Warmus *et al.*, 2008).

1.3.3. Biological inhibitors

1.3.3.1. Anthrax lethal toxin

The MEK-specific inhibitory activity of anthrax lethal toxin (LeTx) was revealed in the National Cancer Institute Antineoplastic Drug Screen project (Duesbery *et al.*, 1998). In this study, sixty human cancer cell lines (termed NCI-60 cell lines) were tested for their sensitivity to a panel of anti-neoplastic molecules. It was shown that the sensitivity profile of the MEK inhibitor PD 098059 was very similar to that of LeTx, raising the possibility that they sensitized the cells by a similar mechanism. Based on this, Duesbery *et al.* (1998) characterized the MEK-specific protease activity of LeTx. About the same time, Vitale *et al.* independently demonstrated the same proteolysis of MEK by LeTx (Vitale *et al.*, 1998).

Anthrax lethal toxin is a binary toxin secreted by the bacterium *Bacillus anthracis*. It is composed of a binding moiety called protective antigen (PA) and an enzymatic moiety, lethal factor (LF). During cellular intoxication, PA binds to the anthrax receptors expressed on the host cell surface and then is cleaved by a furin-like protease. This cleavage removes a 20-kDa N-terminal fragment and leaves a 63-kDa C-terminal truncation, PA_{63}, on the cell surface. PA_{63} then forms an oligomerized channel to which the LF binds. After the binding of LF, the complex is internalized into cells through the endosomal internalization pathway. The acidic environment of the endosome causes a conformational change in PA_{63} that results in the formation of pores through which LF is released into cytosol [reviewed by Singh *et al.* (2005)].

Since its initial identification as a MEK1/2-specific protease (Duesbery *et al.*, 1998), additional members of the MAP kinase kinase family, including MKK3, 4, 6 and 7

but not MEK5, have also been found to be substrates of LF [(Vitale *et al.*, 1998; Pellizzari *et al.*, 1999; Vitale *et al.*, 2000) and discussed by Duesbery *et al.* (2001)]. However, unexpected results from this dissertation research suggested that MKK7 might not be a preferred LF substrate. This will be discussed in Chapter II. LF specifically cleaves the N-terminus of MEK and other MKK proteins at the consensus cleavage site: three to four basic or proline residues followed by three variable residues followed by an aliphatic residue: $(B/P)_{3-4}$-$(X)_3$-Al (Table II). The N-termini of this family of proteins harbor MAP kinase docking sites that are required for the interaction between MEK/MKK and MAPK (Tanoue *et al.*, 2000). Not surprisingly, after LF cleavage, the C-terminal part of MEK/MKK, which contains the kinase domain, loses its affinity for the downstream MAP kinases (Chopra *et al.*, 2003; Bardwell *et al.*, 2004). In addition, biochemical evidence has shown that loss of the amino terminus may destabilize MEK, leading to the decreased intrinsic kinase activity that is observed following LF-mediated proteolysis (Chopra *et al.*, 2003). Thus, cleavage of MEK/MKK by LF results in a blockade of not only the ERK pathway but also of the p38 MAPK and JNK pathways.

Because increased MAP kinase activity has been detected in many types of human cancers, LeTx has potential as a cancer therapeutic. The first evidence for the anti-tumor activity of LeTx was provided by Friedlander *et al.* (1998). Duesbery *et al.* (2001) then assessed its effects on cancer cells and found that LeTx not only efficiently inhibited the proliferation and the soft agar colony formation of oncogenic Ras-transformed NIH-3T3 cells, but it also caused the cells to revert to a nontransformed morphology. LeTx treatment also inhibited the growth of Ras-transformed cells implanted in nude mice, with no overt toxicity. Interestingly, LeTx-treated xenograft

tumors had a pale appearance whereas control tumors were dark red-purple. This study demonstrated the *in vivo* antitumor activity of LeTx and also suggested that LeTx could inhibit tumor growth by targeting cell proliferation pathways as well as angiogenesis pathways.

This finding has been confirmed in several tumor models including melanoma (Koo *et al.*, 2002; Abi-Habib *et al.*, 2005), Kaposi's sarcoma (Depeille *et al.*, 2007), fibrosarcoma (Ding *et al.*, 2008), kidney cancer (Huang *et al.*, 2008), neuroblastoma, and colorectal adenocarcinoma (Rouleau *et al.*, 2008) cells *in vitro*, as well as in xenograft tumor growth *in vivo*. In the earliest xenograft studies, LeTx was not administrated systemically, but intratumorally. In these studies it was noted that intratumoral injection of LeTx had a growth inhibitory effect on distal, uninjected tumors (Duesbery *et al.*, 2001; Koo *et al.*, 2002). These observations revealed the systemic anticancer potential of LeTx. Abi-Habib *et al.* (2006a) then determined the *in vivo* potency and safety of systemically (intraperitoneally) administrated LeTx in athymic nude mice bearing human melanoma xenograft tumors. In this study, the ratios of PA to LF giving the highest potency were determined to be 3:1 and 5:1, and LeTx was well tolerated at a cumulative dosage of 24 μg total LF at a 5:1 ratio of PA to LF. An LD_{10} for a cumulative dose was estimated at 30–36 μg total LF. Since this preclinical study, a standard LeTx systemic treatment has been established for human cancer xenograft tumors in nude mice: 10 μg of PA and 2 μg of LF are pre-mixed and injected intravenously through tail vein every other day, for a total of six injections in two weeks (a cumulative does of 12 μg total LF, which is less than half the LD_{10} dose). At 12 μg, LeTx effectively inhibits the growth of xenograft tumors without apparent animal toxicity (Depeille *et al.*, 2007; Ding *et al.*, 2008; Huang

et al., 2008). In addition LeTx has been modified to selectively target cancer cells expressing high levels of urokinase plasminogen activators or matrix metalloproteases, features of metastatic cancer cells (Abi-Habib *et al.*, 2006b; Liu *et al.*, 2008).

Several lines of evidence support the conclusion that LeTx acts in an anti-angiogenic fashion. First, as noted above, gross inspection reveals that LeTx-treated tumors have a pale appearance when compared to untreated tumors. Second, the mean vascular density for LeTx-treated tumors is dramatically reduced (Depeille *et al.*, 2007; Ding *et al.*, 2008; Huang *et al.*, 2008). Finally, a recent study using high-resolution ultrasound enhanced with contrast microbubbles revealed the rapid (within 24 hours) inhibitory effect of LeTx on the perfusion of fibrosarcoma xenograft tumors, but interestingly not in non-tumor host tissues (Ding *et al.*, 2008). This suggests that the inhibitory effect of LeTx on endothelial function is highly selective for tumor-associated blood vessels.

Although it is clear that LeTx reduces tumor vascularity, the mechanism by which it does this is uncertain. The initial explanation that LeTx acted directly on tumor cells to suppress the release of pro-angiogenic factors was supported by *in vitro* studies demonstrating that LeTx suppressed release of angiogenic cytokines such as vascular endothelial growth factor (VEGF), interleukin-6 (IL-6) and basic fibroblast growth factor (bFGF). However, this hypothesis was questioned after LeTx was demonstrated in subsequent studies to inhibit the growth of tumors that do not express toxin receptors (Liu *et al.*, 2008). Moreover, results from this dissertation research show that systemic LeTx administration can inhibit growth of human melanoma SK-MEL-28 xenograft tumors without directly targeting the MEK-ERK pathway in tumor cells (presented in Chapter

III). These observations indicate that LeTx targets a non-tumor compartment, perhaps endothelial cells. In support of this, endothelial cells have been reported to be potential targets of LeTx (Kirby, 2004; Warfel *et al.*, 2005; Alfano *et al.*, 2009), and the MEK signaling pathway is required for tumor-associated endothelial function (Mavria *et al.*, 2006). Regardless of the cellular target, these observations establish LeTx as an anti-angiogenic agent. However, LeTx appears to be unique in this aspect since an anti-angiogenic effect of other MEK inhibitors has not been reported. Thus this activity may be related to its effects on other MKK signaling pathways

In summary, LeTx is a highly selective biological inhibitor of MEK and most other members in the MKK protein family, and it shows very good potential to be a potent cancer-targeting therapeutic. Although LeTx is unlikely to enter clinical trials owing to its toxicity, it has become a powerful tool for studying the involvement of MEK/MKK signaling pathways, not only in cancers but also in other diseases such as inflammatory diseases (Pellizzari *et al.*, 1999; Park *et al.*, 2002; Agrawal *et al.*, 2003) and eye diseases (Bromberg-White *et al.*, 2009).

1.3.3.2. YopJ

YopJ is a member of the *Yersinia* outer protein (Yop) family of effectors proteins. The Yops are virulence factors produced by *Yersinia* species including *Yersinia pestis*, the bacterial pathogen that caused the bubonic plague or Black Death in the Middle Ages. Upon infection, Yops are translocated into host cells through a contact-dependent type III secretion system. Initial studies showed that YopJ was necessary and sufficient for the pathogen to inhibit multiple eukaryotic signaling pathways, including all the parallel

MAPK pathways (Palmer *et al.*, 1998; Palmer *et al.*, 1999) and the nuclear factor kappa B (NF-κB) pathway (Ruckdeschel *et al.*, 1998; Schesser *et al.*, 1998). Inhibition of these multiple signaling pathways by YopJ results in disruption of cytokine secretion (which in turn disrupts the innate immune response) and an induction of apoptosis in infected cells. Later, Orth *et al.* (1999) confirmed the direct and physical interactions of YopJ with multiple signaling molecules (including IKKβ, an NF-κB activator, and MKK1-5), but not with the members of MKKK or MAPK. This finding suggested that YopJ inhibited these signaling pathways by a mechanism that required direct binding to these signaling molecules. Sequence comparisons showed that YopJ has a secondary structure similar to that of the adenoviral protease (AVP) family. From this, Orth *et al.* (2000) demonstrated the protease activity of YopJ and suggested that YopJ proteolytically inhibited the MAPK and NF-κB pathways. However, whether proteolysis was the mechanism for YopJ inhibition of the MAPK and NF-κB pathways was questionable, because the total amount and molecular weight of MKK or IKKβ were not affected by YopJ treatment (Orth *et al.*, 1999).

The biochemical mechanism for YopJ-mediated inhibition of eukaryotic signaling pathways was not elucidated until recently, when studies identified YopJ as an O-acetyl transferase that acetylates the serine/threonine residues in the activation loop of MEK/MKK and IKK (Mittal *et al.*, 2006; Mukherjee *et al.*, 2006). Once acetylated, those residues can no longer be phosphorylated and activated, resulting in inhibition of the downstream MAPK and NF-κB pathways. A recent mutagenesis study has identified the conserved G α-helix in the kinase domain of MEK as a YopJ-binding motif (Hao *et al.*, 2008). In the study, a PCR random mutagenesis library was screened for mutant

Pbs2 (MKK yeast homologue) proteins that were able to suppress YopJ-induced growth inhibition in yeast. The conserved Ile579 residue of Pbs2 (corresponding to Ile317 of human MEK1) was shown to be required for YopJ to bind and acetylate Pbs2. This residue is in the conserved G α-helix in the kinase domain of MEK, and mutation of several residues in this region has been shown to prevent interaction with YopJ (Hao *et al.*, 2008). Interestingly, the same region has been implicated in binding anthrax LF (Chopra *et al.*, 2003), and the G helix is also a part of the MEK homodimer interface (Ohren *et al.*, 2004). Although the link between MEK dimerization and LF/YopJ binding has not been established, it is tempting to speculate that dimer disruption may be a factor in MEK inhibition.

Based on the specific inhibitory effects of YopJ on the MAPK and NF-κB signaling pathways, YopJ also has potential as a therapeutic for cancers and inflammatory diseases. However, unlike LeTx, which can be internalized by host cells, the delivery of YopJ into host cells is dependent on a type III secretion system that requires a direct interaction between the pathogen and host cells (Ghosh, 2004). Although YopJ can be expressed following transfection into mammalian cells, efficient delivery of YopJ in a clinical setting must be realized in order to develop YopJ as a therapeutic agent.

1.3.4. MEK inhibitors fail to generate clinical responses

Two categories of MEK inhibitors that inhibit the pathway activity were reviewed in this chapter: small-molecule inhibitors that bind and inactivate MEK by a non–ATP-competitive mechanism, and biological inhibitors that are produced by bacteria and

inactivate MEK by posttranslational modifications. The MEK inhibitors in each of these categories have advantages and disadvantages as therapeutic agents. Small-molecule inhibitors are generally orally active and non-immunogenic, whereas the biological inhibitors need to be administrated by injection and may cause an undesirable immune response. On the other hand, small-molecule inhibitors are "washable" and they do not physically destroy MEK, whereas the posttranslational modifications of MEK by biological inhibitors are enzyme-mediated and irreversible in cells. Despite their pre-clinical successes, the MEK small-molecule inhibitors have not performed well in cancer clinical trials because of issues such as a lack of clinical response, insufficient efficacy, and safety concerns. Several facts may explain why these MEK inhibitors work well on xenograft tumors in nude mice but fail to generate clinical responses in human patients. First, individuals enrolled in cancer clinical trials are generally those patients who do not respond to conventional treatments and whose diseases have progressed to late stages with metastasis. The tumor responses in these patients to MEK inhibitors may not be well represented by subcutaneous xenografts in nude mice. Second, it has been shown that cancer cells having constitutively active mutations in MEK activators are relatively sensitive to MEK inhibition, whereas cells without these mutations are resistant (Yeh *et al.*, 2004; Solit *et al.*, 2006; Yeh *et al.*, 2007; Haass *et al.*, 2008). However, patients enrolled in most of the cancer clinical trials for MEK inhibitors were not initially selected for the preferred mutations. Therefore, patients' responses may not correlate well with preclinical predictions. In the Phase I study of ARRY-142886, Ras and Raf mutations were determined in biopsies, and 38% (10 of 26 assessable biopsies) had Ras (n = 9) or Raf (n = 1) mutations (Adjei *et al.*, 2008). Although the three tumors showing the

strongest reduction in Ki-67 staining were positive for Ras or Raf mutations, no statistically significant difference in response was observed, possibly due to the small sample number in this study. Third, along with cancer progression, tumor cells in late-stage patients acquire more and more genetic alterations, which may activate MEK-independent survival pathways, leading to a resistance to MEK-dependent growth inhibition. This could explain why in the clinical studies of PD 184352 and its derivatives, MEK inhibitors did show desirable ERK inhibition but failed to generate clinical responses.

1.4. Introduction to cutaneous melanoma

Cutaneous melanoma is a malignancy of melanocytes, which develops in the skin. Rarely melanomas can also develop in other parts of the body, such as brain, uvea, and the interior of the body. Cutaneous melanomas count only 4% of all the skin malignancies. However, 80% of deaths from skin cancers are melanoma. Two facts result in the challenging management of melanoma. First, melanomas usually progress rapidly without obvious changes on skin surface. Second, metastatic melanomas are very resistant to radiation and currently available systemic therapies. Therefore, once melanomas progress to metastatic stages, most patients are refractory to treatments. In this section, an overview of melanoma will be presented with a focus on molecular mechanisms of melanoma formation and currently available animal models for melanoma research.

1.4.1. Melanoma statistics

The American Cancer Society (2010) estimates that 68,130 new cutaneous melanoma cases will be diagnosed in the United States this year. This ranks melanoma the 5th and the 7th most common cancer type in men and women respectively. The incidence rate of melanoma has a race-dependent trend. It is more than 20 times higher in whites than in African Americans (Altekruse *et al.*, 2010). Among whites, the rate is about 50% higher in men than in women. In the past 35 years, melanoma incidence rates have been increasing in the population of white adults of 65 years and older (5.1% per year in men since 1985 and 4.1% per year in women since 1975). Interestingly, a rapid increasing of the incidence rate has also been observed among young white women aged 15 to 39 years (3.0% per year since 1992).

The American Cancer Society (2010) also estimates that 8,700 deaths from melanoma will occur in the United States this year. If detected in the earliest stage, melanoma is also highly curable. The 5-year survival rate for localized melanoma (confined to primary site) is 98%. Unlike other types of skin cancers, however, melanoma is more likely to spread to other parts of the body, possibly due to its highly motile nature inherited from neural-crest progenitors. If melanoma has spread to regional lymph nodes, the 5-year survival rates range from 78% to 39%, depending on the numbers of metastatic lymph nodes (Balch *et al.*, 2009). If systemic metastasis has occurred, the 5-year survival rate drops to 15% (Altekruse *et al.*, 2010) or even lower than 10% depending on the substages (Balch *et al.*, 2009). Therefore, early detection of melanoma is necessary for better prognosis.

1.4.2. Risk factors

The two major risk factors of melanoma are ultraviolet (UV) exposure (environmental risk factor) and genetic abnormality (genetic risk factor). Higher sensitivity to sunburn and/or a history of excessive sun exposure (including both sunburns and use of tanning booths) increase the risk. Like many other types of cancers, family history of melanoma is a strong risk factor. Many melanoma patients have affected family members (Lynch *et al.*, 1983). This led to cytogenetic studies and mutation screenings in familial melanoma tumor samples. Genetic abnormalities of several oncogenes and tumor suppressor genes are believed to be risk factors of melanoma. These will be discussed later in the following sections.

1.4.3. Melanoma progression, the Clark model.

In 1984, Clark *et al.* reported a study of melanoma tumor progression. This flow of melanoma progression, known as the Clark model, describes the six steps of melanoma progression from normal melanocytes to metastatic melanoma. Each of these steps is accompanied by histological changes. Table III summarizes these six steps. At the first step, melanocytes may focally proliferate and the lesions are considered benign. The proliferating melanocytes may follow a programmed differentiation pathway which leads to disappearance of a nevus. If the differentiation pathway is not followed the melanocytes become hyperplastic (the second step). At step 3, random dysplastic melanocytes with atypical nuclei form. According to Clark's observations, the vast majority of dysplastic precursors are terminal lesions that do not progress to the next step and form melanomas. If the dysplastic precursors do progress, they follow a two-phase

growth pattern before they metastasize. The first phase is the radial growth phase (step 4 of the Clark model), which is characterized by an enlargement of the tumor lesion at its periphery. Tumors at this step grow in the epidermis, and are not metastatic. The second phase is the vertical growth phase (step 5 of the Clark model). In this step tumors acquire the competence for metastasis. Tumors at this step grow vertically into the epidermis in an expansive manner forming metastases, the last step of the Clark model.

1.4.4. Melanoma staging

The American Joint Committee on Cancer (AJCC) staging system is most often used to describe the stages of melanoma. This system, also referred to as the TNM staging system, is based on the size of the tumor (T), the extent of spread to the regional lymph nodes (N), and the presence of distal metastasis (M). Combining these three categories (T, N, and M), a grouped staging system is described using 0 and Roman numerals from I to IV for melanoma (Balch *et al.*, 2009; Gershenwald *et al.*, 2010). In melanoma staging system, subgroups are defined in each of Stages I to III depending of the TNM status.

Stage 0. At this stage, the melanoma is in situ, and stays in the epidermis but has not spread to the dermis. This stage is equivalent to the first step of the Clark model.

Stage I and Stage II. Melanomas at these two stages are still localized in the skin and have not spread to regional lymph nodes. Therefore, melanomas at these two stages may be between the second step and the fifth step of the Clark model. The major criterion distinguishing the two stages is the tumor size. The melanoma with its thickness smaller than 1 mm is defined as Stage I, while the melanoma with its thickness between 1

and 2 mm is defined as Stage II. Depending on the tumor size and ulceration, each of these two stages is subclassified to substages (IA, IB, IIA, IIB, and IIC).

Stage III. At this stage, the melanoma has spread to regional lymph nodes, but distal metastasis has not occurred. Depending on the tumor size, ulceration, and the numbers of regional lymph nodes with evidence of melanoma spread, this stage is subclassified to substages of IIIA, IIIB, and IIIC.

Stage IV. If the melanoma has spread beyond the regional lymph nodes and has metastasized to distal lymph nodes and/or other organs (mostly the lung, liver, or brain), it is defined as a Stage IV melanoma.

1.4.5. Treatment of melanoma

Surgical removal of the primary growth and surrounding normal tissues is essential for melanomas at early stages. Sentinel lymph nodes are sometimes biopsied for stage determination. If lymph node metastases are present, more extensive lymph node surgery may be needed. For melanomas with deep invasions or metastasis to regional lymph nodes, immunotherapy, chemotherapy, and/or radiation therapy may be necessary. Unfortunately, none of these therapeutics prolongs survival in patients with metastatic melanoma. For metastatic melanoma, currently dacarbazine (DTIC) is the only US Food and Drug Administration (FDA)-approved chemotherapy agent, and high-dose interleukin-2 (IL-2) is the only FDA-approved immunotherapy (Tarhini & Agarwala, 2006). However, DTIC is effective in less than 10% of patients, and IL-2 has a high toxicity and gives a low response rate. As discussed earlier in this Chapter (section 1.3.1), several MEK inhibitors have failed in melanoma clinical trials. A number of clinical

trials are ongoing to evaluate the clinical efficacy of some other novel agents for melanomas.

1.4.6. Common genetic abnormalities of melanoma

The most common genetic abnormalities found in melanomas are those of *BRAF*, *NRAS*, *CDKN2A*, and *PTEN* (Miller & Mihm, 2006; Gray-Schopfer *et al.*, 2007). The involvement of the products of these genes in melanoma formation and progression will be the focus in the following sections.

1.4.6.1. *BRAF* and *NRAS*

As discussed in the earlier sections in this chapter, oncogenic mutations of *BRAF* and *NRAS* lead to a constitutive activation of the MEK-ERK survival pathway, which may cause cancer. In fact, before the members in the Raf-MEK-ERK pathway were identified, mutations in *NRAS* had been linked to cancers. van 't Veer *et al.* (1989) screened a panel of melanoma tumor samples and cell lines for *NRAS* mutation and found that *NRAS* mutations were detected only in melanomas from sun-exposed skin. Since *NRAS* mutations were also found in four of the ten primary melanomas examined, van 't Veer hypothesized that UV exposure causes *NRAS* mutation in melanocytes which occurs at a premetastatic stage. This hypothesis was supported by Ball et al. (1994) who examined 100 melanoma tumor samples and found *NRAS* mutations in 36 samples (36%). In addition, they found that *NRAS* mutations occurred in 19% of the melanoma tumors that were in the second step of the Clark's model, and at a higher frequency (56%) in primary tumors from continuously sun-exposed skin. In 2000, Tsao et al. (2000)

evaluated 53 cutaneous melanoma cell lines for *NRAS* mutation, and found activating mutations in 21% (11 of 53) of the cell lines. Downstream, *BRAF* mutations were found in 66% of melanomas examined and at lower frequency in other types of human cancers (Davies *et al.*, 2002). Interestingly, Davies found that all of the identified *BRAF* mutations were within the kinase domain and the V600E oncogenic mutation accounted for 80%. Collectively these studies show oncogenic mutations in *NRAS* and *BRAF* play a critical role in melanoma development.

Based on Davies' finding, Pollock et al. (2003) examined *BRAF* status in nevi, primary melanoma tumors, and melanoma metastases to evaluate the timing of oncogenic *BRAF* mutation. Unexpectedly they detected *BRAF* mutations resulting in V600E substitution in 82% (63 of 77) of nevi. Since most nevi do not progress to malignant melanoma, this finding suggests that oncogenic BRAF alone is insufficient for melanoma tumorigenesis. To support this, Michaloglou *et al.* (2005) expressed B-Raf_V600E in normal human melanocytes and found that sustained expression of B-Raf_V600E resulted in cell cycle arrest, which was accompanied with inductions of tumor suppressor p16 and other senescence markers. This led them conclude that oncogenic B-Raf induced cell senescence in normal melanocytes. Moreover, Wajapeyee *et al.* (2008) performed an shRNA screening and identified the insulin growth factor binding protein 7 (IGFBP7) as a candidate required for B-Raf_V600E-induced melanocyte senescence, and proposed the therapeutic potential of IGFBP7 for melanoma treatment.

Collectively, data from these studies indicate (1) the Ras-Raf-MEK-ERK signaling pathway is essential for melanoma formation, (2) elevated activity of this

pathway due to mutations is not sufficient for melanoma tumorigenesis, and (3) other molecular events are required for melanoma development.

1.4.6.2. *CDKN2A* ($p16^{INK4}$ and $p19^{ARF}$)

In 1986, Pedersen *et al.* reported abnormalities of chromosome 9 in malignant melanoma tumors (10/10 melanomas derived from 8 patients). This was the first report of chromosome 9 abnormality in non-cell line melanoma samples. A similar study was also presented by Limon *et al.* (1988) showing that chromosome 9 was one of the chromosomes that were most frequently found to be structurally aberrant in melanoma cells from patients with metastasis. Later studies of dysplastic nevi and malignant melanomas showed this structural aberrancy of chromosome 9 was a deletion of chromosome 9p21 in (Cannon-Albright *et al.*, 1992; Fountain *et al.*, 1992; Petty *et al.*, 1993). A melanoma susceptibility gene was therefore believed to reside in this region.

Using yeast two-hybrid screening, Serran *et al.* (1993) cloned *p16* from a HeLa cell cDNA library, and characterized p16 as an inhibitor of cyclin-dependent kinase 4 (CDK4). Therefore *p16* was also named $p16^{INK4}$ or cyclin-dependent kinase inhibitor 2A (*CDKN2A*). Within half a year, *p16* was mapped to a locus at chromosome 9p21, and the high frequency of homozygous deletions or mutations of *p16* was confirmed in melanoma as well as other types of human cancer cell lines (Kamb *et al.*, 1994; Nobori *et al.*, 1994). Germline mutations of *p16* were also detected at a high frequency (92%) in familial melanoma cases and at a lower frequency (30%) in dysplastic nevus cases (Hussussian *et al.*, 1994). The *p16* gene was therefore proposed as a candidate of tumor suppressor gene for melanoma.

Interestingly, when mapping the *CDKN2A* locus to chromosome 9p21, Stone and Kamb (Stone *et al.*, 1995) identified a novel form of *CDKN2A* transcript which contained a different first exon resulting in an entirely different open reading frame from the original *p16* transcript that was initially reported in 1994. This alternative first exon of *p16* was later cloned and mapped to chromosome 9p at about 20-kb upstream to the original *p16* exon 1 (Mao *et al.*, 1995). In the same year, Quelle *et al.* (1995) cloned the full-length coding sequence of this novel gene and named it $p19^{ARF}$ (ARF stands for alternative reading frame) as it encoded a protein with a predicted molecular mass of 19.3 kDa. What was surprising was not only the fact that this dual-utilized DNA sequence gave rise to two different open reading frames for distinct gene products, but that expression of p19 in $p16^{INK4}$-deleted cells could induce cell cycle arrest, like p16 (Quelle *et al.*, 1995). The mechanism by which p19 induced cell cycle arrest was not clear at that time.

Since $p16^{INK4}$ and $p19^{ARF}$ were cloned and mapped, groups of studies have reported mutations in the *CDKN2A* locus which harbors both $p16^{INK4}$ and $p19^{ARF}$, in familial melanomas in Australia, Europe and the United States (Walker *et al.*, 1995; Borg *et al.*, 1996; FitzGerald *et al.*, 1996; Flores *et al.*, 1997; Harland *et al.*, 1997; Platz *et al.*, 1997; Soufir *et al.*, 1998; Aitken *et al.*, 1999). These findings support the link between loss of p16/p19 tumor suppressor function and melanoma formation. After years of studies of these tumor suppressors, the mechanisms by which p16 and p19 suppress tumor formation are better understood. Both p16 and p19 inhibit G_1/S cell cycle transition through different but related pathways [reviewed by (Lowe & Sherr, 2003;

Polager & Ginsberg, 2009)]. The tumor suppressor p16 binds to and inhibits cyclin-dependent kinase 4 (CDK4), the activity of which is required to release the transcription factor E2F from Rb, and in turn, promote cell cycle progression through the G1/S check point. On the other hand, p19 stabilizes p53 (which is also a tumor suppressor inducing G_1/S cell cycle transition and/or apoptosis) by binding and inhibiting Mdm2, a p53 negative regulator.

Before p16 and p19 were cloned and mapped, Cowan *et al.* (1988) reported an interesting correlation. Loss of one copy of chromosome 9 was detected at a high frequency in melanomas but at a much lower frequency in nevi. Similarly, germline mutations of p16 were detected at a high frequency (92%) in familial melanoma cases, but at a lower frequency (30%) in dysplastic nevus cases (Hussussian *et al.*, 1994). These finding suggested that loss of p16/p19 tumor suppressor function is not likely to be responsible for nevi dysplasia. Instead, it may be a late-stage event during melanoma development.

1.4.6.3. *PTEN*

Since Parmiter *et al.* (1988) presented the first report of chromosome 10q abnormality (including break, translocation, and chromosome loss) in melanoma cell lines and tumor samples, the involvement of a potential tumor suppressor gene residing on chromosome 10 in melanoma formation had been hypothesized. Following Parmiter's initial report, LOH of chromosome 10q22-10qter was found in non-familial melanoma tumor samples (Herbst *et al.*, 1994). In 1997, the putative tumor suppressor gene sequence on human chromosome 10q23 was identified by two independent groups almost

at the same time (Li *et al.*, 1997; Steck *et al.*, 1997). The gene product was predicted to contain a protein tyrosine phosphatase domain and a large region with homology to chicken tensin and bovine auxilin. The gene was therefore named *PTEN* (phosphatase and tensin homolog).

After *PTEN* was mapped and cloned, LOH of the *PTEN* allele was found in 40-60% of primary or metastatic melanoma tumor samples (Teng *et al.*, 1997; Birck *et al.*, 2000), and *PTEN* mutations were found in about 30-50% of examined melanoma cell lines (Guldberg *et al.*, 1997; Teng *et al.*, 1997; Tsao *et al.*, 1998) as well as 10% of primary melanomas (Tsao *et al.*, 1998). The tumor suppression role of PTEN in melanoma formation was then tested and supported by several studies. First, ectopic expression of PTEN suppressed melanoma tumor cell growth (Robertson *et al.*, 1998). Second, over-expression of PTEN inhibited melanoma cell colony formation (Tsao *et al.*, 2000). Third, Hwang *et al.* (2001) showed that PTEN rescue reduced melanoma tumorigenecity and metastasis. Finally, a similar study demonstrated that PTEN re-expression in melanoma cells which lacked PTEN protein expression retarded tumor development in mice (Stahl *et al.*, 2003).

The tumor suppression function of PTEN was also supported by an epigenetic study. Using immunohistochemistry staining, Zhou *et al.* (2000) found no to low PTEN protein expression in 15% and 50% melanoma samples, respectively. Surprisingly, they found that among the examined melanoma samples which had no PTEN protein expression, 80% (4/5) of them showed neither mutation of the PTEN gene nor deletion of the PTEN allele. Their findings not only demonstrated an epigenetic mechanism by which loss of PTEN function is involved in melanoma formation, but also suggested that

the involvement of loss-of-function of PTEN in melanoma might be underestimated. This provides an explanation for the fact that in some studies the PTEN mutation rate in melanomas was very low and no deletion or LOH of PTEN was detected (Wu *et al.*, 2003).

1.4.7. Disease models

Oncogenic mutations and loss of tumor suppressors have been identified as critical drivers of melanoma formation and the disease progression. Based on these findings, great efforts have been made to develop animal models for melanoma research. These melanoma animal models are developed mainly for two purposes. First, these models allow testing the requirements of those genetic alterations and involvements in melanoma tumorigenesis and the disease progression. Second, these melanoma animal models facilitate the development of melanoma therapeutics as the efficacy of novel therapeutic agents and treatment strategies can be tested in these models. This section will discuss these melanoma animal models.

In 1997, Chin *et al.* (1997) reported a cooperation of oncogenic Ras and $p16^{INK4a}$-deficiency for melanoma susceptibility *in vivo*. In this mouse model, the oncogenic Ras (H-ras^{G12V}) was expressed specifically in melanocytes (under the control of tyrosinase promoter) on a $p16^{INK4a}$-deficient background. These mice (with double deficiencies) developed spontaneous melanoma after a short latency, indicating the oncogenic Ras and loss of $p16^{INK4a}$ allele cooperatively promote melanoma formation. In addition, two interesting observations were obtained from this work. First, the

frequency of *H-ras*^{G12V}-transgenic founder production was unusually low (only three founders from a total of 420 pronuclear injections). This raised the possibility of a selective pressure against oncogenic Ras. Second, before the *H-ras*^{G12V}-transgenic founders were crossed with the *p16*^{INK4a}-deficient mice, no melanoma or other malignancy occurred in the three founders (hyper-pigmentation and a proliferating melanocytic mass were the most relevant phenotypes observed). This indicates that activation of Ras is not sufficient for melanoma tumorigenesis, and that a second genetic alternation is required for melanoma tumorigenesis. This was supported by Powell *et al.* (1999) using another similar melanoma mouse model in which a mutant H-Ras was expressed specifically in melanocytes. Powell *et al.* also found that UV radiation or chemical carcinogens such as DMBA and TPA were necessary for melanoma formation in these mice.

Since constitutive activation of Ras may result in low frequency of transgenic founder production, in 1999 Chin *et al.* (1999) developed an inducible melanoma mouse model, in which the melanocyte-specific H-ras^{G12V} expression was induced by doxycycline on a *p16*^{INK4a}*-null* background. Not surprisingly, melanoma developed in doxycycline-treated mice within 60 days. More interestingly, withdrawal of doxycycline resulted in a clinical and histological regression of developed tumors, indicating that a persistent Ras activation is required to maintain melanoma tumor growth.

In 1998, a melanoma mouse model was established by Kelsall *et al.* to test the effect of UV exposure on melanoma formation. In this model, the viral oncoprotein small DNA tumor virus (SV40) early region was engineered to be expressed specifically

in melanocytes under the control of mouse tyrosinase promoter. After UV exposure, primary melanoma and melanoma metastases occurred without the use of other chemical carcinogens. This mouse model not only tested the requirement of oncogenic proteins for melanoma tumorigenesis, but also demonstrated the critical involvement of UV exposure in melanoma initiation. Since SV40 oncoprotein inactivates both Rb and p53 (Levine, 2009) pathways, this work also demonstrated the involvement of loss of the tumor suppressors in UV-induced melanoma formation. More relevant to melanoma-associated genetic abnormalities, Kannan *et al.* (2003) evaluated the effect of UV exposure on active Ras and p16- or p19-deficient mice. The results from this study showed UV treatment accelerated melanoma formation in active Ras and p19-deficient mice, indicating the cooperation between UV exposure and genetic alteration in melanoma formation. In contrast, this UV-induced acceleration of melanoma formation was not observed in the active Ras and p16-deficient mice. This finding indicates that the p53 pathway plays a more critical role in suppressing UV-induced melanoma formation *in vivo* than the Rb pathway.

To evaluate the functional cooperation between PTEN and p16/p19, a dual inactivation of which was found in several types of human cancers, You *et al.* (2002) established a PTEN/INK4a double deficient mouse model. They found that deficiency of either PTEN or INK4a was not sufficient to induce melanoma in mice, and double deficiency of both tumor suppressor genes caused only low frequency of melanoma (7-10%). Although the contribution of an oncogene to melanoma tumorigenesis *in vivo* was not included in this study, they found that an introduction of oncogenic Ras ($H\text{-}ras^{G12V}$) increased the anchorage-independent colony formation of the MEFs isolated from the

PTEN/INK4a double deficient mice. This also supports that melanoma formation requires both oncogene activation and loss of tumor suppressers.

In the past decade, Cre recombinase-mediated conditional gene recombination has been developed as a powerful tool allowing the introduction of desired genetic alternations in a conditional manner. Combining the tissue-specific transgenic approach, Bosenberg *et. al* (2006) recently established a mouse strain in which the expression of Cre recombinase was inducible by 4-hydroxytamoxifen (OHT) specifically in melanocytes(designated *Tyr::CreER*^{T2}). Using this transgenic mouse strain, researchers can conveniently manipulate the genetic context specifically in melanocytes to evaluate the contribution of a molecular event in melanoma tumorigenesis. Most recently, Dankort *et al.* (2009b) demonstrated a great example of this approach by crossing the *Tyr::CreER*^{T2} mice with another strain of mice in which the mutant B-Raf^{V600E} expression was inducible to create an inducible B-Raf^{V600E} melanoma mouse model. Using this Dankort *et al.* found that, again, constitutive activation of B-Raf was sufficient to develop benign melanocytic hyperplasia, but was not sufficient for melanoma formation. Similar to the finding by Chin *et al.* (1997) discussed earlier in this section, Dankort *et al.* concluded that oncogenic B-Raf must cooperate with a loss of tumor suppressor, PTEN in this example, to induce melanoma formation and lung metastasis. In addition, using this melanoma mouse model they demonstrated the efficacy of kinase pathway inhibitors for melanoma prevention and treatment. This work not only demonstrated the efficacy of kinase pathway inhibitors in a non-xenograft melanoma

animal model, but also provided an example of how a melanoma mouse model may be used to test therapeutic agents.

Collectively, these studies using melanoma mouse models indicate that both activation of oncogenes and loss of tumor suppressors are required for melanoma formation. More importantly, these studies provide a molecular mechanism of melanoma progression. Acquiring oncogene activation seems to be the earliest event. This is believed to be the cause of hyperplastic lesions as most benign nevi have Ras or B-Raf oncogenic mutations (Pollock *et al.*, 2003), and loss of tumor suppressors is not frequently found in dysplastic nevi (Cowan *et al.*, 1988; Hussussian *et al.*, 1994). According to the Clark model, most benign nevi at step 1 follow a programmed differentiation pathway and disappear. Supporting this, previous studies have suggested that oncogene acquisition is not sufficient for tumor formation, but instead, induces cell senescence (Michaloglou *et al.*, 2005; Braig & Schmitt, 2006). This also explains why most benign nevi have Ras/Raf mutations but do not progress to malignant melanoma. As shown by several melanoma mouse models discussed above, oncogene activations need to cooperate with loss of tumor suppressors to initiate melanoma. This molecular mechanism of melanoma progression is in consistent with the Knudson two-hit theory (Knudson, 1971).

1.5. Discussion

The Ras-Raf-MEK-ERK signaling pathway plays a critical role in regulating cell cycle progression, cell proliferation, and survival. Deregulation of the pathway activity may cause diseases, including cancers. Somatic mutations of Ras and B-Raf are found in

several types of human cancers at a high frequency particularly in melanomas. Using cell-based *in vitro* studies as well as *in vivo* mouse models, numerous research groups have demonstrated the critical role of this oncogenic signaling as well as other tumor suppressing pathways in melanoma tumorigenesis and survival.

Considerable effort has been made to develop therapeutic agents for treating cancers. Among these potential therapeutic agents, small-molecule inhibitors targeting MEK1 and MEK2 have shown promising anti-cancer effects in laboratories and pre-clinical studies. However, none of them has demonstrated clinical efficacy in cancer patients and proved as anti-cancer drugs. This indicates that our understating of the roles of MEK signaling pathways in cancers is incomplete.

MEK1 and MEK2 are generally thought to be functionally redundant for the following reasons. First, MEK1 and MEK2 share greater than 85% homology in amino acid sequences, and almost identical crystal structures (Ohren *et al.*, 2004). Second, both MEK1 and MEK2 phosphorylate ERK1 and ERK2, and ERK1 and ERK2 are the only known substrates of MEK1 and MEK2. Regardless the high structural and biochemical similarities of MEK1 and MEK2, however, a handful of studies have suggested that these two protein isoforms may have non-overlapping biological functions (Giroux *et al.*, 1999; Belanger *et al.*, 2003). A better understanding of the difference between MEK1 and MEK2 as well as their distinct biological functions may help developing more efficient anti-cancer drugs. For this purpose, using two complementary approaches I evaluated the necessity and sufficiency of MEK1 and MEK2 signaling pathways for melanoma cell

proliferation. This research provides insights into the complexity of the MEK signaling pathway. The results are presented in the following chapters.

1.6. Tables and figures

Table I. Small-molecule IC_{50} values

Compound	IC_{50} (μM)	
	MEK activity (measured by *in vitro* assays)[a]	Cellular events (measured by cell-based assays)[b]
PD 098059	**2 – 50 μM** Ref: (Alessi *et al.*, 1995; Dudley *et al.*, 1995; Favata *et al.*, 1998; Davies *et al.*, 2000; Ahn *et al.*, 2001)	**7 μM** Ref: (Dudley *et al.*, 1995)
U0126	**0.058 – 13 μM** Ref: (Favata *et al.*, 1998; Davies *et al.*, 2000; Ahn *et al.*, 2001)	**0.1 μM** Ref: (Favata *et al.*, 1998)
PD 184352	**0.017 – 0.3 μM** Ref: (Sebolt-Leopold *et al.*, 1999; Davies *et al.*, 2000; Warmus *et al.*, 2008)	**0.024 – 1 μM** Ref: (Sebolt-Leopold *et al.*, 1999; Solit *et al.*, 2006)
PD 0325901	**0.001 μM** Ref: (Kohno & Pouyssegur, 2006)	**0.001 – 0.00043 μM** Ref: (Kohno & Pouyssegur, 2006; Solit *et al.*, 2006)
ARRY-142886	**0.014 μM** Ref: (Yeh *et al.*, 2007)	**0.03 – 0.473 μM** Ref: (Yeh *et al.*, 2007; Friday *et al.*, 2008)

[a] *In vitro* kinase assays were performed by using purified MEK1 or MEK2. Measurements for MEK activity included phosphotransfer from [γ-^{32}P]ATP to ERK and western blot using antibodies against phospho-ERK.

[b] Cellular events included cell proliferation (measured by cell proliferation assays), DNA synthesis (measured by thymidine incorporation assay), and anchorage-independent growth (measured by soft agar assay).

Table II. Alignment of MEK/MKK amino acid sequences flanking the LF cleavage sites.

LF substrates	Amino acid sequences[a]															
Substrate positions (P)[b]:	8	7	6	5	4	3	2	1		1′	2′	3′	4′	5′	6′	7′	8′
MEK1	M	**P**	K	K	K	P	T	$P^{(8)}$	/	**I**	Q	L	N	P	A	P	D
MEK2	A	**R**	R	K	**P**	V	L	$P^{(10)}$	/	**A**	L	T	I	N	P	T	I
MKK3b	S	**K**	R	K	K	D	L	$R^{(26)}$	/	**I**	S	C	M	S	K	P	P
MKK4(K^{45}-L^{46})	Q	G	**K**	R	**K**	A	L	$K^{(45)}$	/	**L**	N	F	A	N	P	P	F
MKK4(R^{58}-F^{59})	P	**P**	F	K	S	T	A	$R^{(58)}$	/	**F**	T	L	N	P	N	P	T
MKK6	K	K	R	N	**P**	G	L	$K^{(14)}$	/	**I**	P	K	E	A	F	E	Q
MKK7(Q^{44}-L^{45})	Q	**R**	**P**	**R**	**P**	T	L	$Q^{(44)}$	/	**L**	P	L	A	N	D	G	G
MKK7(Q^{76}-L^{77})	A	**R**	**P**	R	H	M	L	$G^{(76)}$	/	**L**	P	S	T	L	F	T	P
Consensus sequence		(**B** / **P**)$_{3-4}$				X	X	X	/	**Al**							

[a] Amino acid sequences shown in single-letter codes are aligned to the position where LF cleaves (slash). Aliphatic residues (Al) at the protease cleavage position 1' (bold) are fully conserved in all the LF cleavage sites. The basic (B) or proline residues prior to the cleavage sites are shaded. (X), variable residues.

[b] The substrate positions (P1-P8 and P1′-P8′) are assigned based on the system used by Schechter and Berger (Schechter & Berger, 1967).

Table III. The Clark model of melanoma progression.

Clark model steps	Descriptions
1. Melanocytic nevus	Commonly acquired melanocytic nevi and structurally normal melanocytes (benign lesions).
2. Melanocytic hyperplasia	Melanocytic nevi with persistent but limited lentiginous melanocytic hyperplasia (aberrant differentiation).
3. Melanocytic dysplasia	Melanocytic nevi with persistent lentiginous melanocytic hyperplasia and random cytologic atypia (aberrant differentiation and appearance of cells with nuclear atypia).
4. Radial growth phase of primary melanoma	Primary cancerous lesion without competence for metastasis.
5. Vertical growth phase of primary melanoma	Primary cancerous lesion with competence for metastasis.
6. Metastatic melanoma	Metastatic cancer

Figure 1. Schematic illustration of the Raf-MEK-ERK signaling pathway.

Ras-mediated Raf activation involves a complex series of events, including protein recruitment to the cell membrane and phosphorylation at numerous residues [reviewed by Chong *et al.* (2003)]. Active Raf then activates MEK by phosphorylating the two conserved serine residues in the activation loop. Active MEK then in turn activates ERK by phosphorylating the threonine and tyrosine residues in the conserved T-E-Y motif. After its activation, ERK phosphorylates and activates downstream effectors that regulate a variety of cellular events, including cell cycle progression and cell proliferation at the transcriptional and posttranslational levels. The circled P symbols denote phosphate groups added on the critical serine residues and threonine/tyrosine residues of MEK and ERK, respectively.

Figure 1. Schematic illustration of the Raf-MEK-ERK signaling pathway.

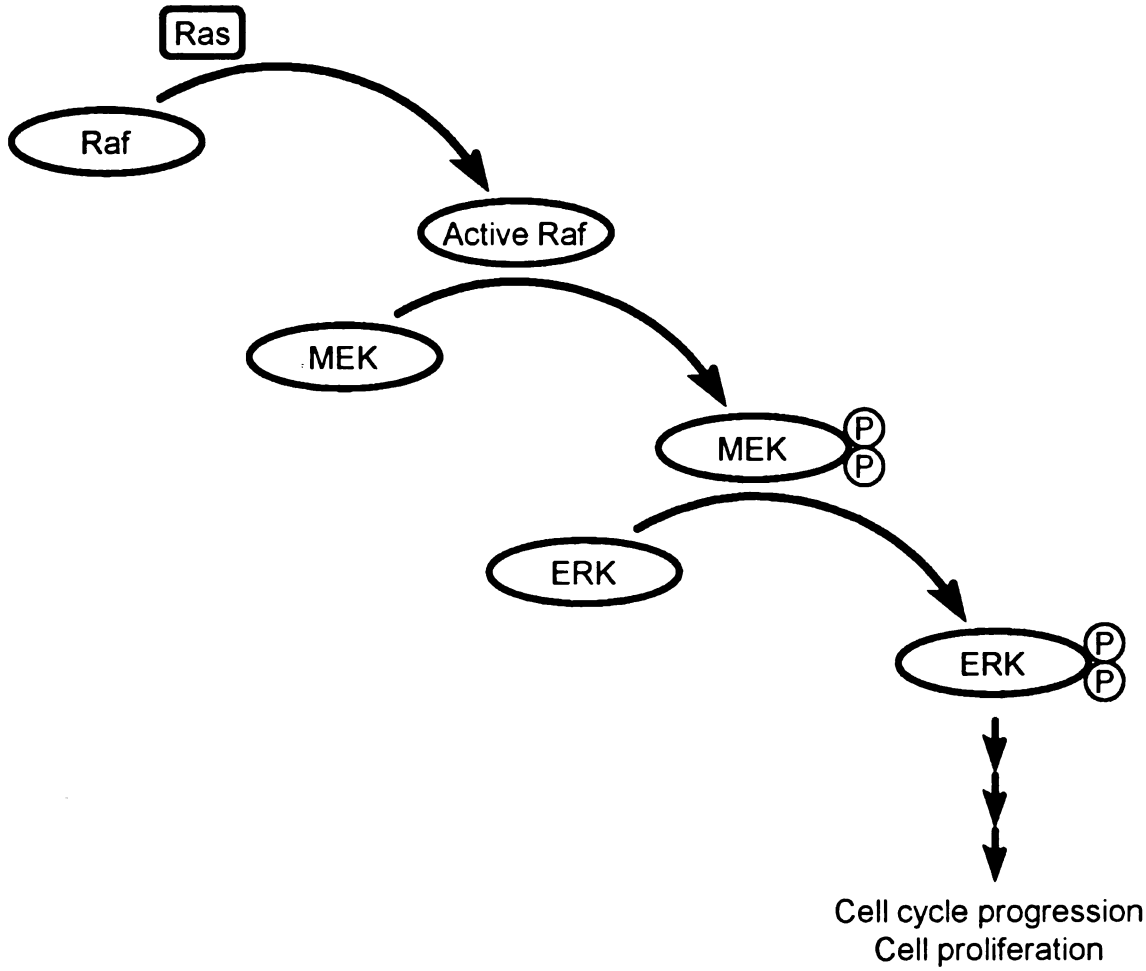

Figure 2. Structures of MEK inhibitors.

(*a*). PD 098015. (*b*). U0126. (*c*). PD 184352. (*d*). PD 0325901. (*e*). PD 318088. (*f*). PD 334581. (*g*). ARRY-142886. (*e-g*). The A and B rings of the diaryl amines of PD 184352 and its derivatives are denoted.

Figure 2. Structures of MEK inhibitors.

a.

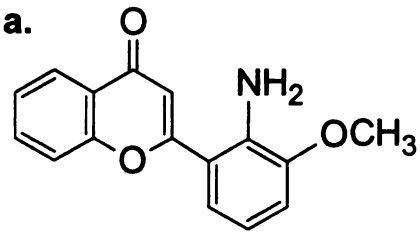

PD 098059

b.

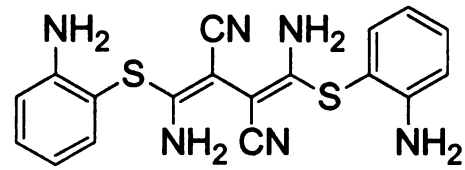

U0126

c.

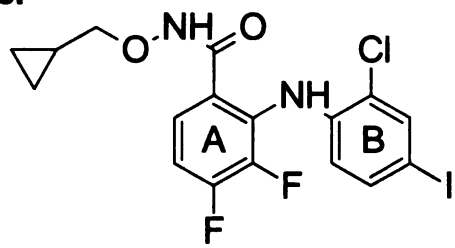

PD 184352

d.

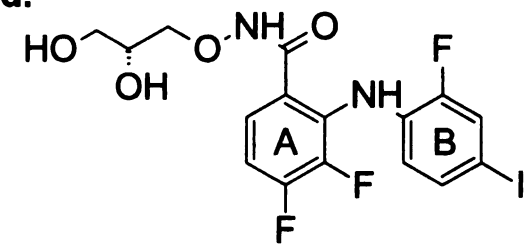

PD 0325901

e.

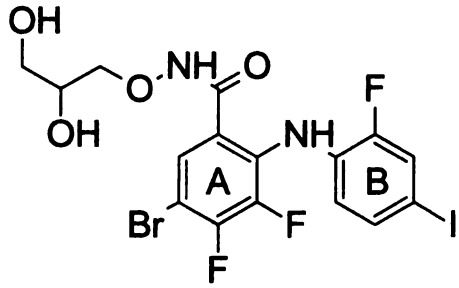

PD 318088

f.

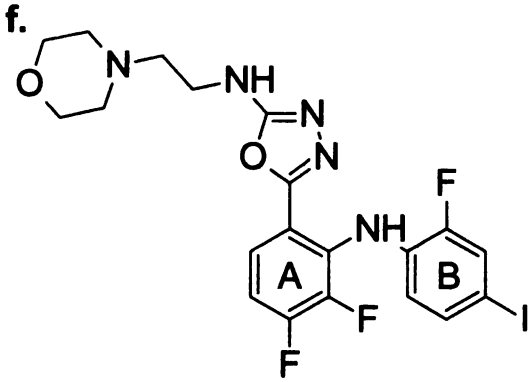

PD 334581

g.

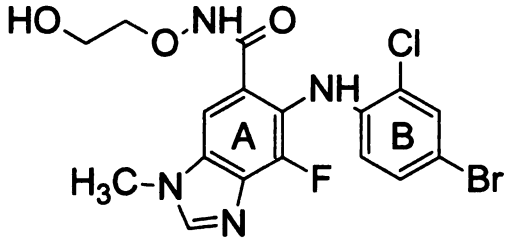

ARRY-142886

Figure 3. Effect of PD 184352 on MEK activation in cells.

Human melanoma SK-MEL-28 cells were cultured as described in the Materials and methods section of Chapter II (page 77). Cells were treated with PD 184352 at the concentrations indicated for 24h. Total cell lysates [prepared as described in the Materials and methods section of Chapter II (page 79)] were subjected to immunoblotting probed with antibodies against phospho-MEK1/2, phospho-ERK1/2, total ERK1/2, and GAPDH.

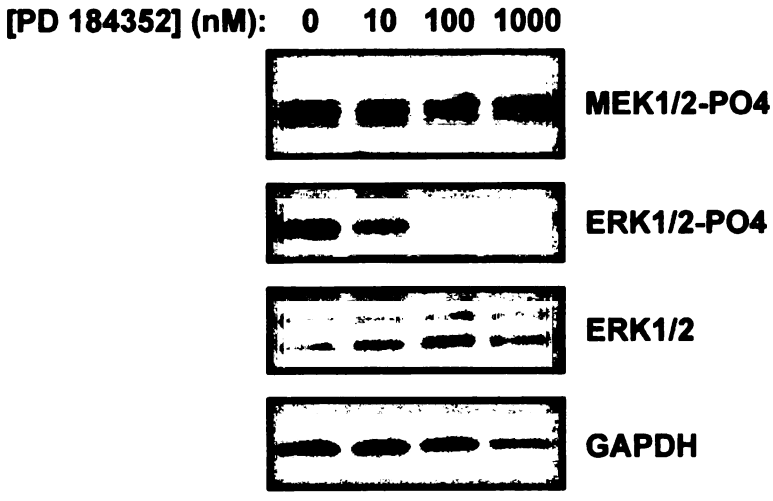

Chapter II. Cleavage-resistant MEK proteins; a novel experimental model to establish MEK sufficiency

1.1. Introduction

In order to determine the sufficiency of a MEK/MKK signaling pathway for a cellular function, the experimental system used will have to inhibit the pathways of multiple MEK/MKK members, but leave only one active. It is not expected to be efficiently achievable by transfecting several interference RNA molecules into cultured cells to target multiple protein molecules. In this chapter, the development of a novel experimental model achieving this challenging task will be presented. In this system, multiple endogenous MEK/MKK proteins and the downstream signaling pathways are inhibited by treating cells with LeTx, a bacterial toxin with MEK/MKK-specific proteolytic activity (see Chapter I section 1.3.3.1 for the introduction). Simultaneously, a mutant MEK/MKK protein that is resistant to LF-mediated cleavage is expressed in cells to preserve the specific MEK/MKK signaling pathway. This achieves a special cellular context in which only one MEK/MKK signaling pathway is present. If a MEK/MKK pathway is sufficient for a cellular function, the cleavage-resistant form of the corresponding MEK/MKK should rescue this cellular function when the cells are treated with LeTx.

1.2. Results

1.2.1. Point mutations at the P1′ site render MEK resistant to LF-mediated cleavage

An alignment of all the MEK and MKK amino acid sequences (Table II) revealed a consensus sequence for LF cleavage: $(B/P)_{3-4}X_3/Al$, where B represents basic residues, P represents proline, X represents variable residues, and Al represents aliphatic residues. The aliphatic residue at the P1′ position is fully conserved in all the MEK/MKK proteins, and has been shown to be critical for the cleavage by LF (Park *et al.*, 2002; Chopra *et al.*, 2003). Therefore, to make MEK resistant to LF-mediated cleavage, I introduced an aliphatic-to-aspartic acid mutation in this position of human MEK and MKK proteins. These cleavage-resistant (cr) mutant proteins are named MEKcr or MKKcr in this dissertation. For the subsequent study, a V5 tag was fused to the amino termini of wild-type and the cleavage resistant mutants of MEK/MKK proteins. This NH_2-terminal V5 fusion was included to examine the cleavage of the proteins by LF at the NH_2-termini (explained below).

To confirm the cleavage resistance of MEKcr, an in-cell LF cleavage assay was developed. In this assay, wild-type V5-MEK or V5-MEKcr proteins were transiently expressed in CHO K1 cells which were then treated with PA alone (1 μg/ml PA as a control) or LeTx (1 μg/ml PA and 0.1 μg/ml LF) for 12h. As transient transfection of plasmid DNA can efficiently over-express exogenous proteins in CKO K1 cells, MEK cleavage by LF may not be clearly observed if an excessive amount of V5-MEK is produced during LF cleavage. To overcome this, cells were co-treated with 10 μg/ml

cycloheximide to block *de novo* protein synthesis during PA or LeTx treatment. To ensure successful internalization of LF and in-cell proteolytic activity of LeTx, cleavage of endogenous MEK1 was first examined by immunoblotting probed with antibodies that specifically recognize the amino terminus of MEK1 (LeTx causes loss of epitope) or the carboxyl-terminus of MEK1 (LeTx causes mobility shift). As shown in Figure 4A, LeTx treatment resulted in a loss of the NH_2-terminal epitope (Figure 4A, second panel) and an increase in the electrophoretic mobility of endogenous MEK1 (Figure 4A, third panel) in control cells as well as in cells transfected with V5-*lacZ* control plasmid. This result indicates LF-mediated MEK cleavage occurs in CHO K1 cells. Under the same conditions, LF-mediated proteolysis resulted in a loss of NH_2-terminal V5 epitope only in CHO K1 cells expressing wild-type V5-MEK1 or V5-MEK2 but not in cells expressing V5-MEK1cr or V5-MEK2cr (Figure 4B and C, top panels). To exclude the possibility that the loss of V5 epitope of wild-type V5-MEK1 and V5-MEK2 was a result of failure in expressing the exogenous proteins, and to further confirm the cleavage of wilt-type V5-MEK proteins, antibodies recognizing carboxyl termini of MEK1 or MEK2 were used to detect the electrophoretic mobility shift of cleaved V5-MEK1 and V5-MEK2. As shown in the second panels of Figure 4B and C, bands with slightly higher electrophoretic mobility were detected by immunoblotting with antibodies recognizing carboxyl-terminus of MEK1 or MEK2 in cells transfected with wild-type V5-MEK1 or V5-MEK2, but not in cells transfected with V5-MEK1cr or V5-MEK2cr. These results demonstrate that V5-MEK1cr and V5-MEK2cr were resistant to LF-mediated proteolysis.

In this experiment, a substantial increase of non-tagged MEK expression along with V5-MEK transfection was noticed (Figure 4B middle panel, compare none-

transfected cells with V5-MEK1 transfected cells). This was caused by internal translation from the original translation initiation codon of the MEK sequence cloned in the V5-expression vector. This was evidenced by the following observation. The original translation initiation codons that were inserted together with MEK sequences into the V5 expression vector were removed from the plasmid by doing a site-directed mutagenesis. The modified expression vectors were then transfected into CHO K1 cells. After this manipulation, the increase of non-tagged MEK expression was no longer observed (Figure 5). These experiments demonstrated that the increased non-tag MEK level after V5-MEK plasmid transfection was due to exogenous expression and not an up-regulation of the endogenous MEK. This dual translation pattern was also observed in V5-MEK-transfected SK-MEK-28 stable cell lines (will be presented in Chapter III).

1.2.2. The cleavage-resistant mutation does not impair MEK activity.

Cleavage by LF removes an amino terminal docking domain that is required for interaction with MAPK (Tanoue *et al.*, 2000; Chopra *et al.*, 2003; Bardwell *et al.*, 2004). To confirm that neither the addition of the V5 tag nor the introduction of the LF cleavage-resistant mutation interferes with MEK's ability to interact with and phosphorylate ERK, the activity of V5-MEK1cr and V5-MEK2cr was examined. To do this, clonal lines of human melanoma SK-MEL-28 cells stably expressing V5-MEK1cr or V5-MEK2cr, or their wild-type counterparts were established. Similar to most melanomas, SK-MEL-28 cells harbor the B-Raf_V600E mutation (Davies *et al.*, 2002), which constitutively phosphorylates and activates MEK1 and MEK2. Therefore, this cell line allows a convenient examination of the status of cellular MEK1 and MEK2. When

an antibody that only recognized activated MEK1 and MEK2 was used in the immunoblotting, the activation status of both V5-MEK1cr and V5-MEK2cr were found to be comparable to that of their wild-type counterparts (Figure 6A). This indicates that (1) neither the NH_2-terminal V5 fusion nor the CR mutation impairs MEK activation and (2) V5-MEK1cr and V5-MEK2cr are activated in SK-MEL-28 cells.

To further examine the ability of V5-MEK1cr and V5-MEK2cr to phosphorylate their only known substrate, ERK, immunoprecipitation-kinase (IP-kinase) assays were performed. To do this, V5-MEK1cr and V5-MEK2cr were immunoprecipitated from SK-MEL-28 cells and used as the kinase source for ERK in the kinase assay. Since saturating the kinase in a kinase assay may result in a false positivity, the optimum amount of wild-type V5-MEK immunoprecipitates in this IP-kinase assay was determined first. A fixed amount of recombinant ERK2 (400 ng) was used as the substrate and mixed with a decreasing amount of the V5-immunoprecipitates in the presence of active B-Raf to determine the minimum amount of the V5-immunoprecipitaes required for the kinase reaction. As shown in Figure 6B, a minimum of 5 μl of V5-MEK1 or V5-MEK2 immunoprecipitates was required to fully phosphorylate 400 ng of ERK2 in the kinase reaction. Based on this optimization experiment, a full set of the IP-kinase assays, in which the V5-MEK immunoprecipitates were mixed with or without active B-Raf and recombinant ERK2, was performed based on the optimized condition to test the kinase activity of V5-MEK1cr and V5-MEK2cr. As shown in Figure 6C, after considering the amount of the V5 immunoprecipitates used for each assay (Figure 6C, lower panel), V5-MEK1cr and V5-MEK2cr were as capable as their wild-type counterparts in phosphorylating ERK2. These results indicate that

neither the addition of the V5 tag nor the introduction of the cleavage-resistant mutation alters the ability of MEK to interact with and phosphorylate ERK.

1.2.3. Point mutations at the P1' site render other MKK members resistant to LF-mediated cleavage

A similar strategy was used to generate cleavage-resistant forms of MKK3, MKK4, MKK6 and MKK7. As expected, the aliphatic-to-aspartic mutation at the P1' position rendered MKK3 and MKK6 resistant to LF cleavage (Figure 7). As MKK4 and MKK7 were previously reported to harbor two LF cleavage sites (Vitale *et al.*, 2000), two cleavage-resistant mutants with the aliphatic-to-aspartic mutation introduced to one of the cleavage sites were generated for each of MKK4 and MKK7: V5-MKK4cr_46 and V5-MKK4cr_59 for MKK4, and V5-MKK7cr_45 and V5-MKK7cr_77 for MKK7. LF completely cleaved wild-type V5-MKK4 in CHO K1 cells (Figure 8A). Unexpectedly, the aliphatic-to-aspartic mutation introduced to Leu^{46} of MKK4 was sufficient to make MKK4 resistant to the cleavage, but the same mutation introduced to Phe^{59} was not. On the other hand, V5-MKK7cr_45 and V5-MKK7cr_77 were both resistant to the cleavage in CHO K1 cells (Figure 8B). However, under the same condition, a convincing cleavage of wild-type MKK7 was not detected (Figure 8B).

1.2.4. MKK4 cleavage in mammalian cells

Further experiments were performed to determine why V5-MKK4cr_46 was not cleaved by LF in CHO K1 cells. As shown in Figure 8A, LeTx treatment of CHO-K1 cells expressing wild-type V5-MKK4 resulted in a complete loss of the V5 epitope,

demonstrating the cleavage of MKK4 by LF. Since two LF cleavage sites were identified on MKK4, a mutant MKK4 with the cleavage-resistant mutation introduced at only one of the cleavage sites would be expected to be still cleaved by LF at the other cleavage site which remained unchanged. As expected, V5-MKK4cr_59 was still sensitive to LF-mediated proteolysis (Figure 8A). Presumably LF cleaved this mutant MKK4 at the Lys^{45}-Leu^{46} position. Unexpectedly, however, the aliphatic-to-aspartic mutation introduced to Leu^{46} of human MKK4 was sufficient to render MKK4 resistant to cleavage, even if the Phe^{59} residue was remained unchanged (Figure 8A). Two possibilities can explain this observation. First, LF cleaves MKK4 only at the Lys^{45}-Leu^{46} position but not at the Arg^{58}-Phe^{59} position (*i.e.*, Arg^{58}-Phe^{59} of MKK4 is not a real LF cleavage site). Alternatively, LF cleaves MKK4 at both positions in a processive manner (*i.e.*, cleavage at Arg^{58}-Phe^{59} requires a prior cleavage at Lys^{45}-Leu^{46}).

To test these two possibilities in an unambiguous way, wild-type human MKK4 fused with a V5 tag followed by a 6xHis tag at the carboxyl terminus was constructed (denoted as MKK4-V5-His6 in this dissertation). The carboxy-terminal fusion allowed more readily determining the molecular weight of the carboxyl terminus of MKK4 after LF cleavage. In addition, two MKK4-V5-His6 deletion mutants were constructed as molecular weight indicators: MKK4 with a deletion of amino acid residues 1-45 (denoted as MKK4_d45-V5-His6), and MKK4 with a deletion of amino acid residues 1-58 (denoted as MKK4_d58-V5-His6). The MKK4_d45-V5-His6 deletion mutant also allowed testing the second possibility that LF cleaves MKK4 at both sites in a processive

manner. The set of these proteins was then expressed in CHO K1 cells and in-cell cleavage assays were performed.

As shown in Figure 9, LeTx treatment on CHO K1 cells expressing wild-type MKK4-V5-His6 resulted in a complete loss of the V5 epitope, indicating MKK4 cleavage by LF. However, under the same conditions I could not detect the LF-cleaved carboxyl terminal fragment of MKK4 using an anti-V5 antibody (Figure 9, lane 2). An explanation for this is that after LF cleavage, the carboxyl terminus of MKK4 is degraded, as previously observed for MEK1 (Duesbery *et al.*, 1998) and MEK2. To test this, MG-132, a proteosome inhibitor, was included in the in-cell cleavage assay. As shown in Figure 9 (lane 4), MG-132 treatment rendered the LF-cleaved carboxyl terminus of MKK4 recognizable by V5 antibody in the immunoblotting, indicating that after LF cleavage MKK4 is degraded through a proteosome-dependent pathway.

The two MKK4 deletion mutants, MKK4_d45-V5-His6 and MKK4_d58-V5-His6, were distinguishable by the differential electrophoretic mobility in an SDS-PAGE gel (Figure 9, land 5-8 and lane 9-12). After LF cleavage, the carboxyl terminus of MKK4-V5-His6 (Figure 9, lane 4) had the same electrophoretic mobility as that of MKK4_d45-V5-His6 (Figure 9, land 5-8) but not MKK4_d58-V5-His6 (Figure 9, lane 9-12). This result demonstrates that wild-type MKK4 is cleaved by LF only at the Lys^{45}-Leu^{46} position but not the Arg^{58}-Phe^{59} position in cells. In addition, co-treatment of LeTx and MG-132 did not result in an electrophoretic mobility shift of the MKK4_d45-V5-His6 deletion mutant. This indicates that MKK4_d45-V5-His6 was not cleaved by LF and that the Arg^{58}-Phe^{59} position of MKK4 was not an LF cleavage site. Taken together, these

data show that MKK4 has only one LF cleavage site, the Lys^{45}-Leu^{46} position, as opposed to two LF cleavage sites as previously observed and reported by Vitale *et al.* (2000) in an *in vitro* assay.

1.2.5. MKK7 cleavage in mammalian cells

As shown in Figure 8B, LeTx treatment resulted in a subtle decrease of the NH_2-terminal V5 epitope of wild-type MKK7 (the second lane of the top panel in Figure 8B). One possible explanation for this is that a limited amount of LF could not cleave the excess of V5-MKK7 that was expressed in the transfected cells. To test this, a decreasing amount of the plasmid DNA encoding for wild-type V5-MKK7 was transfected into CHO K1 cells and the cleavability of MKK7 was tested in cells in the presence of cycloheximide. Under this condition, the expression level of wild-type V5-MKK7 was decreased proportionate with the decreasing amount of the plasmid DNA transfected (Figure 10, upper panel). However, LF was still not able to cleave wild-type MKK7 even when the expression of V5-MKK7 was decreased to a barely-detectable level. The uncleavability of wild-type V5-MKK7 in this experiment was not due to experimental failure as a complete cleavage of endogenous MEK1 by LF was readily detected in the same cell lysates (Figure 10, middle panel). This result indicates that MKK7 might not be an enzymatic substrate of LF in mammalian cells. To further test this, 293FT cells (a human embryonic kidney 293-derived cell line) were treated with LeTx for 24, 48, and 72 hours, and whole cell extracts were prepared for immunoblotting to examine MKK7 cleavage by LF. If LF cleaves MKK7 at Gln^{44}-Leu^{45} and Gln^{76}-Leu^{77} positions as

previously reported by Vitale *et al.* (2000), then a decrease of NH_2-terminal signal and an electrophoretic mobility shift of MKK7 should be detected following cleavage. As shown in Figure 11A, LeTx treatment did not result in a loss or a decrease of the immunoblotting signal of endogenous MKK7 in 293FT cells, even if the cells were treated with LeTx for 72h. In addition, an antibody recognizing the last 20 amino acid of MKK7 failed to detect an electrophoretic mobility shift of MKK7. This result clearly shows that MKK7 is not a preferred LF substrate in mammalian cells, and argues the MKK7 cleavage by LF observed by Vitale *et al.* (2000) may be an *in vitro* artifact.

1.3. Discussion

In this chapter, the design and the engineering of cleavage-resistant forms of MEK and MKK (MEKcr and MKKcr) were presented. This set of MEKcr were designed to be used as a tool to study the sufficiency of MEK1 and MEK2 signaling pathways for melanoma cell proliferation, which will be presented in Chapter III. Cleavage resistant forms of MEK/MKK proteins have been previously reported for MEK1 (Duesbery *et al.*, 1998), MKK3 (Park *et al.*, 2002), and MKK6 (Park *et al.*, 2002; Chopra *et al.*, 2003). Although the mutations were introduced at slightly different positions on each of MEK1 (P1), MKK3 (P1 and P1′), and MKK6 (P1 and P1′, or P1′ alone), all of these studies suggest that hydrophobicity and surface charge surrounding the LF cleavage position are critical for the cleavage. In this dissertation project, aliphatic-to-aspartic acid mutations were introduced only to the P1′ positions of MKK1-4, 6 and 7, and the produced MEKcr and MKKcr were all resistant to LF-mediated proteolysis. These results extend previous observation (Chopra *et al.*, 2003) showing that the aliphatic residue adjacent to the LF

cleavage site are critical for LF-mediated proteolysis.

When V5-MEK1cr and V5-MEK2cr were stably expressed in human melanoma SK-MEL-28 cells, which harbor B-Raf_V600E constitutive activation mutation, these cleavage-resistant MEK mutants were phosphorylated and activated in the cells (examined by immunoblotting with an antibody that specifically recognizes MEK1 and MEK2 with phosphate groups at the activation loops). These MEKcr proteins were phosphorylated to a comparable level as their wild-type counterparts, indicating that introducing the aliphatic-to-aspartic acid mutation to MEK1 and MEK2 does not alter their ability to be activated. Moreover, these V5-MEKcr proteins could be immunoprecipitated from SK-MEL-28 cells and used as kinase source in an *in vitro* kinase assay. These V5-MEKcr proteins were as capable as their wild-type counterparts in phosphorylating their substrate, ERK2, in the assay. Interestingly, immunoprecipitated V5-MEK and V5-MEKcr proteins were not able to phosphorylate ERK2 in the absence of active B-Raf, although they were activated in SK-MEL-28 cells. A few possibilities can explain this. First, during cell lysis and immunoprecipitation, these proteins may have been de-phosphorylated by phosphatases, the activity of which was not fully inhibited by phosphatase inhibitors added in the lysis buffer. Second, in SK-MEL-28 cells, the B-Raf_V600E may have only activated a small portion of V5-MEK, yet this was sufficient to be detected by the phospho-MEK1/2 antibody by immunoblotting. After immunoprecipitation, the vast majority of the immunoprecipitated V5-MEK may not have been activated by B-Raf_V600E and was not able to phosphorylate ERK2 in the kinase assay until after the addition of active B-Raf. Finally, it is also possible that active

V5-MEK may be sequestered in a protein complex that may mask the epitope for antibody recognition. As a result of this, only less active V5-MEK could be immunoprecipitated.

Vitale *et al.* (2000) reported that in addition to MEK1 and MEK2, most members in the MKK family were enzymatic substrates of LF with an exception of MEK5. For the most part the results repeated here support this observation. However, my data do not wholly support their findings. Both MKK4 and MKK7 were previously found to harbor two LF cleavage sites. The data presented above in this chapter show that in mammalian cells LF cleaves MKK4 only at the Lys^{45}-Leu^{46} position but not the Arg^{58}-Phe^{59} position, and that LF does not cleave MKK7 in cells. A comparison of the LF cleavage site consensus sequence [$(B/P)_{3-4}X_3/Al$] and the amino acid sequences of the two reported MKK4 cleavage sites shows that the amino acid sequence of the first LF cleavage site of MKK4, $QGKRKALK^{45}L^{46}$, matches the consensus LF cleavage site whereas the second site, $PPFKSTAR^{58}F^{59}$, does not (Table II in Chapter I, see page 45). This supports that Arg^{58}-Phe^{59} of MKK4 is not a real LF cleavage site in mammalian cells, and that the cleavage at the Arg^{58}-Phe^{59} of MKK4 observed by Vitale *et al.* was possibly an artifact resulted from the *in vitro* experimental system.

Since Vitale's initial report ten years ago, there have been no further reports of LF-mediated MKK7 cleavage published in the literature. The in-cell cleavage assays of

endogenous MKK7 by LF presented in this chapter were carried out in two different mammalian cell lines, Chinese hamster ovary cells (CHO K1) and human embryonic kidney 293-derived cells (293FT). The cleavability of either a low expression level of exogenous MKK7 or of endogenous MKK7 by LF was examined in these two mammalian cell lines, and no MKK7 cleavage was observed. The data strongly suggest that MKK7 is not a preferred LF substrate in mammalian cells. Moreover, on careful analysis of Vitale's initial report, it is not clear whether MKK7 is cleaved by LF *in vitro* [the MKK7 panel of Figure 4 in the report by Vitale *et al.* (2000)]. In their *in vitro* cleavage experiments, LF resulted in a noticeable decrease of GST::MKK3, 4, and 6 Coomassie Blue staining signals. However, LF did not result in any decrease of the GST::MKK7 signal. Both reported MKK7 cleavage sites were identified by isolating two very weak Coomassie Blue bands with higher electrophoretic mobility in the gel. These two truncated MKK7 may alternatively be explained by protein degradation, which is commonly observed in GST-fusion protein purification. Collectively, the results presented in this chapter argue against the cleavability of MKK7 by LF.

Unlike MKK4, the amino acid sequences of both cleavage sites of MKK7 match the consensus sequence of LF cleavage site perfectly (Table II in Chapter I, see page 45). If the amino acid sequences match the LF cleavage site consensus sequence and MKK7 also contains the conserved the LF-interacting region (Chopra *et al.*, 2003), then why is MKK7 not cleaved by LF in cells? Perhaps the sequence of the LF cleavage site gives an answer to this question. The consensus sequence of LF cleavage site is generalized based on an alignment of all the reported MEK/MKK cleavage sites, including the two of

MKK7. If MKK7 is not an LF substrate, the two reported cleavage sites of MKK7 should not be included in the alignment, and the consensus of LF cleavage site may be different. In other words, if the two reported LF cleavage sites of MKK7 are excluded from Table II, then a better consensus sequence of LF cleavage site would be $(B)_3X_{2-4}(B/P)_1/Al$, where B represents basic residues, X represents variable residues, P represents proline, and Al represents aliphatic residues. In this new consensus sequence, a proline residue or a basic residue at the P1 position is conserved in MEK1, MEK2, MKK3, 4, and 6, but not in MKK7. Therefore, it is very possible that the amino acid residue at the P1 position of MEK/MKK is also critical for LF cleavage. Two previous studies support this possibility. First, Duesbery *et al.* (1998) have demonstrated a mutant MEK1 with an alanine substitution for this critical proline residue was resistant to LF cleavage. Second, the critical role of the amino acid at P1 position of MEK/MKK for LF cleavage is supported by a crystal structure study of LF. Pannifer *et al.* (2001) have shown that the side chain of proline or arginine at the P1 position of MEK/MKK sits in the S1 substrate-binding pocket of LF to generate a productive cleavage complex.

This chapter describes the development of a novel experimental system that allows evaluating sufficiency of an individual MEK/MKK signaling pathway when multiple other parallel family pathways are inhibited by LeTx. This system was then utilized and coupled with isoform-specific MEK knockdown to determine both sufficiency and necessity of MEK1 and MEK2 signaling pathways for melanoma cell proliferation. This will be presented in Chapter III.

1.4. Figures

Figure 4. Resistance of V5-MEKcr to LF-mediated proteolysis.

(A) Non-transfected (None), mock-transfected (Mock), and V5-*lac*Z-transfected CHO K1 cells, as well as cells transfected with **(B)** wild-type V5-MEK1 or V5-MEK1cr, or **(C)** wild-type V5-MEK2 or V5-MEK2cr, were treated with PA alone control (PA) or LeTx (LT) in the presence of cycloheximide for 12 h as described in Materials and methods. Total cell lysates were then harvested and subjected to immunoblotting probed with the antibodies indicated on the right of each panel. V5 antibody (V5) and an antibody against NH_2-terminus of MEK1 (MEK1 (NH_2)) were used to detect loss of NH_2-terminal epitopes following LF-mediated proteolysis. Antibodies against the carboxyl terminus of MEK1 (MEK1 (COOH)) and MEK2 (MEK2 (COOH)) were used to detect cleaved MEK1 and MEK2, respectively, with increasing electrophoretic mobility. Antibodies against α-tubulin and β-tubulin were used as loading controls.

Figure 4. Resistance of V5-MEKcr to LF-mediated proteolysis.

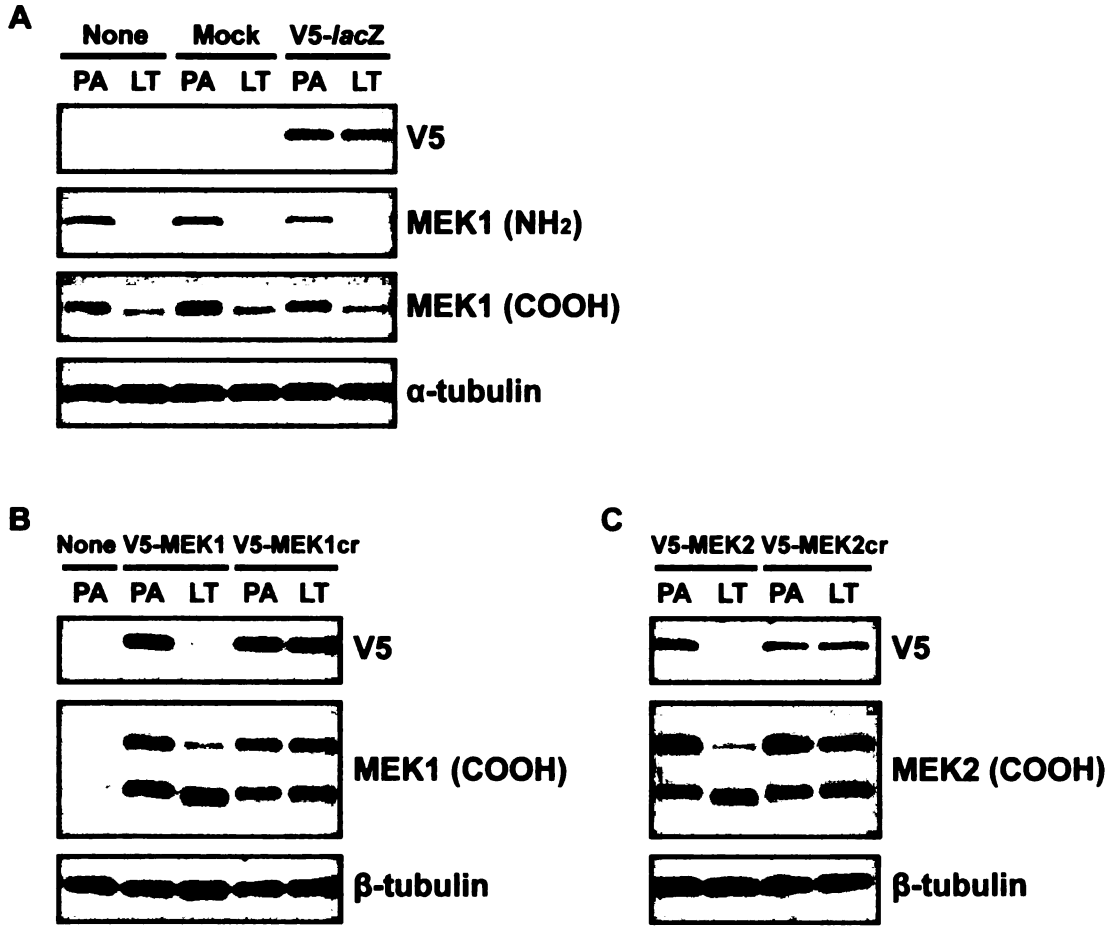

Figure 5. Dual translation of V5-MEK expression vectors.

CHO K1 cells were transfected with plasmids encoding for V5-MEK1 or V5-MEK1cr, or the modified plasmids in which the original translation initiation codons of MEK sequences were removed (V5-MEK1_dATG and V5-MEK1cr_dATG). Non-transfected cells (None) or cells transfected with V5-*lacZ* were used as controls. After transfection, cells were treated with PA alone (PA) or LeTx (LT) in the presence of cycloheximide for 12 h as described in Materials and methods. Total cell lysates were then harvested and subjected to immunoblotting probed with antibodies against NH_2-terminus of MEK1 (top panel) and GAPDH (bottom panel). V5-MEK1 and non-tagged MEK1 are indicated. Lane numbers are labeled at the bottom of the blots.

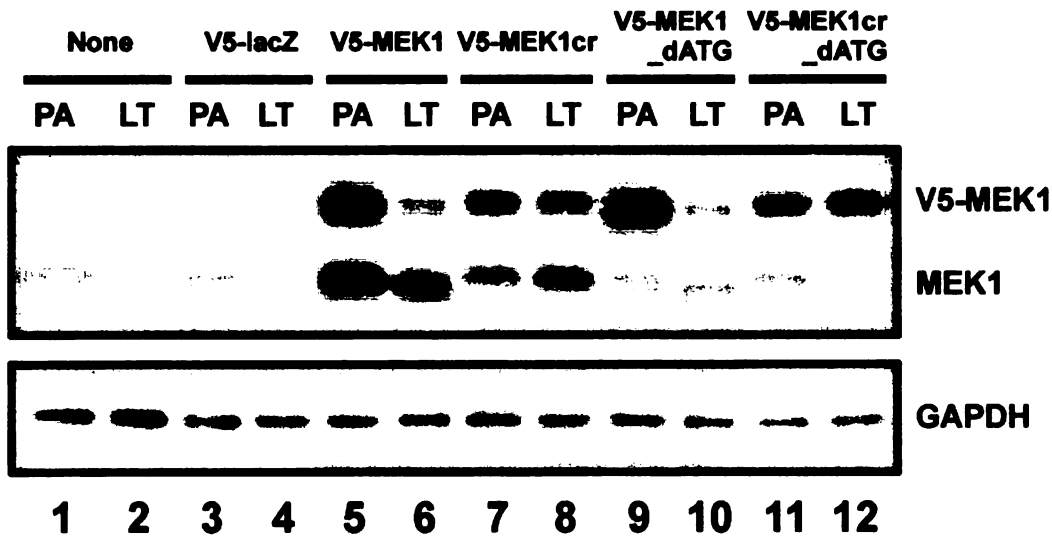

Figure 6. Activity of V5-MEKcr.

(A) Phosphorylation and activation of V5-MEKcr in cells. SK-MEL-28 cells stably expressing V5-MEK or V5-MEKcr were treated with PA alone (PA) or LeTx (LT) for 24 h. Whole cell lysates were prepared and immunoblotted with anti-phosphoMEK1/2 antibody to examined the activation status of cellular V5-MEK1cr and V5-MEK2cr (upper panel), or with anti-GAPDH antibody as a loading control (lower panel). **(B)** Optimization of V5-MEK IP-kinase assay. V5-*lacZ*, V5-MEK1, V5-MEK1cr, V5-MEK2, and V5-MEK2cr were immunoprecipitated from SK-MEL-28 cells as described in Material and methods. A decreasing amount (5, 0.5, and 0.05 μl) of the V5-MEK immunoprecipitates was added into *in vitro* kinase assay reactions which were then carried out as described in Material and methods. **(C)** Kinase activity of V5-MEKcr. Anti-V5 immunoprecipitates were prepared from SK-MEL-28 cells as described in Material and methods, and then used for *in vitro* kinase assays (top panel) in the presence or absence of active B-Raf and/or recombinant ERK2. Equal amounts of V5 immunoprecipitates were subjected to V5 immunoblotting (bottom panel) as the V5-MEK input control.

Figure 6. Activity of V5-MEKcr.

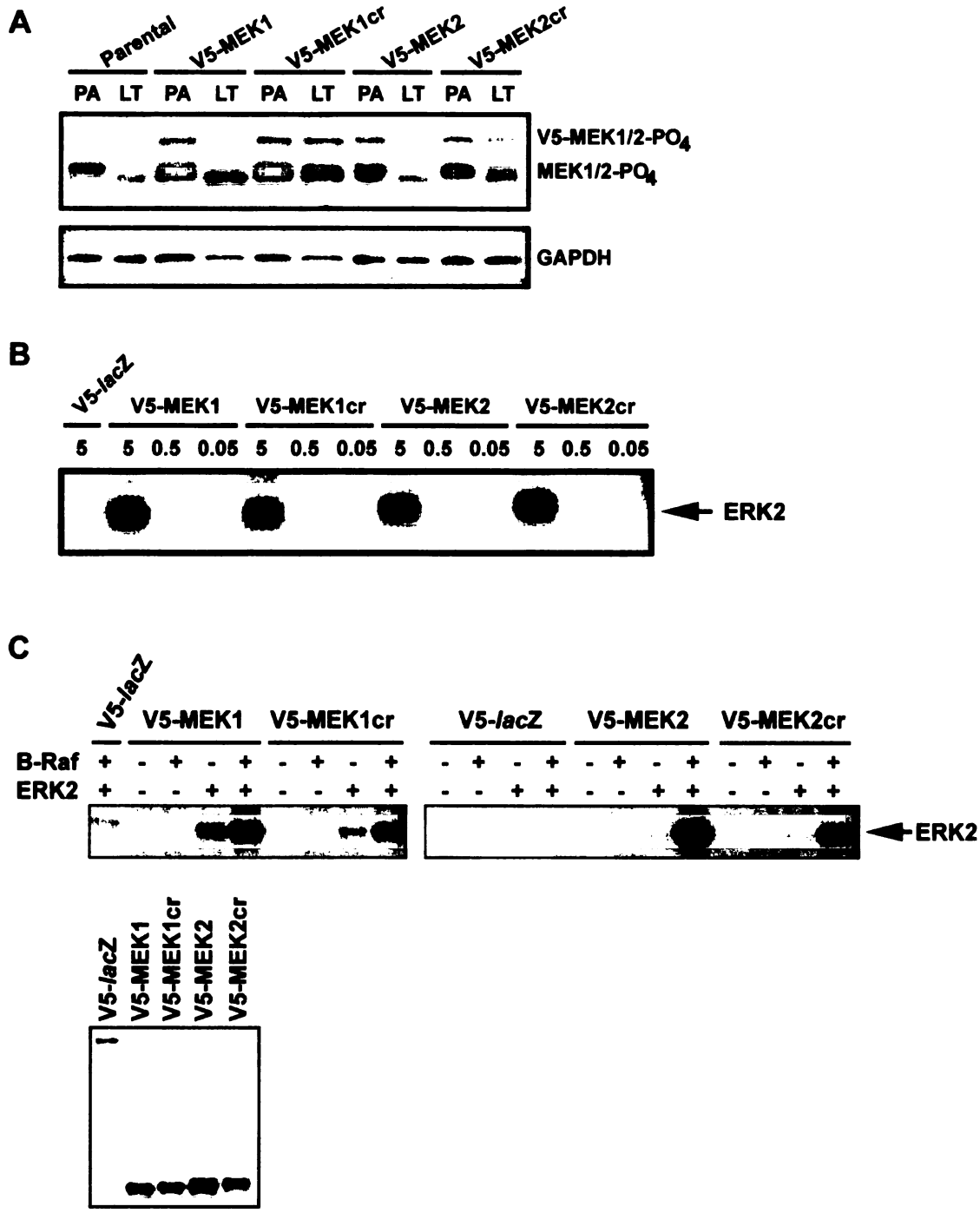

Figure 7. Resistance of MKK3cr and MKK6cr to LF-mediated proteolysis.

(**A**) Human melanoma SK-MEL-28 cells stably expressing V5-MKK3 or V5-MKK3cr were treated with LeTx in an LF concentration-dependent manner (indicated) for 24h. Total cell lysates were harvested and subjected to immunoblotting probed with antibodies against V5 epitope (top panel), carboxyl terminal of MKK3 (middle panel), and α-tubulin (bottom panel). (**B**) CHO K1 cells were transfected with V5-MKK6, or V5-MKK6cr. In-cell cleavage assays were performed as described in Materials and methods. Total cell lysates were then collected and immunoblotted with antibodies against V5 epitope (top panel), carboxyl terminus of MKK6 (middle panel) and α-tubulin (bottom panel).

Figure 7. Resistance of MKK3cr and MKK6cr to LF-mediated proteolysis.

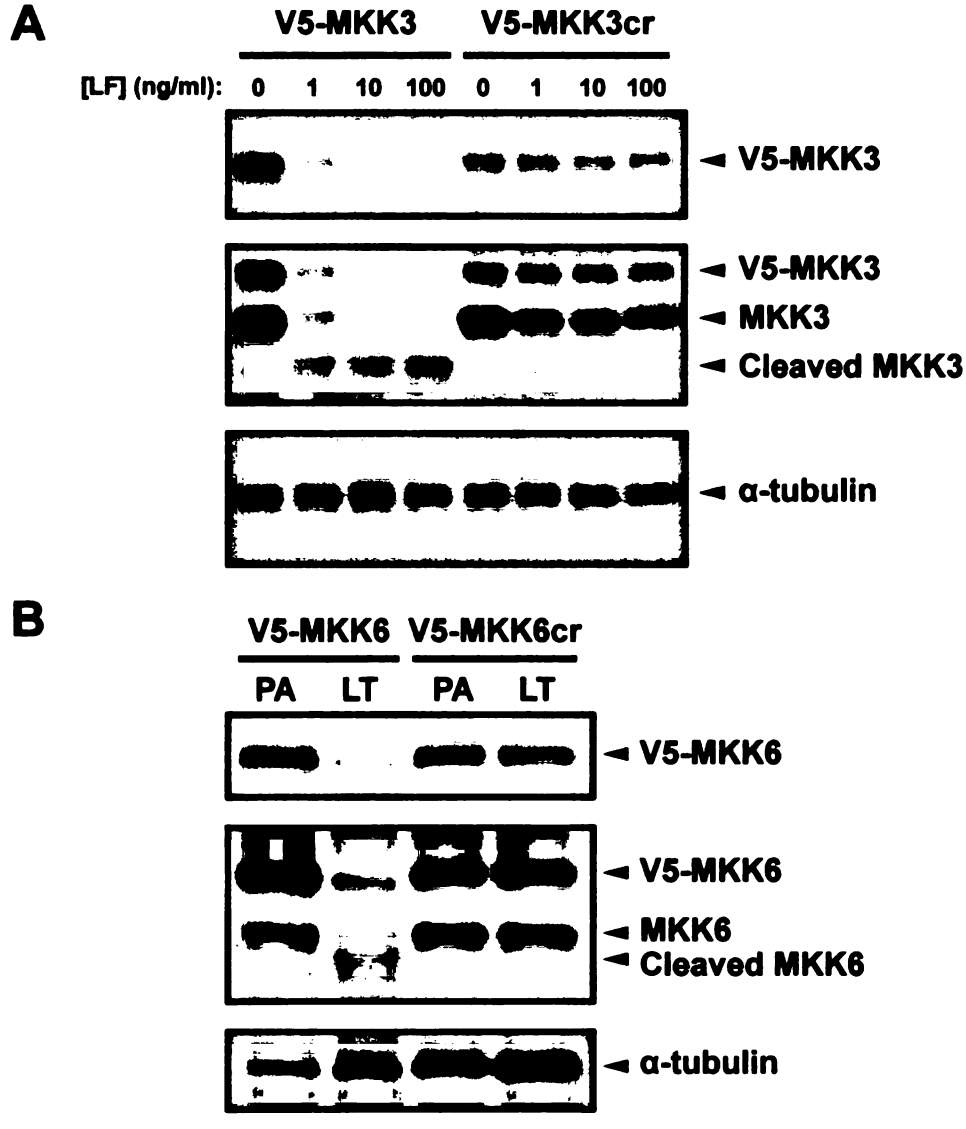

Figure 8. Resistance of MKK4cr and MKK7cr to LF-mediated proteolysis.

CHO K1 cells were transiently transfected with (**A**) V5-MKK4, V5-MKK4cr_46, or V5-MKK4cr_59, or (**B**) V5-MKK7, V5-MKK7cr_45, or V5-MKK7cr_77. In-cell cleavage assays were performed as described in Materials and methods. Total cell lysates were then collected and immunoblotted with antibodies against V5 epitope (top panels), α-tubulin and β-actin (indicated).

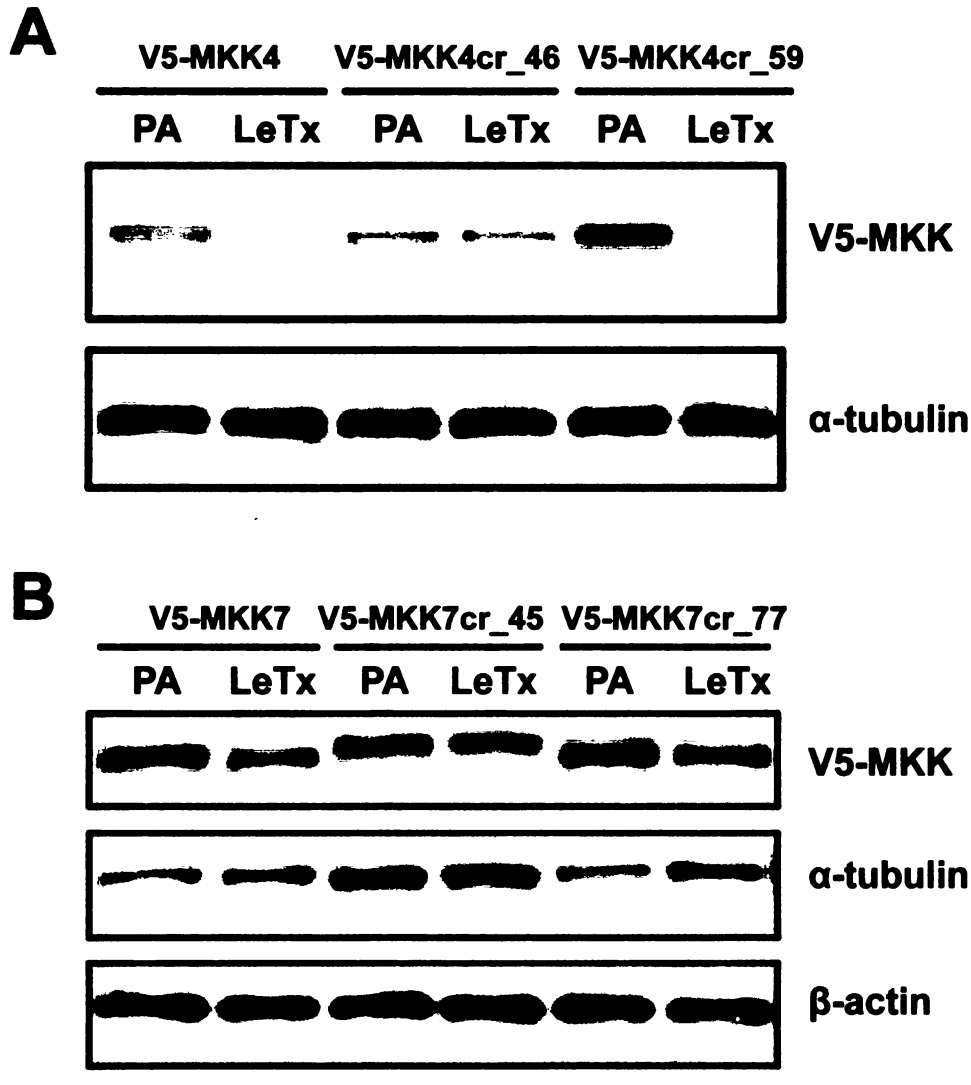

Figure 9. In-cell cleavage of MKK4 by LF.

CHO K1 cells were transfected with MKK4-V5-His6, MKK4_d45-V5-His6, or MKK4_d58-V5-His6 plasmids. After transfection, cells were split to four dished and cultured for 12h. Cells in each dish were treated with PA alone (1 μg/ml PA) or LeTx (1 μg/ml PA plus 0.1 μg/ml LF) in the presence of 0.1% DMSO or 10 μg/ml MG-132 for 24h. Total cell lysates were collected and immunoblotted with antibodies against V5 epitope (top panel) and GAPDH (bottom panel).

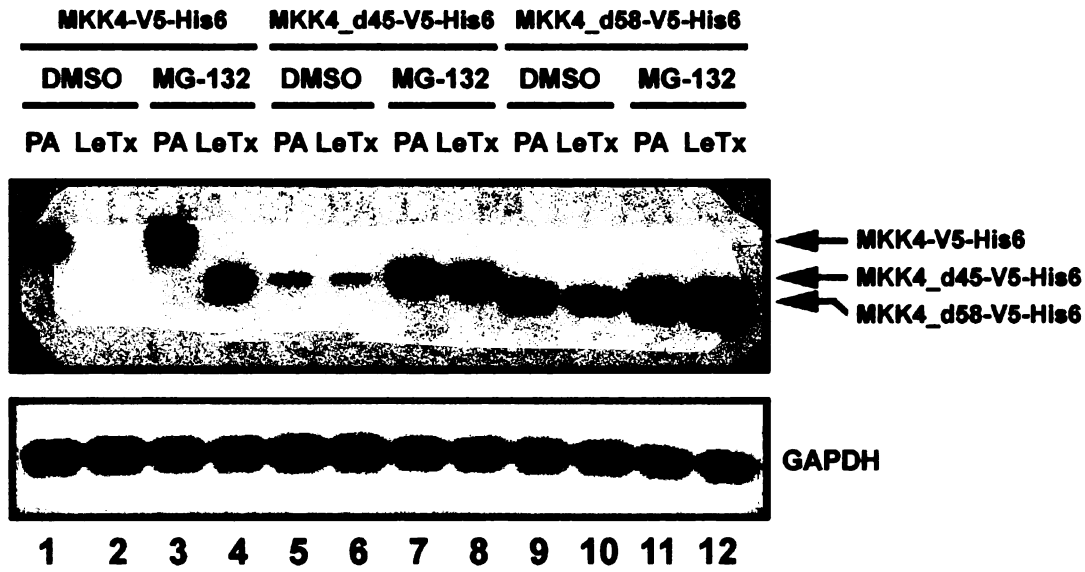

Figure 10. Wild-type MKK7 is not cleaved by LF in cells.

Non-transfected (None) CHO K1 cells and cells transfected with a decreasing amount of V5-MKK7 plasmids (8, 4, 2, and 1 μg as indicated) were treated with PA alone (PA) or LeTx (LT) for 12h in the presence of cycloheximide as described in Material and methods. Total cell lysates were collected and immunoblotted with antibodies against V5 epitope (top panel), NH_2-terminus of MEK1 (middle panel), and β-actin (bottom panel).

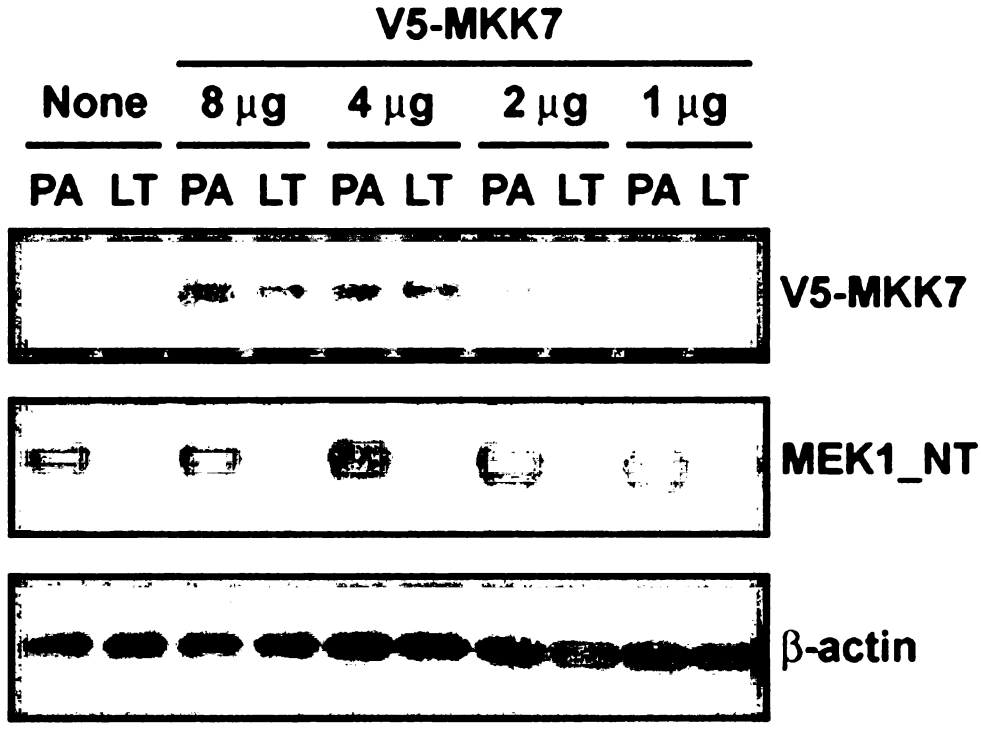

Figure 11. LF does not cleave endogenous MKK7 in mammalian cells.

293FT cells were treated with PA alone (PA) or LeTx (LT) for 24, 48, and 72h (indicated). Total cell lysates were collected and immunoblotted with antibodies against the last 20 amino acids of human MKK7 (top panel), NH_2-terminus of MEK1 (middle panel), and β-actin (bottom panel).

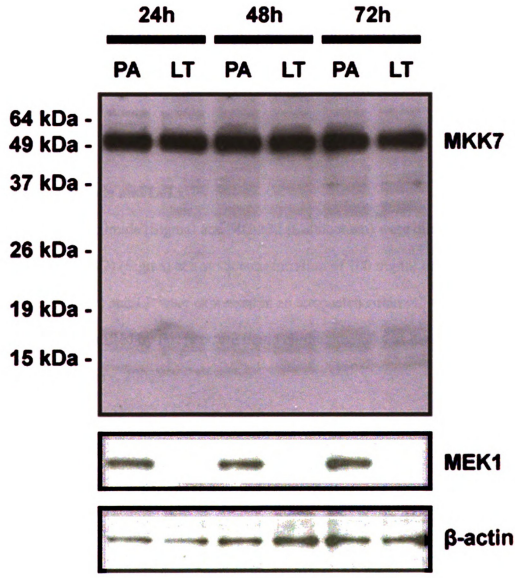

1.5. Materials and methods

1.5.1. Cell lines and stable cell line establishment.

Chinese hamster ovary (CHO) K1 cells were purchased from ATCC and grown in Dulbecco's minimal essential medium (DMEM) supplemented with 10% fetal bovine serum (FBS) and 50 units/ml penicillin/streptomycin (Invitrogen). SK-MEL-28 cells were obtained from CeeTox Inc. and grown in RPMI 1640 medium supplemented with 5% FBS and 50 units/ml penicillin/streptomycin. 293FT cells were purchased from Invitrogen and grown in DMEM medium supplemented with 10% FBS and 50 units/ml penicillin/streptomycin (Invitrogen). All the cells were cultured at 37°C in a humidified 5% CO_2 incubator.

1.5.2. Chemicals and LeTx

Cycloheximide (Sigma) and MG-132 (Calbiochem) were dissolved in dimethyl sulfoxide (DMSO) (Sigma) at a stock concentration of 100 mg/ml and 10 mg/ml, respectively. PA and LF were expressed in an attenuated strain of Bacillus anthracis (BH445) and purified by fast pressure liquid chromatography as described (Bromberg-White & Duesbery, 2008).

1.5.3. V5-MEKcr construction.

All the plasmids used for transient transfection were prepared by using the QIAprep® Spin Miniprep Kit (Qiagen). Human MEK1 (NM_002755.2) sequence was PCR-amplified from the pREST-A/MKK1 vector, which was a generous gift from Natalie Ahn (Mansour *et al.*, 1994b). Human MEK2 (NM_030662.2), MKK3

(NM_145109.2), MKK4 (NM_003010.2), and MKK6 (NM_002758.2) sequences were PCR-amplified from the following I.M.A.G.E. clones (Open Biosystems). MEK2, clone #2961198; MKK3, clone #5215093; MKK4, clone #5272439; MKK6, clone #4499772. Human MKK7 (NM_145185.2) sequences were PCR-amplified from the pcDNA3/MKK7 vector. Amplified sequences were then inserted into pENTR™ Directional TOPO® vector (Invitrogen) according to the manufacturer's instructions. To generate MEKcr/MKKcr, aspartic acid residues were introduced into the P1′ position of LF cleavage sites (the 9^{th}, 11^{th}, 27^{th} and 15^{th} amino acid of MEK1, MEK2, MKK3 and MKK6, respectively; the 46^{th} and 59^{th} amino acids of MKK4; 45^{th} and 77^{th} amino acids of MKK7.) by using QuikChange® Site-Directed Mutagenesis (Stratagene). All the wild-type MEK/MKK and MEKcr/MKKcr sequences were verified by DNA sequencing. V5-MEK/MKK mammalian expression vectors were created by performing LR recombination reactions to move MEK/MKK sequences from the Entry vectors to the pcDNA3.1/nV5-DEST Destination vectors (Invitrogen) according to the manufacturer's instructions.

1.5.4. Construction of MKK4-V5-His6 and deletion mutants.

To make MKK4 carboxyl terminal fusion, the stop codon of MKK4 sequence was removed from the MKK4 Entry vector by using QuikChange® Site-Directed Mutagenesis (Stratagene) with modified PCR reaction in which 10% DMSO was included to solve secondary structure. A second run of modified Site-Directed Mutagenesis reaction was

performed to remove amino acid 2-45 and 2-58 of MKK4 from the modified Entry vector in order to generate the deletion mutant MKK4_d45 and MKK4_d58, respectively. The coding regions of MKK4 on all the Entry vectors were verified by DNA sequencing. MKK4-V5-His6 mammalian expression vectors were created by performing LR recombination reactions to move MKK4 sequences from the modified Entry vectors to the pcDNA-DEST40 Destination vectors (Invitrogen) according to the manufacturer's instructions.

1.5.5. In-cell MEK cleavage assay.

To examine the cleavage of wild-type MEK/MKK or the cleavage resistance of MEKcr/MKKcr in CHO K1 cells, cells were transfected with V5-MEK/MKK expression vectors or V5-*lacZ* (as a control) by using Lipofectamine™ 2000 (Invitrogen) according to the manufacturer's instructions. After transfection, cells were trypsinized and split into two dishes, and cells in each dish were treated with either PA alone control (1 μg/ml PA) or LeTx (1 μg/ml PA plus 0.1 μg/ml LF) in the presence of 10 μg/ml cycloheximide (Sigma) for 12h. Total cell lysates were collected on ice in RIPA lysis buffer [50 mM Tris-HCl pH 7.5, 150 mM NaCl, 1 mM EDTA, 1 mM EGTA, 2 mM Na_3VO_4, 20 mM sodium pyrophosphate, 1% sodium deoxycholate, 1% Triton X-100, 0.1% SDS, and 1 × EDTA-free protease inhibitor cocktail (Roche)] and homogenized by sonication in ice bath. Protein concentrations were determined by BCA™ Protein Assay Kit (Pierce) according to the manufacturer's instructions. Total cell lysates were then prepared in 1×SDS sample buffer [47.5% Laemmli Sample Buffer (Bio-Rad) and 2.5% β-

mercaptoethanol]. Five micrograms of total cell lysates were subjected to immunoblotting to detect LF-mediated cleavage as described in the results.

To examine the cleavage of MEK1, MEK2, and MKK3 in SK-MEL-28 cells (presented in Figure 6A and Figure 7A), clonal lines of cells stably expressing V5-MEK1cr, V5-MEK2cr, V5-MKK3cr, or their wild-type counterparts were established (described in the Material and methods of Chapter III, see page 143). For examining cleavages of MEK1 and MEK2 (Figure 6A), cells were treated with PA alone control (1 μg/ml PA) or LeTx (1 μg/ml PA plus 0.1 μg/ml LF) for 24h. For examining the cleavage of MKK3 (Figure 7A), cells were treated with LeTx in a LF concentration-dependent manner (1 μg/ml PA plus 0, 1, 10, 100 ng/ml LF) for 24h. Total cell lysates were collected and prepared for immunoblottings.

1.5.6. Immunoblotting.

Five micrograms of total cell lysates were separated in 10% Novex® Pre-Cast Tris-Glycine Gels (Invitrogen). To examine cleavage of endogenous MKK7 in 293FT cells (Figure 11), 4-20% gradient gels were used. After electrophoresis, proteins were electro-transferred onto polyvinylidene fluoride (PVDF) membranes (Millipore) according to the manufacturers' instructions. Membranes were then soaked in 5% non-fat milk for 30 min and hybridized with primary antibodies against V5 epitope (Bethyl Laboratories), NH_2-terminus of MEK1 (Upstate, #07-641), COOH-terminus of MEK1 (Santa Cruz Biotechnology, SC-219), COOH-terminus of MEK2 (Santa Cruz Biotechnology, SC-525), phospho-MEK1/2 (Cell Signaling #9154), COOH-terminus of MKK3 (Santa Cruz Biotechnology, SC-961), COOH-terminus of MKK6 (Epitomics,

1 821-1), COOH-terminus of MKK7 (Epitomics, 1949-1), α-tubulin (Sigma, T9026), β-tubulin (Sigma, T5201), β-actin (Sigma, A1978), or GAPDH (Cell Signaling, #2118) at 4°C for overnight. Conditions for primary antibody hybridizations were followed according to the antibody datasheets. After primary antibody hybridization, membranes were washed three times in TBST buffer (50 mM Tris, 150 mM NaCl, and 0.1% Tween-20), hybridized with HRP-conjugated secondary antibodies (Kirkegaard & Perry Laboratories) according to the instructions of the antibodies, and then washed three times in TBST buffer. Immunoblotting signals were then detected by LumiGLO™ Reagent and Peroxide (Cell Signaling) and exposed to X-Ray files (Kodak).

1.5.7. Immunoprecipitation

To immunoprecipitate V5-MEK from SK-MEL-28 cells, 5×10^6 cells were washed with ice-code PBS (Invitrogen) three times. Whole cell extracts were prepared on ice in 1 ml of lysis buffer (20 mM Tris-HCl pH 7.5, 150 mM NaCl, 1.5 mM $MgCl_2$, 2 mM EGTA, 1% Triton X-100, 2 mM DTT, 10 mM NaF, 1 mM Na_3VO_4, and 12 mM β-glycerophosphate), and then homogenized by sonication in ice bath. Soluble fraction of cell extracts was isolated by centrifugation at 12,000*g* at 4°C for 10 min. Protein concentrations were determined by BCA™ Protein Assay Kit (Pierce) according to the manufacturer's instructions. Two hundred mg of clear extracts were incubated with 25 μl of agarose-immobilized V5 antibody (Bethyl Laboratories) in a total volume of 500 μl of lysis buffer on a rotator at 4°C for 12h. The precipitates were then washed twice with the

lysis buffer and twice with kinase assay buffer (25 mM Tris-HCl pH 7.5, 5 mM β-glycerophosphate, 2 mM DTT, 0.1 mM Na_3VO_4, and 10 mM $MgCl_2$), and resuspended in 50 µl of kinase assay buffer as the kinase source for the following kinase assay.

1.5.8. *In vitro* kinase assay.

Five microlitters of prepared V5 immunoprecipitates were incubated on ice with or without 0.05 µg of active B-Raf (Upstate Biotechnology) and 400 ng of recombinant ERK2 in a total volume of 2 µl of assay dilution buffer (20 mM MOPS pH 7.2, 25 mM β-glycerophosphate, 5 mM EGTA, 1 mM Na_3VO_4 and 1 mM DTT), and then 3 µl of ATP mixture [0.5 µl of [γ-^{32}P]ATP (Amersham; 10 mCi/ml, 3000 mCi/mmole) in 250 µM ATP and 37.5 mM $MgCl_2$] was added. *In vitro* phosphorylation reaction was carried out by incubating the reactions in 30°C water bath for 30 min, and then stopped by addition of 10 µl of 2×SDS sample buffer. Proteins in the reactions were then separated in 10% Tris-Glycine gels, and ERK2 phosphorylation was visualized by using a FLA-5000 PhosphoImager (Fuji). The input of 5 ul of V5-fusion proteins was shown by immunoblotting using V5 antibody.

Chapter III. Sufficiency and necessity of MEK signaling pathways for melanoma cell proliferation

1.1. Introduction

MEK1 and MEK2 share greater than 85% amino acid homology in their kinase domains. Therefore, currently available MEK small-molecule inhibitors target both MEKs. Since the only known substrates of both MEK 1 and 2 are ERK1 and ERK2, it has generally been assumed that MEK1 and MEK2 functions are overlapping and redundant. However, studies of mouse knockouts as well as recent studies in cultured cells indicate these molecules may have distinct biological functions. Whereas MEK1 deficiency results in embryonic lethality and a reduction in placental vascularization (Giroux *et al.*, 1999), MEK2 knock-out mice are viable and fertile (Belanger *et al.*, 2003). In addition, *in vitro* studies indicate MEK1 and MEK2 have non-redundant roles in colon cancer cell proliferation (Voisin *et al.*, 2008) and epidermal neoplasia (Scholl *et al.*, 2009b).

The B-Raf/MEK/ERK pathway is constitutively activated in many cancers including melanoma. Indeed, more than eighty percent of human melanomas harbor somatic B-Raf and N-Ras mutations (Tsao *et al.*, 2000; Davies *et al.*, 2002) that cause constitutive activation of MEK 1 and 2. Elevated MEK 1 and 2 activities promote melanoma tumorigenesis, angiogenesis, and progression (Cohen *et al.*, 2002; Govindarajan *et al.*, 2003; Tanami *et al.*, 2004; Wellbrock *et al.*, 2004; Trisciuoglio *et al.*, 2005). Conversely, biological and small molecule inhibitors targeting MEK 1 and 2 inhibit melanoma cell proliferation and xenograft tumor growth as well as metastasis (Koo *et al.*, 2002; Collisson *et al.*, 2003; Abi-Habib *et al.*, 2005; Solit *et al.*, 2006).

Consequently, a great deal of effort has been placed on developing inhibitors of MEK1 and 2 (Roberts & Der, 2007). Despite this, MEK1/2 inhibitors have failed to meet expectations in clinical trials owing to poor efficacy and unexpected toxicities (LoRusso *et al.*, 2005b; Eisen *et al.*, 2006; Lee & Duesbery, 2010). This indicates we do not yet fully appreciate the role of MEK signaling in melanoma. A better understanding of the relative roles of MEK1 and MEK2 may aid in the design of more effective therapies for treating melanoma and other MEK-dependent cancers.

To test the hypothesis that the functions of MEK1 and MEK2 are critical and interchangeable for melanoma cell proliferation, two series of experiments were performed. In the first approach, the necessity of MEK1 and MEK2 signaling pathway for SK-MEL-28 cell proliferation was determined using MEK-specific siRNA. In this experiment, either MEK1 or MEK2 was knocked-down by the specific siRNA while the other MEK isoform and other MKK family proteins were present. In the second approach, the novel experimental system presented in Chapter II was used to evaluate the sufficiency of MEK signaling pathways for cell proliferation by making either MEK1 or MEK2 active in SK-MEL-28 cells. Briefly, this system takes advantage of the MEK/MKK-specific proteolytic activity of anthrax lethal toxin (LeTx). LeTx is a binary toxin composed of protective antigen (PA) and lethal factor (LF). PA binds to the anthrax toxin receptors on cell surface to form a complex, which mediates the internalization of LF into cells (reviewed by Singh *et al.*, 2005). LF proteolytically inactivates MEK 1 and 2, (Duesbery *et al.*, 1998; Vitale *et al.*, 1998), MKK 3-4, 6 and 7 (Vitale *et al.*, 1998; Pellizzari *et al.*, 1999; Vitale *et al.*, 2000) at the amino-terminal consensus cleavage site, although results presented in Chapter II show that MKK7 may

not be a preferred LF substrate in mammalian cells (Chapter II, section 1.2.5, page 60). As a result of the cleavage, MEK loses a critical docking domain which is required for interacting with the downstream substrate ERK (Chopra *et al.*, 2003; Bardwell *et al.*, 2004). As a consequence MEK signaling is blocked (Duesbery *et al.*, 1998; Park *et al.*, 2002; Depeille *et al.*, 2007; Ding *et al.*, 2008). Taking advantage of this, LeTx was used as a global MEK/MKK inhibitor to inhibit both of MEK1 and MEK2 as well as most other MKK signaling pathways in SK-MEL-28 cells. Simultaneously, a cleavage-resistant form of MEK (MEK1cr or MEK2cr) was expressed to rescue the individual MEK signaling pathway in cells. Sufficiency of MEK1 and MEK2 signaling pathways for melanoma cell proliferation was then evaluated.

1.2. Results

1.2.1. Necessity of MEK1 and MEK2 signaling pathways for melanoma cell proliferation

1.2.1.1. Necessity of MEK1 and MEK2 signaling pathways for ERK activation in melanoma cells

To test the hypothesis that MEK1 and MEK2 are redundant and interchangeable, the necessity of MEK1 and MEK2 signaling pathways for ERK activation in melanoma cells was evaluated first by performing siRNA-mediated MEK knock-down. To do this, human melanoma SK-MEL-28 cells were transfected with individual siRNA or pools of siRNAs that specifically target either MEK1 or MEK2. These siRNAs were designed and validated by QIAGEN Inc. (Valencia, CA). The knock-down efficiency of each

siRNA was estimated to be 75% or greater based on immunoblotting and the effects of each siRNA appeared to alter the targeted MEK without affecting the other (Figure 12). Individual knock-down of either MEK1 or MEK2 had no effect on ERK activation in SK-MEL-28 cells. In contrast, however, pooled siRNA targeting both MEK1 and MEK2 did cause a decrease in ERK phosphorylation (Figure 12). This indicates that neither MEK1 nor MEK2 is necessary for ERK activation, and that MEK1 and MEK2 can compensate for each other to activate ERK in SK-MEL-28 cells.

1.2.1.2. Necessity of MEK1 and MEK2 signaling pathways for melanoma cell cycle progression

The necessity of MEK1 and MEK2 signaling for cell cycle progression was then further determined in SK-MEL-28 cells using fluorescence-activated cell sorting (FACS). Under normal cell culture conditions, about 70% of SK-MEL-28 cells are in G_0/G_1 phase. Whereas knockdown of either MEK1 or MEK2 had no effect on cell cycle progression, the combined knockdown of MEK1 and MEK2 resulted in a significant 10% increase in cells at G_0/G_1 ($p < 0.0001$) (Table IV). These data indicate that neither MEK1 nor MEK2 signaling is necessary for ERK activation or cell cycle progression in SK-MEL-28 cells, and that MEK1 and MEK2 can compensate for each other to activate ERK and to promote cell cycle progression in SK-MEL-28 cells. This supports the hypothesis that MEK1 and MEK2 are interchangeable for melanoma cell proliferation.

1.2.2. Sufficiency of MEK1 and MEK2 signaling pathways for melanoma cell proliferation

To confirm the feasibility of the novel experimental system (presented in Chapter II) in SK-MEL-28 cells, V5-MEK1cr, V5-MEK2cr, or their wild-type counterparts (as controls) were stably transfected into SK-MEL-28 cells. These cells were then treated with LeTx in a LF concentration-dependent manner (1μg of PA plus 0, 1, 10, and 100 ng/ml of LF) for 24h, and the cellular levels of MEK1 and MEK2 were then examined using immunoblotting. LF-mediated proteolysis caused loss of the NH_2-terminal V5 epitope in cells expressing wild-type V5-MEK1 and V5-MEK2 within 24 hours, even when the cells were treated with low concentrations of LF (1 ng/ml). This loss of V5 epitope did not appear to be a result of decreasing cytomegalovirus (CMV) promoter activity (due to the down regulation of c-jun and c-fos by LeTx treatment) as the expression level of V5-*lac*Z in SK-MEL-28 cells remained unchanged in the presence of LF (Figure 13B). In contrast, V5-MEK1cr and V5-MEK2cr were much more resistant and showed only partial cleavage at the highest LF concentration used (100 ng/ml) (Figure 13A, top panels). These data confirm the earlier results showing that V5-MEK1cr and V5-MEK2cr remained intact in V5-MEKcr-expressing CHO K1 cells after with LeTx treatment (presented in Chapter II). In addition, following LeTx treatment, MEK1 and MEK2 were not detectable in V5-MEK2cr-expressing cells and V5-MEK1cr-expressing cells, respectively (Figure 13A, the second panels for MEK1, and the third panels for MEK2). It was noted that in SK-MEL-28 cells, the V5-MEK expression vectors also gave the same dual-translation pattern which was described earlier in Chapter II (see the text in page 54 and Figure 5). Taken together, these results validate

observations in CHO K1 cells and confirm MEK1 or MEK2 expression can be stably maintained in the absence of other MKK.

1.2.2.1. MEK2, but not MEK1, is sufficient to maintain ERK2 activity

ERK1 and ERK2 are the only identified enzymatic substrates of MEK1 and MEK2. To evaluate the sufficiency of MEK1 and MEK2 to phosphorylate ERK in melanoma cells, I examined the status of ERK phosphorylation when SK-MEL-28 cells expressed MEK1 or MEK2. As expected, ERK2 was more abundant than ERK1 in SK-MEL-28 cells (Figure 13A, the fifth panels), and ERK2 activation was dramatically inhibited by LeTx in SK-MEL-28 parental cells as well as in cells expressing wild-type V5-MEK1 or wild-type V5-MEK2 (Figure 13A, the fourth panels). In contrast, V5-MEK2cr maintained ERK2 phosphorylation in the presence of LeTx. Surprisingly, ERK2 activation was not maintained in V5-MEK1cr-expressing cells treated with LeTx, although V5-MEK1cr was activated in SK-MEL-28 cells and the kinase activity of V5-MEK1cr was confirmed by the earlier IP-kinase assay result. These results indicate that in SK-MEL-28 melanoma cells, MEK2 alone is sufficient to maintain ERK2 activity in the presence of LF, but MEK1 is not, and that MEK1 and MEK2 are not interchangeable for ERK2 activation in this cellular context.

1.2.2.2. Genome-wide cDNA microarray reveals non-overlapping transcriptional patterns downstream of MEK1 and MEK2

In response to extracellular signals, MAP kinase pathways regulate gene expression at the translational and/or post-translational level. Therefore, if MEK1 and

MEK2 are redundant and interchangeable, transcriptional targets downstream of MEK1 and MEK2 should overlap. In contrast, if MEK1 and MEK2 are not redundant, they should have non-overlapping transcriptional effects. To test this, SK-MEL-28 cells were treated with LeTx, so that (i) V5-*lacZ*-expressing cells had neither MEK1 nor MEK2 (as both were cleaved by LeTx); (ii) V5-MEK1cr-expressing cells had only MEK1 (V5-MEK1cr) but not MEK2; and (iii) V5-MEK2cr-expressing cells had only MEK2 (V5-MEK2cr) but not MEK1 (Figure 14A). Under these conditions, endogenous MEK and other MKK proteins were cleaved and inactivated by LF in LeTx-treated cells (data not shown). After LeTx treatment, total RNA was collected from the cells, and global gene expression change was analyzed by using the Agilent 60-mer Whole Human Genome Microarrays. The microarray data analysis was performed in collaboration with Mr. Karl Dykema from Dr. Kyle Furge's laboratory at the Van Andel Research Institute. Comparing the gene expression patterns in these cells, we found that relative to control treatment (PA plus LF_E687C, an inactive LF mutant) in V5-*lacZ*-expressing cells, LeTx treatment resulted in statistically significant changes in expression of 2,560 genes out of the 18,359 genes represented on the microarray. Of the 2,560 genes, 268 were rescued in V5-MEK1cr-expressing cells, and 1,214 were rescued in V5-MEK2cr-expressing cells. Surprisingly, when we compared the LeTx effect on these two types of cells, we found that the rescued genes were incompletely overlapping (Figure 14B). This indicates that MEK1 and MEK2 have both overlapping and non-overlapping downstream targets, and that MEK1 and MEK2 are not absolutely redundant and interchangeable with respect to gene expression in melanoma cells.

1.2.2.3. MEK2cr, but not MEK1cr, rescued proliferation-related pathways in LeTx-treated cells

We examined the pathway outputs in LeTx-treated cells by performing a gene set enrichment analysis (Furge *et al.*, 2007a; Furge *et al.*, 2007b). We found that in SK-MEL-28 cells LeTx treatment resulted in down-regulation of several transcriptional signatures, most of which were associated with cell proliferation, such as those of E2F transcription factor, RNA processing, DNA replication and recombination, and cell cycle progression, as well as oncogenic pathways. This supports previous findings that LeTx inhibits melanoma cell proliferation *in vitro* (Koo *et al.*, 2002; Abi-Habib *et al.*, 2005). Interestingly, 49 of these signatures were uniquely rescued in V5-MEK2cr-expressing cells whereas no signatures appeared to be uniquely rescued by V5-MEK1cr-expressing cells (see Table V for representative pathways, and Appendix I for the full pathway list). This finding indicates that MEK1 and MEK2 signaling pathways are not equally sufficient for gene expression associated with melanoma cell proliferation and suggests that MEK2 has a more substantial role in driving melanoma cell proliferation.

1.2.2.4. MEK2, but not MEK1, is sufficient for melanoma cell proliferation *in vitro*.

To test whether MEK2 and not MEK1 is sufficient to drive SK-MEL-28 melanoma cell proliferation, additional clonal SK-MEL-28 cells stably expressing the V5-fusion proteins were established and included in the following experiments. After SK-MEL-28 cells were transfected with wild-type V5-MEK or V5-MEKcr expression vectors, three independent stable clones displaying different levels of V5-fusion protein

expression were selected (Figure 15). SK-MEL-28 cells stably expressing V5-*lac*Z were established as a control. In this set of stably transfected cell lines, expression levels of V5-MEKcr were comparable to their wild-type counterparts, and expression levels of V5-MEK1 were comparable to V5-MEK2 (Figure 15). These stable cell lines were then tested for their sensitivity to LeTx *in vitro* by performing a LeTx toxicity assay. To do this, cells were cultured in the presence of PA and various concentrations of LF for 72h, and relative viability (compared to no LF) of LeTx-treated cells was then determined (Figure 16). Whereas parental SK-MEL-28 cells and the cells expressing V5-*lac*Z, V5-MEK1, V5-MEK1cr, and V5-MEK2 had similar sensitivities to LeTx (with IC_{50} values around 0.5 ng/ml of LF), cells expressing V5-MEK2cr showed a significantly lower sensitivity to LeTx-induced proliferation inhibition *in vitro* (Figure 16 and Figure 17). Importantly, the resistance of V5-MEK2cr-expressing cells to LeTx positively correlated with expression levels of V5-MEK2cr. The IC_{50} of LF on SK-MEL-28 cells expressing low, moderate, and high levels of V5-MEK2cr was 3-, 8-, and 21-fold higher than that for parental cells, respectively (Figure 16 and Figure 17). Furthermore, if resistance to LF is strictly dependent upon expression of MEK2cr then these cells should retain their sensitivity to MEK small-molecule inhibitors. To test this, cells were tested for their sensitivity to two MEK inhibitors, U0126 and PD 184352, in a dose-dependent manner. Consistent with the hypothesis, V5-MEK2cr-expressing cells were as sensitive as other V5-MEK-expressing cells to the MEK inhibitors U0126 and PD184352 (Figure 17). Taken together, these experiments demonstrate that SK-MEL-28 cells expressing V5-MEK2cr are relatively resistant to LeTx-induced proliferation inhibition *in vitro*, and

indicate that the MEK2, but not MEK1, signaling pathway is sufficient for SK-MEL-28 melanoma cell proliferation *in vitro*.

1.2.2.5. Neither MKK3 nor MKK6 is sufficient for SK-MEL-28 cell proliferation *in vitro*.

It was recently reported that cross talk between ERK and p38 MAPK stimulates melanoma proliferation (Estrada *et al.*, 2009). Despite the low basal level of p38 MAPK activity in SK-MEL-28 cells under the cell culture conditions that were used (Figure 18), the sufficiency of MKK3 or MKK6 signaling pathways for SK-MEL-28 cell proliferation was tested. When SK-MEL-28 cells stably expressing V5-MKK3cr or V5-MKK6cr were tested for their sensitivities to LeTx-induced proliferation inhibition *in vitro*, none of these stable cell lines were resistant to LeTx (Figure 19). This result indicates that neither MKK3 nor MKK6 is sufficient for melanoma cell proliferation *in vitro*.

1.2.2.6. MEK2 signaling is sufficient for anchorage-independent growth

The results presented above show the sufficiency of the MEK2 signaling pathway for melanoma SK-MEL-28 cell proliferation *in vitro*. Next I attempted to determine the sufficiency of MEK1 and MEK2 signaling pathways for melanoma tumor growth *in vivo* using a xenograft mouse model. However, as shown in section 1.2.3 of this chapter, I was not able to answer this question due to technical limitations of the xenograft model. Despite this, the xenograft experiment results revealed valuable information regarding the *in vivo* targeting of LeTx. This part of the data is presented in the next section.

Using a soft agar colony forming assay as an alternative strategy, I evaluated the ability of these cells to grow in an anchorage-independent fashion. Parental SK-MEL28 as well as SK-MEL28 cells expressing V5-*lac*Z, V5-MEK and V5-MEKcr readily formed colonies (>50 μm diameter) within 21 days (Figure 20A, top panels). However, in the presence of LeTx, colony formation of all cell types tested was inhibited, except for V5-MEK2cr-expressing cells (Figure 20A, lower panels). When these results were quantified, it was noted that expression of V5-MKK2cr in SK-MEL-28 cells resulted in a significant rescue of 70% of the colony formation in the presence of LeTx (Figure 20B). This result, in agreement with the proliferation results presented earlier, demonstrates that the MEK2 signaling pathway alone is sufficient for anchorage-independent growth of SK-MEL-28 cells.

1.2.3. A xenograft model to test the sufficiency of MEK1 and MEK2 signaling pathways for melanoma tumor growth *in vivo*

As discussed in the General Introduction (Chapter I), LeTx possesses a potent inhibitory activity on tumor growth *in vivo* in different cancer xenograft models (Duesbery *et al.*, 2001; Koo *et al.*, 2002; Depeille *et al.*, 2007; Ding *et al.*, 2008). A similar approach was used in this dissertation project to determine the sufficiency of MEK signaling pathways for melanoma tumor growth *in vivo*.

1.2.3.1. SK-MEL-28 xenograft tumor growth

To grow SK-MEL-28 xenograft tumors in nude mice, cells were subcutaneously injected into the right side of the dorsalateral area of a group of athymic nude mice.

Tumor volumes were measured every two days by using a caliper. Figure 21 shows a representative SK-MEL-28 xenograft tumor growth curve. Shortly after subcutaneous inoculation, lesions were measurable due to swelling. The swellings generally disappeared within two weeks and the volume of the lesions remained not measurable for the next five weeks. Seven weeks after cell inoculation, xenograft tumors started growing in an exponential manner (Figure 21). Although considerable variation of tumor size between mice was normally observed in this xenograft model, the experimental reproducibility was revealed when tumor growth curves from multiple independent experiments were overlaid on the same plot (Figure 22).

1.2.3.2. LeTx systemic treatment of SK-MEL-28 xenograft tumors

In this dissertation project, an established approach for LeTx systemic treatment of cancer xenograft tumors in nude mice was used. Xenograft tumors were allowed to grow to an average volume of 50 mm^3, at which time mice were divided into two groups. Mice in each group were then intravenously injected with LeTx (PA plus LF) or control (PA plus LF_E687C) at a dosage of one standard dose (1 ×SD equals 10 μg PA plus 2 μg LF or LF_E687C) every two days for a total of six injections (6 standard doses). Previous studies have shown that this treatment has no obvious adverse effects on the health of athymic nude mice while xenograft tumor growth is inhibited (Abi-Habib *et al.*, 2006a; Depeille *et al.*, 2007; Ding *et al.*, 2008; Huang *et al.*, 2008). As shown in Figure 21, SK-MEL-28 xenograft tumor growth was also inhibited by the same systemic LeTx treatment.

1.2.3.3. Sensitivity of MEKcr-expressing xenograft tumors to LeTx systemic treatment

The inhibitory effect of LeTx on SK-MEL-28 xenograft tumor growth suggests that MEK signaling pathways are required for melanoma tumor growth *in vivo*. Based on this, sufficiency of MEK signaling pathways for SK-MEL-28 xenograft tumor growth should be testable by expressing MEKcr proteins in xenograft tumors. If the MEK1 or MEK2 signaling pathway individually is sufficient for SK-MEL-28 xenograft tumor growth *in vivo*, tumors expressing V5-MEK1cr or V5-MEK2cr are expected be resistant to the growth inhibition effect of LeTx systemic treatment. To test this, SK-MEL-28 parental cells or cells expressing high levels of V5-MEK1, V5-MEK1cr, V5-MEK2, or V5-MEK2cr were subcutaneously injected into groups of athymic nude mice to establish SK-MEL-28 xenograft tumors expressing each of these V5-fusion proteins. After these tumors reached an average volume of 50 mm^3, mice received LeTx or control (PA plus LF_E687C) systemic treatment as described. As shown in Figure 23, V5-MEK1cr-exressing tumors were still sensitive to LeTx although a slight decrease in sensitivity was observed when compared with parental and wild-type V5-MEK1-expressing tumors. Similarly, tumors expressing V5-MEK2cr were also sensitive to LeTx systemic treatment of LeTx (Figure 24). These results suggest that although the MEK2 signaling pathway alone was sufficient to drive SK-MEL-28 cell proliferation *in vitro*, neither MEK1 nor MEK2 was sufficient for SK-MEL-28 xenograft tumor growth *in vivo*.

1.2.3.4. Dose-dependent effects of LeTx on SK-MEL-28 xenograft tumor growth

When the MEKcr proteins were tested for their resistance to LF-mediated proteolysis in SK-MEL-28 cells, restored cleavage of MEK1cr and MEK2cr by LF was observed at the highest concentration of LF (Figure 13A, top panels). Therefore, it was possible that elevated LeTx levels in SK-MEL-28 xenograft tumors were sufficient to overcome the cleavage resistance of MEKcr and masked their sufficiency for tumor growth. To test this, a LeTx dose-dependency xenograft study was conducted. In this experiment, cells were inoculated into groups of 20 mice. After tumors were established, mice were divided into four groups, and mice in each group were intravenously injected with either 1×SD control (PA plus LF_E687C) or a decreasing dose of LeTx (1×SD, 0.5×SD, and 0.25×SD). Systemic treatment with LeTx inhibited SK-MEL-28 parental xenograft tumor growth in a dose-dependent manner (Figure 25, parental tumors), indicating that the one standard dose of LeTx used in the previous experiments was not an over dosage. Under these conditions, no obvious therapeutic resistance of V5-MEK2cr-expressing tumors was observed when compared with parental or wild-type V5-MEK2-expressing tumors (Figure 25). This result excluded the possibility that an exposure of high concentration of LeTx proteolytically inactivated V5-MEKcr and masked the potential resistance of V5-MEK2cr-expressing tumors, and confirmed that MEK1 or MEK2 signaling pathway individually was not sufficient for melanoma tumor growth *in vivo*.

1.2.3.5. Loss of V5-MEKcr expression in SK-MEL-28 xenograft tumors

To confirm the finding that MEK1 or MEK2 signaling pathway was not sufficient for SK-MEL-28 xenograft tumor growth *in vivo* as presented above, MEK cleavage as well as the cleavage-resistance of MEKcr in tumor cells were examined. To do this, at the end of the xenograft experiment, mice were euthanized and the xenograft tumors were dissected. Tumor lysates were then prepared and subjected to immunoblotting. Surprisingly, a loss of V5-MEKcr expression, both of V5-MEK1cr and V5-MEK2cr, in the xenograft tumor cells was observed at the end of the experiment (about three months from cell inoculation) (Figure 26). The loss of V5-MEKcr expression was independent from LeTx systemic treatment as it was also observed in control-treated tumor cells. Before I could accept this as an explanation for why V5-MEKcr-expressing tumors were not resistant to LeTx, I needed to confirm that MEK proteins were indeed cleaved in LeTx-treated tumors.

1.2.3.6. LeTx systemic treatment does not cause MEK cleavage in tumor cells.

When ERK activation status was further examined in the xenograft tumor lysates, an unexpected result was observed: ERK activation was maintained in LeTx-treated tumor cells even if the treated tumors were responding (Figure 26). In addition, LeTx treatment did not result in a loss of V5 epitope immunoblotting signal in the lysates prepared from tumor cells expressing wild-type V5-MEKs (Figure 26). This observation raised a possibility that for some unknown reason LF did not cleave MEK in SK-MEL-28 tumor cells, and led to a further examination of cleavage of endogenous MEK in LeTx-treated tumors. Surprisingly, no cleavage of endogenous MEK was observed in LeTx-

treated SK-MEL-28 parental xenograft tumor cells (Figure 27). Two possibilities could explain this surprising result. First, the endogenous MEK in SK-MEL-28 xenograft tumor cells became biochemically uncleavable by LF due to an unknown reason. Second, LF was not delivered into the tumor cells when LeTx was administrated intravenously. To test these two possibilities, the 6^{th} LeTx or control injection for half of the mice in the xenograft experiment was switched from intravenous injection to intratumoral injection by which tumor cells would be directly exposed to LeTx. One day after the last injection, tumors were dissected and tumor lysates were prepared to examine endogenous MEK cleavage by immunoblotting. As shown in Figure 27, a loss of endogenous MEK1 NH_2-terminal epitope and a slight electrophoretic mobility shift of cleaved MEK1 (indicating MEK1 cleavage by LF) were observed in tumor cells only when the last LeTx injection was administrated intratumorally. In addition, in those tumor cells whose endogenous MEK was cleaved, ERK activation was inhibited. This result indicates that MEK did not become uncleavable by LF in xenograft tumors, but rather that systemic injection of LeTx is not able to deliver LF into tumor cells. Therefore, the inhibitory effect of LeTx on xenograft tumor growth must be mediated by a non-tumor compartment.

1.2.3.7. Sufficiency of MEK signaling pathways for SK-MEL-28 tumor growth *in vivo* was not testable due to technical difficulties.

As shown above, after three-month growth in nude mice, SK-MEL-28 xenograft tumors cells lost V5-MEKcr expression. In addition to this, it was also found that LeTx was not delivered into tumor cells if injected intravenously. This makes the sufficiency of MEK signaling pathways for melanoma tumor growth *in vivo* non-testable. However,

clinical-valuable information was also obtained from this unexpected observation. This will be discussed later in this chapter.

1.3. Discussion

Kinase inhibitors have been extensively used as tools to study signal transduction pathways. However, most kinases share high sequence homology and similar structures with their family members, making it difficult to discriminate between kinase isoforms using small molecule inhibitors. Although RNA interference can specifically target one of the protein isoforms, concerns about incomplete protein knockdown can confound interpretation, especially when these proteins are highly expressed or slowly turned over in cancer cells. In addition, in order to study the sufficiency of an individual protein belonging to a family which has several members and isoforms (*e.g.* the MEK/MKK protein family), multiple protein members in the family need to be simultaneously inhibited or knocked down. Combining several siRNA molecules decreases the efficiency of RNA interference and increases the likelihood of off-target effects. Due to these limitations, studies of the function of a protein are restricted to evaluating necessity but not sufficiency. This impedes a better understanding of individual protein functions, especially for those involved in complicated signaling networks.

In this Chapter, a novel experimental system which allows one to determine the sufficiency of MEK/MKK signaling pathways for a specific phenotype or cellular function was presented. This system utilizes the specific proteolytic activity of anthrax

lethal toxin (to globally inhibit multiple MEK/MKK signaling pathways) and a set of mutant MEK/MKK proteins that are resistant to LF-mediated proteolysis (to rescue one specific MEK or MKK signaling pathway in cells treated with LeTx). This system is applicable to most mammalian cells because anthrax toxin receptors are ubiquitously expressed in many different types of cells (Bradley *et al.*, 2001; Scobie *et al.*, 2003). With an appropriate phenotype as a readout (*e.g.*, proliferation in this study), this system is a powerful tool allowing dissection of the roles of each MEK/MKK signaling pathway. Since LF efficiently cleaves and inactivates multiple members in the MKK family and inactivates the three canonical MAPK pathways, this experimental approach eliminates the potential cross talk between MKK family proteins. To the best of my knowledge, this is the only available approach for evaluating the sufficiency of individual MEK/MKK signaling pathways.

Combining RNA interference technology with this novel experimental system, both necessity and sufficiency of MEK1 and MEK2 signaling pathways for melanoma cell proliferation were determined in order to test the hypothesis that MEK1 and MEK2 signaling pathways are interchangeable and redundant for melanoma cell proliferation. In the first series of experiments, MEK-directed siRNA were used to selectively knock-down either MEK1 or MEK2, or both, in human melanoma SK-MEL-28 cells. Doing this I found that only simultaneous knock-down of both MEK1 and MEK2 could block ERK activation and cell cycle progression. This indicates that neither MEK1 nor MEK2 is necessary for melanoma cell proliferation, and that they can compensate for each other. These results are consistent with the hypothesis that MEK1 and MEK2 are

interchangeable and redundant for melanoma cell proliferation. Other studies support this conclusion. For example, Scholl *et al* show that stepwise deletion of MEK 1 or MEK 2 alleles reduce Ras-induced epidermal hyperplasia to a similar extent (Scholl *et al.*, 2009a).

In the second series of experiments, V5-MEKcr constructs were stably expressed in SK-MEL28 cells so that when the cells were treated with LeTx, multiple endogenous MEK and MKK were inactivated with the exception of the cleavage-resistant mutants which remained intact and capable of signaling. Doing this, I found first that MEK1 and MEK2 are not equally sufficient for ERK activation in SK-MEL-28 cells. MEK2 signaling pathway alone was sufficient for ERK activation, but MEK1 was not. This led me to use whole genome cDNA microarrays to examine the transcriptional patterns downstream of MEK1 and MEK2. This approach revealed the non-overlapping transcriptional effect of MEK1 and MEK2. Further, collaborating with the bioinformatics group at the Van Andel Research Institute, we performed a gene set enrichment analysis to look for transcriptional signatures that can be rescued by V5-MEK1cr and V5-MEK2cr. We found that LeTx treatment down-regulated many proliferation-associated transcriptional signatures, many of which were able to be rescued only by V5-MEK2cr but not by V5-MEK1cr (Appendix I). Although another group of signatures was rescued by both of V5-MEK1cr and V5-MEK2cr (Appendix II), *in vitro* assays confirmed MEK2 signaling was sufficient for SK-MEL-28 cell proliferation but MEK1 signaling was not, suggesting that (1) rescuing this group of transcriptional activities was not sufficient to rescue cell proliferation and/or (2) these transcriptional

activities were rescued by V5-MEK1cr to a less extent. Consistent with the *in vitro* proliferation assay, soft agar assays showed that MEK2 signaling was sufficient for the anchorage-independent growth of SK-MEL-28 cells, and V5-MEK1cr expression was not sufficient to rescue colony formation of SK-MEL-28 cells in the presence of LeTx. Collectively, these findings lead me to conclude that (1) MEK2 signaling pathway is sufficient for ERK activation, *in vitro* proliferation, and anchorage independent growth of SK-MEL-28 melanoma cells, whereas MEK1 is not, and (2) though they are critical for SK-MEL28 cell proliferation, MEK 1 and MEK 2 are not interchangeable. Additional studies provide compelling evidence that under some conditions MEK1 and MEK2 are not functionally interchangeable. During mouse embryonic development, loss of MEK1 expression is lethal, likely because of reduced blood vessels in the labyrinthine layer of the placenta (Giroux *et al.*, 1999). In contrast, MEK2 is dispensable as MEK2 deficient mice are viable and fertile (Belanger *et al.*, 2003). Voisin *et al* (2008) have shown that although both of the constitutively active MEK1 and MEK2 isoforms individually are sufficient to transform normal intestinal epithelial cells, shRNA-mediated MEK2 knockdown has much stronger inhibitory effect on colon cancer cell proliferation than MEK1 knockdown does, leading them to conclude that MEK1 and MEK2 may be differentially regulated or may target distinct effector pathways in certain cellular and/or genetic contexts. Scholl *et al* (2009b) demonstrated that MEK1 but not MEK2 is required for DMBA/TPA-induced benign epidermal papilloma formation. Also, Catalanotti *et al* (2009) have recently reported that MEK1 and MEK2 form heterodimer complexes in which MEK1 serves as a negative regulator of MEK2.

These two sets of experiments led to apparently contradictory conclusions. In the first set (the necessity study) MEK1 and MEK can compensate for each other, whereas in the second MEK1 cannot compensate for loss of MEK2. In fact, these are not truly contradictory as the two experimental approaches are fundamentally different. In the siRNA experiments, only one of the MEK/MKK signaling pathways was inhibited, whereas in the LeTx plus MEKcr experiments, multiple MEK and MKK pathways were blocked. These two experimental strategies resulted in different cellular backgrounds. Taking this into consideration, these results can be explained by formulating a new hypothesis: while MEK2 is sufficient for SK-MEL28 melanoma tumor growth, MEK1 can compensate for loss of MEK2 only in the presence of an as yet unidentified factor. This factor is likely an MKK or is regulated by an MKK since the sufficiency of MEK2 is revealed only in the presence of LF, an MKK-specific protease. However, this factor likely is not p38 MAPK or JNK since the basal activities of these kinases are too low to be detected in SK-MEL-28 cells by immunoblotting (Figure 18). Identification of this LF-sensitive factor may have important clinical consequences since its targeted inactivation would block the ability of MEK1 to compensate for loss of MEK2 activity and as a consequence increase the dependency on signaling through MEK2 for survival.

The novel experimental system presented in this dissertation relies on MEKcr rescue. Therefore, it is important to make sure that the aliphatic-to-aspartic acid mutation does not alter the activity of MEK. Thus far, the only known biochemical activity of MEK is its kinase activity. In addition, in order to be an active kinase, MEK needs to be phosphorylated and activated by a MEK kinase such as B-Raf. The validation

experiments (Figure 6) presented in Chapter II indicate that (1) both MEK1cr and MEK2cr are phosphorylated in SK-MEL-28 cells, and (2) both MEK1cr and MEK2cr are capable of phosphorylating ERK2 in an IP-kinase assay. These results indicate that the aliphatic-to-aspartic acid mutation introduced to MEK1 and MEK2 neither impairs MEK's kinase activity nor interferes with the Raf:MEK and MEK:ERK interactions. However, it may be argued that the *in vitro* interaction between MEKcr and ERK does not accurately represent the physical interaction occurring in cells, although the amount of V5-MEK immunoprecipitates added to the *in vitro* kinase assay reactions was not saturating (as shown in Figure 6B). I reasoned that if the CR mutation made MEK incapable of interacting and phosphorylating ERK in cells, then (1) expressing V5-MEKcr should be the same as expressing V5-*lacZ*, and (2) the transcriptional changes caused by LeTx treatment in V5-MEKcr-expressing cells should be very similar to that in V5-*lacZ*-expressing cells. To test this, we performed a clustering analysis on the microarray data (see section 1.2.2.2 in page 88) to compare the global transcriptional changes in LeTx-treated SK-MEL-28 cells expressing V5-*lacZ*, V5-MEK1cr, or V5-MEK2cr. The clustering analysis revealed a higher similarity between LeTx-treated V5-MEK1cr-expressing cells and V5-MEK2cr-expressing cells than V5-MEK1cr-expressing cells and V5-*lacZ*-expressing cells (Figure 28), indicating that the introduced cleavage-resistant mutation did not disrupt MEK1 function. This result argues against the possibility that the CR mutation disrupts the interaction of MEK with ERK, and supports the interpretation presented in section 1.2.2.1 (page 88) that MEK1 individually is not sufficient to phosphorylate ERK in SK-MEL-28 cells.

As discussed in Chapter I, LeTx treatment has shown very promising anti-cancer activities in cultured tumor cell lines as well as xenograft models (Duesbery *et al.*, 2001; Koo *et al.*, 2002; Depeille *et al.*, 2007; Ding *et al.*, 2008; Huang *et al.*, 2008; Rouleau *et al.*, 2008). In addition, it has become a very powerful tool for studying MEK/MKK signaling pathways and their roles in human diseases. As a global MEK/MKK protease, LF cleaves multiple MEK/MKK proteins and LeTx treatment results in a global inhibition of the ERK, p38 MAPK, and JNK pathways. In this chapter, I presented an effort to combine LeTx systemic treatment and V5-MEKcr-melanoma xenograft model for evaluating the sufficiency of MEK1 and MEK2 signaling pathways for melanoma tumor growth *in vivo*. Although this was eventually not testable due to technical limitations, the series of xenograft experiments have provided valuable information. This is discussed as follows.

As presented in this chapter, it took about 3-4 months to complete an SK-MEL-28 xenograft experiment. This was due to the 7-to-8-week dormancy before tumors started growing. This relatively long-term tumor dormancy was not commonly observed in the literature and it does not seem to be mouse strain- or animal facility-specific as other cancer cell-derived xenograft tumors grown in the same strain of athymic nude mice at the Van Andel Research Institute do not require this long-term tumor dormancy. Therefore, it appears to be cell line-specific. On the other hand, however, this long-term tumor dormancy was not observed in other reports when SK-MEL-28 cells were xenotransplanted (Rouleau *et al.*, 2008). It seems that this tumor dormancy is specific to the SK-MEL-28 cells that we obtained. Although the molecular mechanism of this tumor

dormancy is not clear, it has been hypothesized that during this period of time tumor cells are switching to an angiogenic phenotype, which is essential for tumor growth [reviewed by Naumove *et al.* (2006)].

When V5-MEK-expressing cells were xenografted, a few interesting observations were obtained. First, V5-MEK-expressing xenograft tumors required shorter terms of dormancy (Figure 23 and Figure 24). This was particularly obvious for V5-MEK1cr-expressing tumors which bypassed the dormancy and directly grow up after tumor inoculation (Figure 23). Second, whereas V5-MEK1cr-expressing tumors required a shorter term of dormancy than wild-type V5-MEK1-expressing tumors (Figure 23), V5-MEK2cr-expressing tumors required a longer term of dormancy than wild-type V5-MEK2-expressing tumors (Figure 24). Third, these differences appear to be only in tumor dormancy, not tumor growth rate, as these different xenograft tumors had similar exponential growth rates after they broke dormancy. It is possible that MEK overexpression reduced the period of tumor dormancy (*i.e.*, the MEK signaling pathway positively regulates the development of the tumor microenvironment), and MEK1 and MEK2 might have different effects on this process. However, since V5-MEKcr expression was lost during the course of xenograft tumor growth, it is not clear if this shorter period of tumor dormancy was due directly to MEK expression level. Besides, since each SK-MEL-28 stable clone was isolated from a single cell colony by selection with antibiotics, the possibility of clonal effects cannot be excluded. To directly address this question, V5-*lacZ*-expressing cells should be xenografted as a control, and other

moderate- and low-MEK expressors should be included to test a correlation with MEK expression levels.

As shown in Figure 26, the expression levels of V5-MEKcr were dramatically decreased in xenograft tumors during the course of subcutaneous growth and the expression level of V5-MEKcr was not comparable to its wild-type counterpart. This is one of the reasons why it was not possible to test the sufficiency MEK signaling pathways for SK-MEL-28 xenograft tumor growth *in vivo*. Although it was not clear when the tumors started losing the V5-MEKcr expression, this loss of V5-MEK expression appears to be MEKcr-specific. Possibilities to explain this include (1) the aliphatic-to-aspartic mutation makes MEK less stable, and (2) wild-type MEK and MEKcr have different transcriptional effects which have an autoregulatory feedback effect. Both of these possibilities appear to be culture environment-specific since this loss of V5-MEKcr expression was not observed in cultured cells. On the other hand, the possibility of clonal effects cannot be excluded since only one (the high expressor) of the three stable clones in each set was inoculated for xenograft tumor establishment and it was not clear if this loss of V5-MEKcr expression in xenograft tumors would also be observed if the moderate- or low-expressors were also inoculated. To address this, other stable clones should be included in this study and expression levels of V5-MEK and V5-MEKcr in tumor cells should be examined. In addition, in order to understand when the V5-MEKcr expression was lost in tumor cells, more nude mice should be included in the study and tumors should be dissected at different time points during the study.

It was assumed that systemic LeTx treatment *via* tail vein injection delivered LeTx to xenograft tumors, LF was internalized into tumor cells, and LF cleaved MEK/MKK proteins and blocked multiple MEK/MKK signaling pathways in tumor cells. It was further assumed that as a result of this, tumor cell proliferation was inhibited, and in turn, tumor growth was inhibited. However, a surprising observation from the SK-MEL-28 xenograft model and LeTx systemic treatment was that the endogenous MEK was still intact in LeTx-treated tumor cells even if the tumor growth was inhibited (Figure 26 and Figure 27). This resistance of MEK to LF cleavage was not due to a change in MEK cleavability *per se* as the endogenous MEK was still sensitive to LF cleavage if LeTx was directly injected into tumor cells *via* intratumoral injection (Figure 27). If endogenous MEK proteins were not cleaved by LeTx in tumor cells, then the special cellular context in which only one individual MEK pathway was active in tumor cells was not achievable. This was another reason why I was unable to determine the sufficiency of MEK signaling pathways for melanoma tumor growth *in vivo*. However, this observation provided valuable information. This result clearly indicates that LeTx systemic treatment inhibits xenograft tumor growth without targeting tumor cells. If LeTx does not target tumor cells, why can it inhibit tumor growth? It is possible that LeTx systemic treatment inhibits xenograft tumor growth by inhibiting tumor-associated endothelial function, considering that endothelial cells are potential targets of LeTx (Kirby, 2004; Warfel *et al.*, 2005; Alfano *et al.*, 2009) and that LeTx treatment decreases microvessel density in xenograft tumors (Duesbery *et al.*, 2001; Depeille *et al.*, 2007; Ding *et al.*, 2008). This gives valuable clinical information: targeting tumor-associated endothelial cells may be sufficient to inhibit xenograft tumor growth, and targeting

melanoma-associated endothelium could be another strategy to treat melanoma. In addition, this raises an alternative hypothesis that MEK signaling pathways in melanoma-associated endothelium are essential for tumor survival *in vivo*.

In summary, using complementary experimental approaches I have tested the redundancy of MEK1 and MEK2 signaling in the *in vitro* proliferation of SK-MEL-28 melanoma cells. I observed that (1) neither MEK1 nor MEK2 is necessary for melanoma cell proliferation and (2) MEK2, but not MEK1, is sufficient for melanoma cell proliferation. These results lead to an alternative hypothesis that while MEK2 can compensate for loss of MEK1, MEK1 can compensate for the loss of MEK2 function only when an unidentified factor is present. This study provides novel insight into the complicated interplay between MEK1 and MEK2 that may have significant clinical impact.

1.4. Tables and figures

Table IV. Percentage of G_1 population of MEK siRNA-treated SK-MEL-28 cells.

siRNA experiments	G_1 population (% ± S.D.)*
None	69.45 ± 0.91
Lipid only	69.68 ± 1.21
Non-silencing	70.49 ± 0.16
MEK1 siRNA-7	70.45 ± 3.27
MEK1 siRNA-8	71.30 ± 3.07
MEK1siRNA-11	70.43 ± 1.83
MEK1 siRNA-7811	72.92 ± 1.71
MEK2 siRNA-9	70.65 ± 0.48
MEK2 siRNA-14	71.21 ± 0.86
MEK2 siRNA-914	71.53 ± 1.24
P1 (MEK1 siRNA-811 + MEK2 siRNA-914)	81.33 ± 1.48 **
P2 (MEK1 siRNA-7811 + MEK2 siRNA-914)	78.24 ± 3.41 **

* Data were obtained from at least three independent experiments.
** $p < 0.0001$, determined by one-way ANOVA followed by Bonferroni post-hoc analysis.

Table V. MEK2cr-rescued transcriptional signatures that are significantly affected by LeTx treatment.

Signatures/Pathways/Gene sets [a]	t-statistics [b] V5-*lacZ*	V5-MEK1cr	V5-MEK2cr	Reference [c]
Myc	-7.14	0.32	4.53	Ref: (Bild *et al.*, 2006)
E2F1, TFDP1, RB1 transcription factors	-6.28	1.07	3.29	MSigDB Gene Set: SGCGSSAAA_V$E2F1DP2_01
rRNA processing	-5.44	0.33	2.74	GO: 0006364
Ribosome biogenesis	-6.46	0.67	3.80	GO: 0042254
DNA recombination	-5.00	1.39	3.30	GO: 0006310
Nucleotidyl-transfer reaction	-3.63	1.39	2.93	Ref: (Ashburner *et al.*, 2000); MSigDB Gene Set: Nucleotidyltransferase_activity
G_1/S cell cycle transition	-3.67	1.49	2.77	MSigDB Gene Set: G1PATHWAY

[a] The complete list of transcriptional signatures is presented in Appendix I

[b] t-statistics were obtained from three independent microarray experiments, and the scores in V5-MEK1cr-expressing cells have *p* values greater than 0.005.

[c] MSigDB Gene Sets: http://www.broadinstitute.org/gsea/msigdb/search.jsp; GO (Gene Ontology): http://www.geneontology.org/.

Figure 12. Necessity of MEK1 and MEK2 signaling pathways for ERK activation in SK-MEL-28 cells.

SK-MEL-28 cells were transfected with nothing (N); lipid only (L); non-silencing control siRNA (NS); MEK-specific siRNA (MEK1 siRNA 7, 8, or 11, and MEK2 siRNA 9 or 14), or pools of MEK-specific siRNA (MEK1 siRNA 7+8+11 or MEK2 siRNA 9+14) as described in Materials and methods. As controls, cells were transfected with combinations of both MEK1- and MEK2-specific siRNA (P1, MEK1 siRNA 8+11 plus MEK2 siRNA 9+14; P2, MEK1 siRNA 7+8+11 plus MEK2 siRNA 9+14). After transfection, cells were trypsinized and split to two dishes for cell lysate collection and for cell cycle analysis (results shown in Table IV). Seventy-two hours later, whole cell lysates were harvested and immunoblotted. The efficiency of siRNA-mediated MEK knock-down was examined by immunoblottings with antibodies against MEK1 or MEK2. ERK activation was detected by antibodies specifically against phospho-ERK. Total ERK expression was detected by ERK antibody as a control. Antibody against GAPDH was used as an equal loading control.

Figure 12. Necessity of MEK1 and MEK2 signaling pathways for ERK activation in SK-MEL-28 cells.

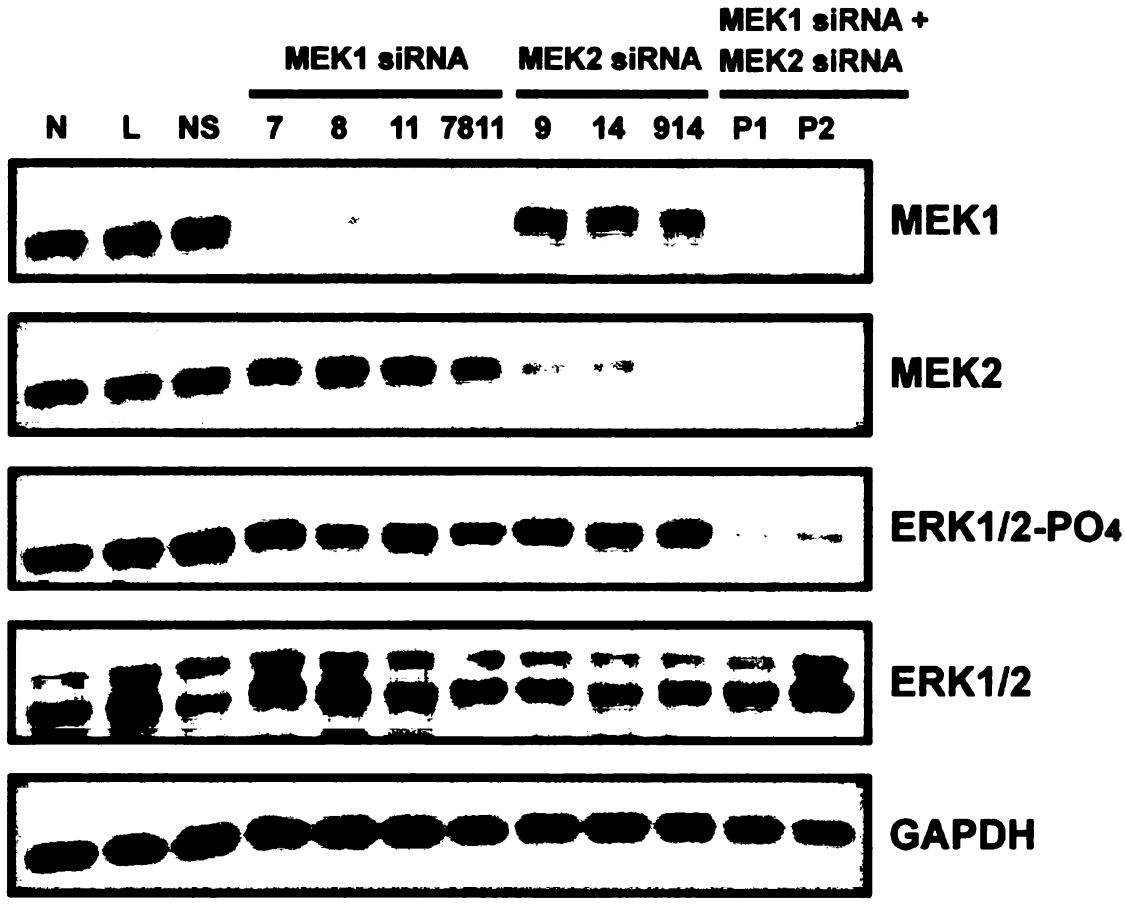

Figure 13. Individual MEK signaling in LeTx-treated SK-MEL-28 cells.

SK-MEL-28 parental cells and cells stably expressing **(A)** V5-MEK or V5-MEKcr, or **(B)** V5-*lacZ* were treated with LeTx (1 μg/ml PA plus 0, 1, 10, or 100 ng/ml LF) for 24 h. Total cell lysates were then harvested and immunoblotted with antibodies against the V5 epitope to confirm the cleavage resistance of V5-MEKcr (top panels). Antibodies against the carboxyl terminus of MEK1 (second panel) and the carboxyl terminus of MEK2 (third panel) were used to demonstrate individual MEK expression in LeTx-treated cells. Antibodies against phospho-ERK1/2 (fourth panel) and total ERK1/2 (fifth panel) were used to examine ERK activation, and an antibody against β-actin and β-tubulin were used as a loading control (bottom panels).

Figure 13. Individual MEK signaling in LeTx-treated SK-MEL-28 cells.

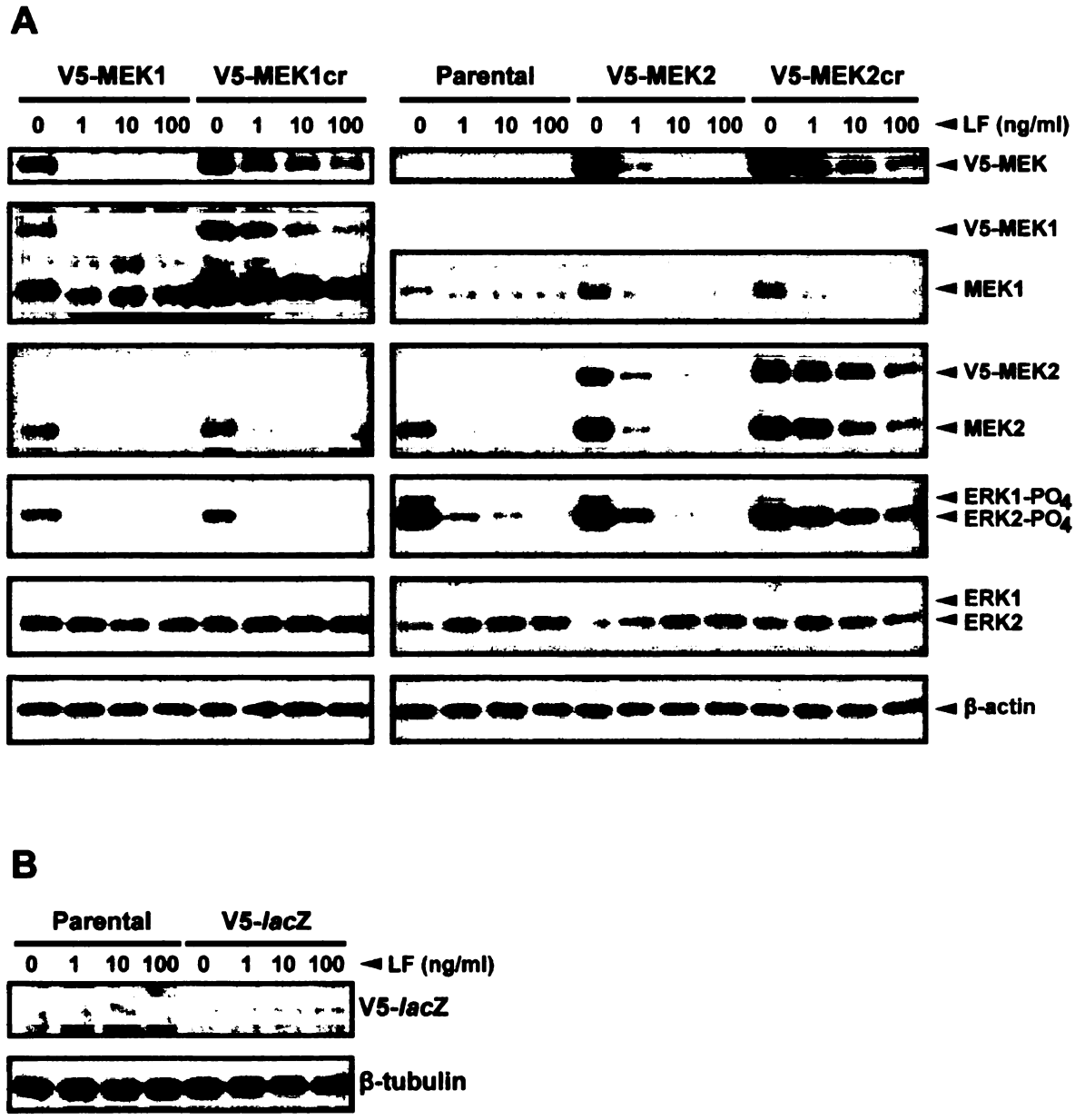

Figure 14. Overlapping and non-overlapping transcriptional targets downstream of MEK1 and MEK2.

Two sets of SK-MEL-28 parental cells and the cells stably expressing V5-*lac*Z, V5-MEK1, V5-MEK1cr, V5-MEK2, or V5-MEK2cr were treated with PA plus LF_E687C control (EC) or LeTx (LF) for 24h as described in Material and methods. **(A)** Total cell lysates were collected from cells in one of the sets for immunoblotting probed with antibodies against V5 epitope (top panel), NH_2-terminus of MEK1 (the second panel), NH_2-terminus of MEK2 (the third panel), phospho-ERK1/2 (the fourth panel), total ERK1/2 (the fifth panel), and GAPDH (bottom panel). **(B)** After control or LeTx treatment, total RNA samples were collected from the other set of cells, and subjected to cDNA microarray hybridization and data analysis. The gene expression profile in control-treated V5-*lac*Z-expressing cells was compared to that in LeTx-treated cells to generate a list of genes that were significantly changed by LeTx treatment (shaded circle). The lists of genes that were significantly rescued by MEK1 (solid circle) or MEK2 (dashed circle) were generated by comparing the gene expression profile in LeTx-treated V5-*lac*Z-expressing cells with LeTx-treated V5-MEK1cr-expressing cells or LeTx-treated V5-MEK2cr-expressing cells, respectively. The numbers of genes that were significantly changed are labeled.

Figure 14. Overlapping and non-overlapping transcriptional targets downstream of MEK1 and MEK2.

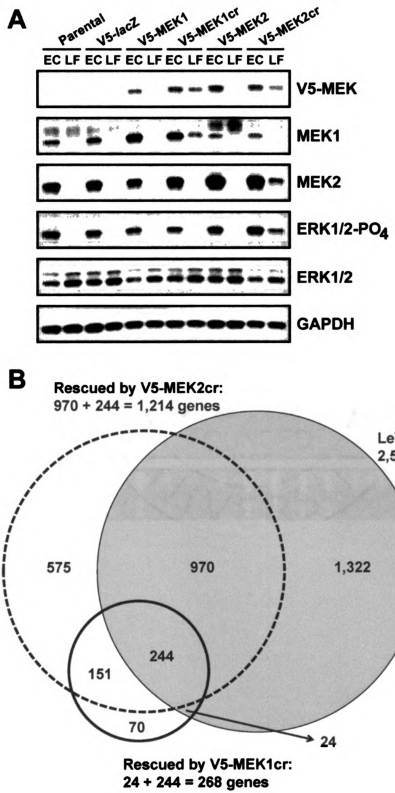

Figure 15. Expression levels of V5 fusion proteins in SK-MEL-28 cells.

Clonal SK-MEL-28 cells stably expressing V5-*lacZ* (Z) and cells expressing high (H), moderate (M), or low (L) expression levels of wild-type V5-MEK or V5-MEKcr were established as described. Parental SK-MEL-28 cells (P) were used as a control. Total cell lysates were harvested and immunoblotted with antibody against V5 epitope to detect expression levels of V5 fusion proteins (upper panel) and antibody against α tubulin for equal loading control (lower panel).

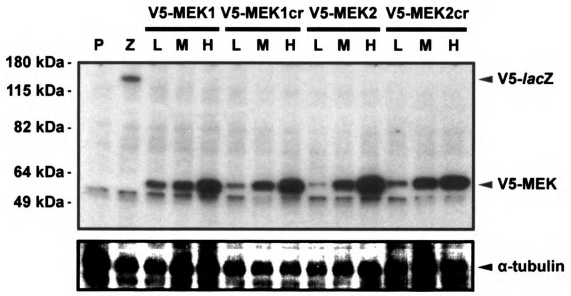

Figure 16. Inhibitory effect of LeTx on proliferation of SK-MEL-28 stable clones.

SK-MEL-28 parental cells (**A**, solid line) and the cells stably expressing V5-*lacZ* (**A**, dashed line), V5-MEK1 (**B**, green lines), V5-MEK1cr (**B**, red lines), V5-MEK2 (**C**, green lines) or V5-MEK2cr (**C**, red lines) with different V5-fusion protein expression levels: low (**B** and **C**, dashed lines), moderate (**B** and **C**, thin solid lines) or high (**B** and **C**, thick solid lines) were tested for their sensitive to LeTx by doing a toxicity assay as described. The *x* axis represents the concentration of LF. The *y* axis represents relative viability normalized by PA alone control. Data presented in this figure is a representative of three independent experiments. Error bars represent standard divisions of triplicate wells in the assay. Images in this figure are presented in color.

Figure 16. Inhibitory effect of LeTx on proliferation of SK-MEL-28 stable clones.

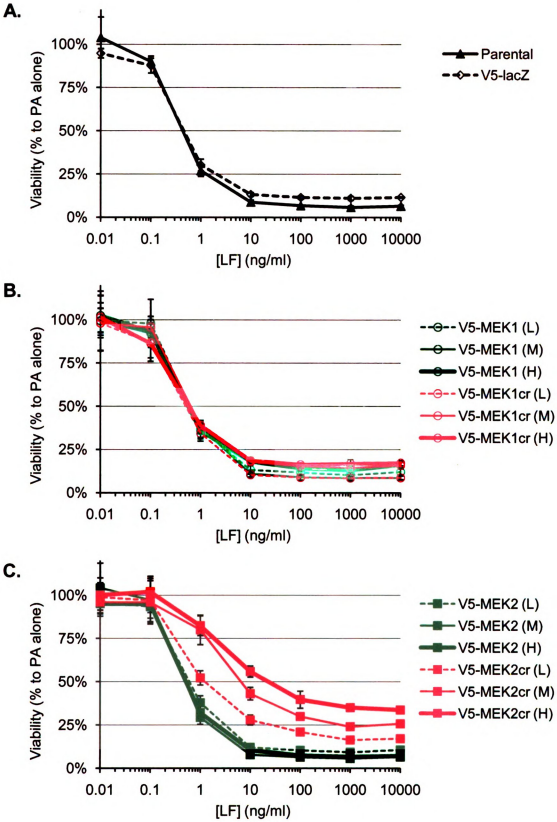

Figure 17. Sensitivities of SK-MEL-28 cells to LeTx and MEK inhibitors.

SK-MEL-28 parental cells and the cells stably expressing V5-*lac*Z, or expressing low (L), moderate (M), or high (H) levels of wild-type V5-MEK or V5-MEKcr, were tested for their sensitivities to LeTx, U0126, or PD184352 by use of toxicity assays as described in Materials and methods. (A set of representative proliferation curves is shown in Figure 16). The IC_{50} values for each stable cell line were normalized to the IC_{50} of parental cells. Results are presented as an average of the change of at least three independent experiments ± S.D. Statistical significance was determined by one-way ANOVA (http://www.physics.csbsju.edu/stats/anova_NGROUP_NMAX_form.html) followed by post-hoc analysis (http://graphpad.com/quickcalcs/posttest1.cfm). *P* values were greater than 0.05 except for (*) $p < 0.005$, and (**) $p < 0.00001$.

Figure 17. Sensitivities of SK-MEL-28 cells to LeTx and MEK inhibitors.

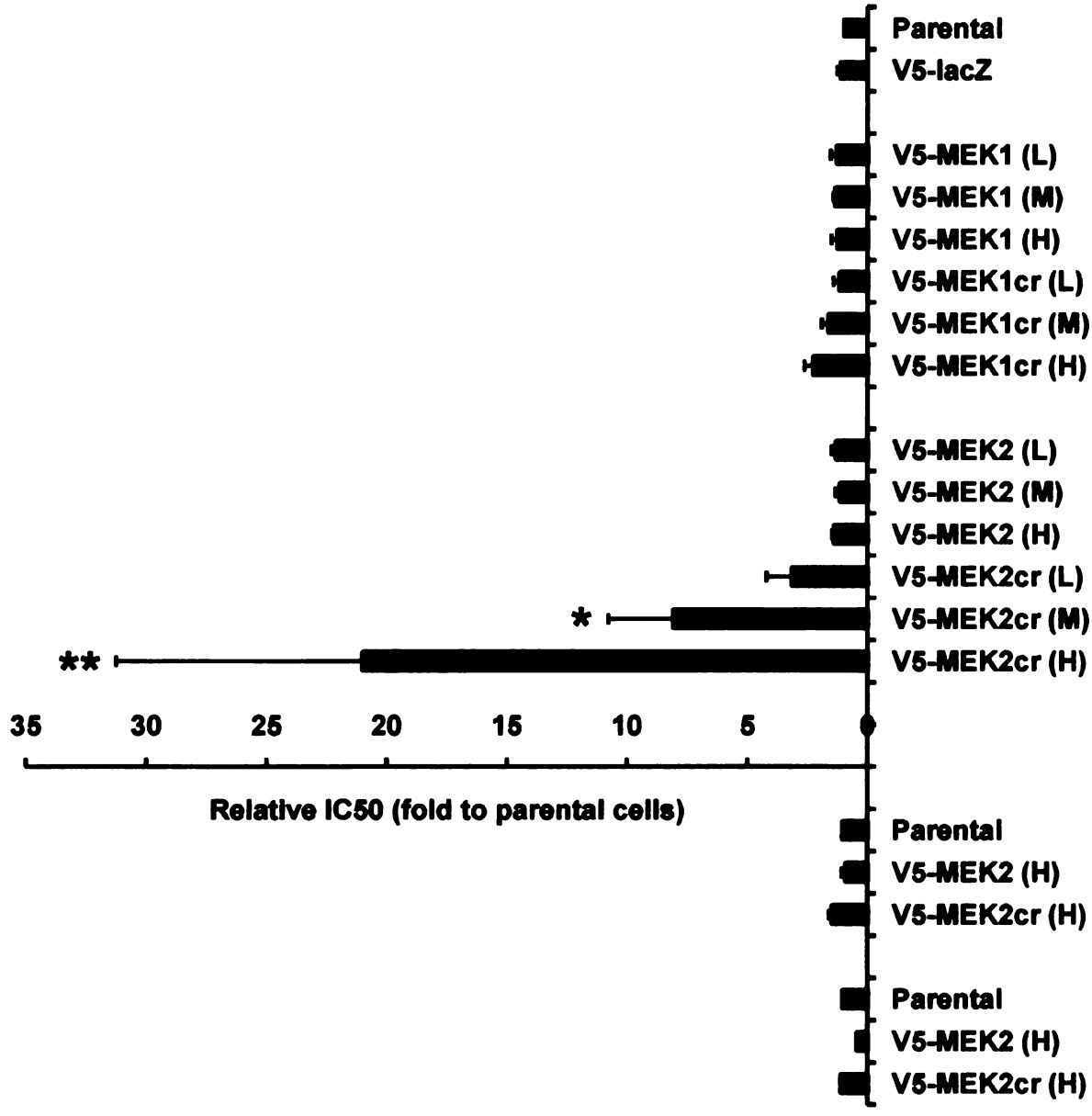

Figure 18. LeTx treatment inhibits p38 and JNK MAP kinase activation in SK-MEL-28 cells.

SK-MEL-28 cells were treated with PA alone control or LeTx for 24 h followed by UV treatment as described in Materials and methods. Whole cell extracts were prepared and subjected to immunoblotting as described in Materials and methods. Activities of p38 MAPK (top panel) and JNK (middle panel) were detected by antibodies against phospho-p38 MAPK and phospho-JNK respectively. GAPDH (bottom panel) expression levels were detected as the equal loading control.

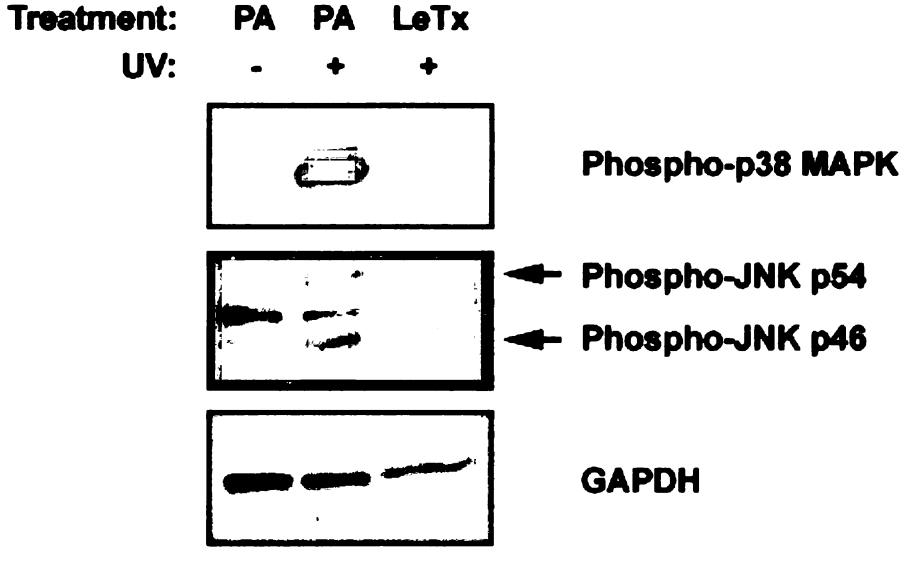

Figure 19. Sensitivity of V5-MKK3cr- and V5-MKK6cr-expressing cells to LeTx.

SK-MEL-28 parental cells and the cells stably expressing V5-*lacZ*, or expressing low (L), moderate (M), or high (H) levels of V5-MKK3, V5-MKK3cr, V5-MKK6, or V5-MKK6cr were tested for their sensitivities to LeTx as described in Material and methods and the legend of Figure 17. The IC_{50} values for each stable cell line were normalized to the IC_{50} of parental cells. Results are presented as an average of the change of at least three independent experiments ± S.D. Statistical significance was determined by one-way ANOVA (http://www.physics.csbsju.edu/stats/anova_NGROUP_NMAX_form.html) followed by post-hoc analysis (http://graphpad.com/quickcalcs/posttest1.cfm). *P* values were greater than 0.05 except for (*) $p < 0.05$. Image in this figure is presented in color.

Figure 19. Sensitivity of V5-MKK3cr- and V5-MKK6cr-expressing cells to LeTx.

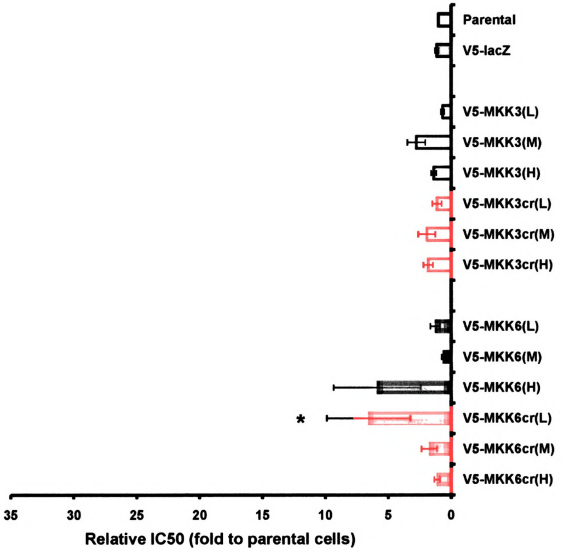

Figure 20. Sufficiency of MEK2 signaling pathway for anchorage-independent growth of SK-MEL-28 cells.

SK-MEL-28 parental cells and cells stably expressing V5-*lac*Z or high levels of wild-type V5-MEK or V5-MEKcr were seeded as single-cell suspensions in soft agar and then treated with PA alone control or LeTx, as described in Materials and methods. After treatment (21 days), colonies were fixed and stained with 1% crystal violet prepared in 10% ethanol. **(A)** Representative images of colonies grown in soft agar in the presence of PA alone or LeTx. Bars, 1mm. **(B)** Anchorage-independent growth was quantified, and the colony density was determined by dividing the number of colonies by the area and then normalizing to the colony density of the parental cells treated with PA alone. One-way ANOVA followed by post-hoc analysis were performed to determine statistical significance. *P* values were greater than 0.05 except for (*), $p < 0.00001$.

Figure 20. Sufficiency of MEK2 signaling pathway for anchorage-independent growth of SK-MEL-28 cells.

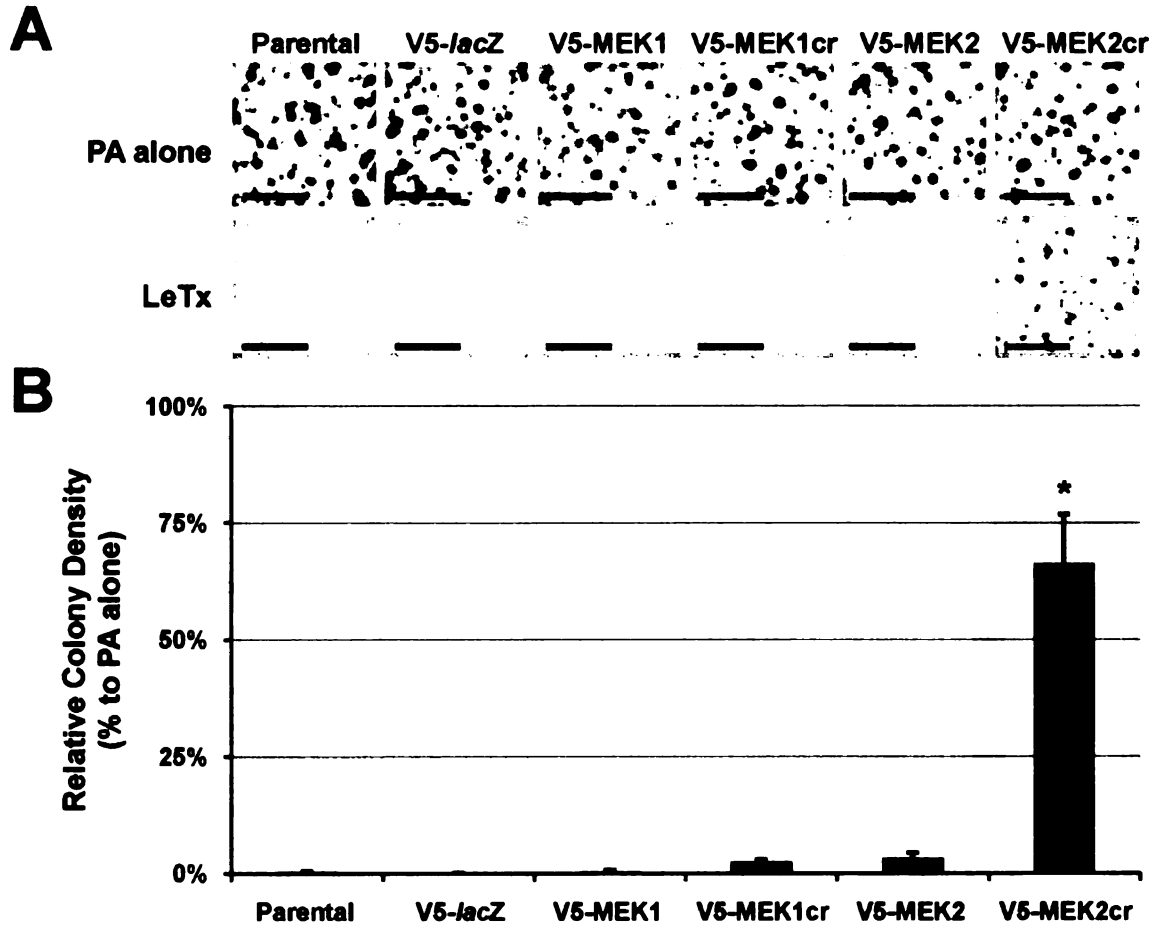

Figure 21. SK-MEL-28 xenograft tumor growth and systemic treatment with LeTx.

SK-MEL-28 xenograft tumors were established as described in Material and methods. Briefly, cells were subcutaneously injected at a number of 10^7 cells in 100 μl of Hanks' balanced salt solution (HBSS) into the right side of the dorsalateral area of groups of ten athymic nude mice. Tumor volumes were measured every two days by using a caliper. After the average volume of tumors in the group reached to 50 mm^3, mice were divided to two groups. Five mice in each group were intravenously injected with either LeTx (PA plus LF) or control (PA plus LF_E687C, an inactive form of LF) prepared in 50 μl of HBSS at a dosage of one standard dose (1×SD) every two days for a total of six injections (6×SD total). One standard dose equals 10 μg of PA plus 2 μg of LF or LF_E687C. Xenograft tumor growth is presented by average tumor volume (*y axis*) as a function of time (*x axis*). The thick solid line represents the tumor growth before treatment. The dashed line represents the growth of control-treated tumors. The thin solid line represents the growth of LeTx-treated tumors. Error bars represent standard deviations of tumor volumes.

Figure 21. SK-MEL-28 xenograft tumor growth and systemic treatment with LeTx.

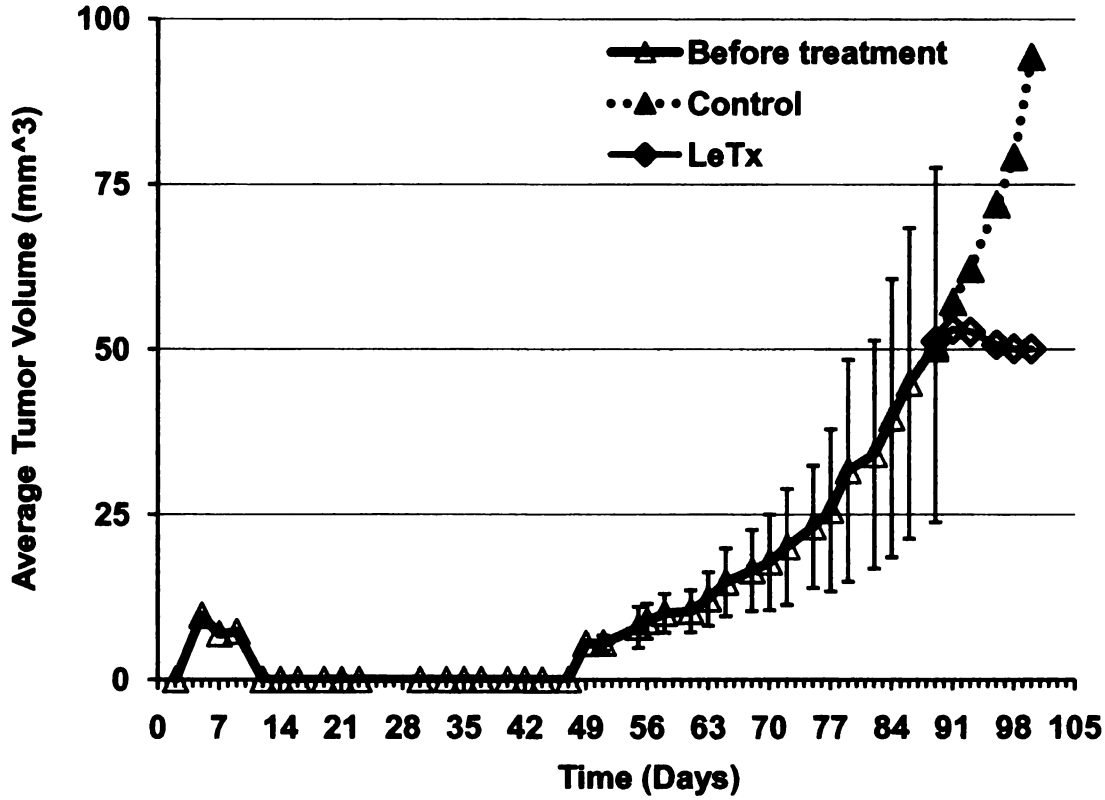

Figure 22. Reproducibility of SK-MEL-28 xenograft tumor growth in athymic nude mice.

SK-MEL-28 xenograft tumors were established as described in Material and methods and the legend of Figure 21. Xenograft tumor growth is presented by average tumor volume (*y axis*) as a function of time (*x axis*). Tumor growth curves from five independent experiments are presented as lines with different colors and indicated by ND xenograft project numbers. Total numbers (*n*) of mice used in each project are indicated. Image in this figure is presented in color.

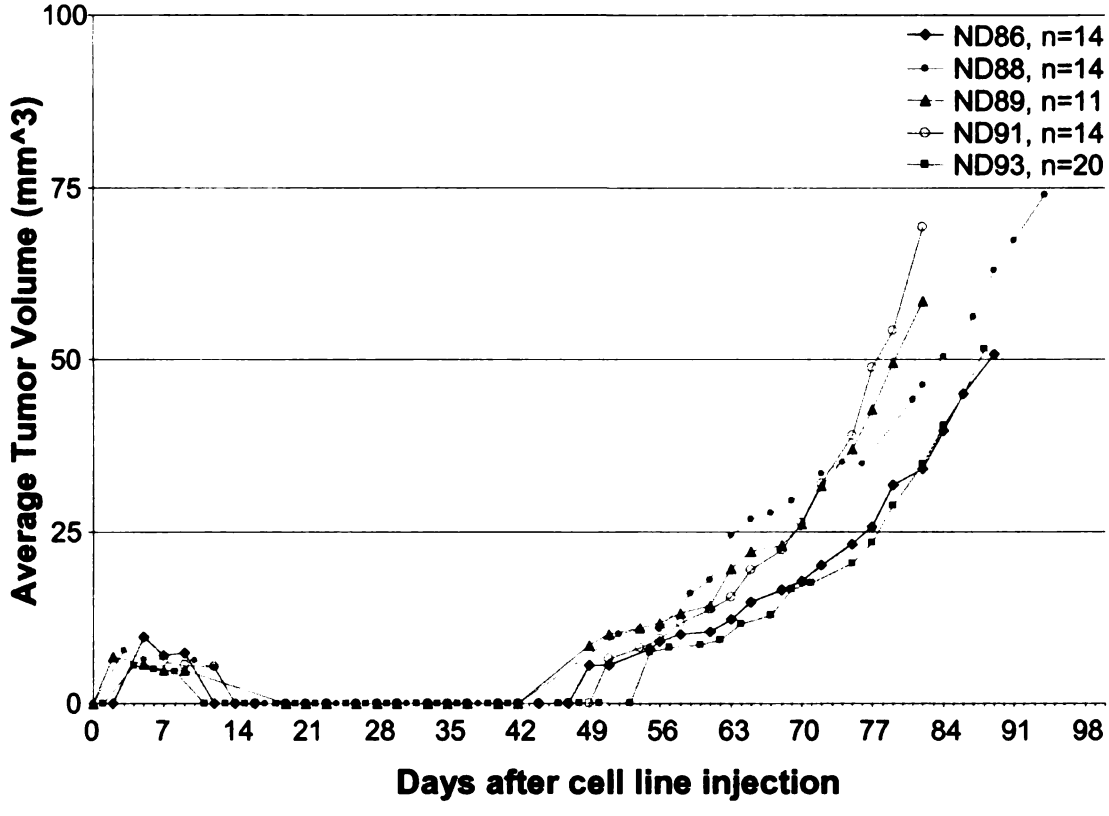

Figure 23. Sensitivity of V5-MEK1cr-expressing xenograft tumors to LeTx.

SK-MEL-28 parental xenograft tumors (black lines) and tumors expressing V5-MEK1 (green lines) or V5-MEK1cr (red lines) were established as described in Material and methods and the legend of Figure 21. After the average volume of tumors in each group reached to 75 mm^3, mice were divided to two groups. Five mice in each group were intravenously injected with either LeTx (PA plus LF) or control (PA plus LF_E687C) at a dosage of one standard dose (1×SD) every two days for a total of six injections (6×SD total). One standard dose equals 10 μg of PA plus 2 μg of LF or LF_E687C. Xenograft tumor growth is presented by average tumor volume (*y axis*) as a function of time (*x axis*). The thick solid lines represent the tumor growth before treatment. The dashed lines represent the growth of control-treated tumors. The thin solid lines represent the growth of LeTx-treated tumors. Error bars represent standard deviations of tumor volumes. Image in this figure is presented in color.

Figure 23. Sensitivity of V5-MEK1cr-expressing xenograft tumors to LeTx.

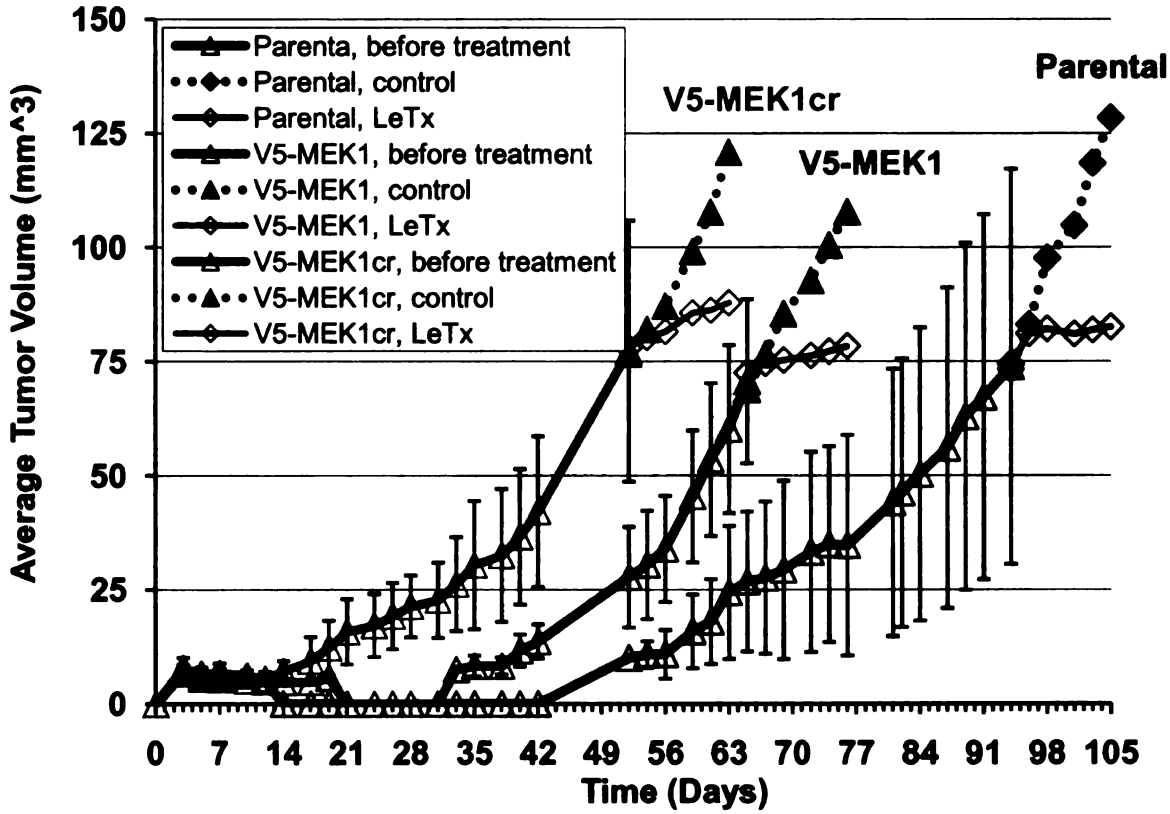

Figure 24. Sensitivity of V5-MEK2cr-expressing xenograft tumors to LeTx.

SK-MEL-28 parental xenograft tumors (black lines) and tumors expressing V5-MEK2 (green lines) or V5-MEK2cr (red lines) were established as described in Material and methods and the legend of Figure 21. After the average volume of tumors in each group reached to 50-70 mm^3, mice were divided to two groups. Five mice in each group were intravenously injected with LeTx (PA plus LF) or control (PA plus LF_E687C) at a dosage of one standard dose (1×SD) every two days for a total of six injections (6×SD total). One standard dose equals 10 μg of PA plus 2 μg of LF or LF_E687C. Xenograft tumor growth is presented by average tumor volume (*y axis*) as a function of time (*x axis*). The thick solid lines represent the tumor growth before treatment. The dashed lines represent the growth of control-treated tumors. The thin solid lines represent the growth of LeTx-treated tumors. Error bars represent standard deviations of tumor volumes. Image in this figure is presented in color.

Figure 24. Sensitivity of V5-MEK2cr-expressing xenograft tumors to LeTx.

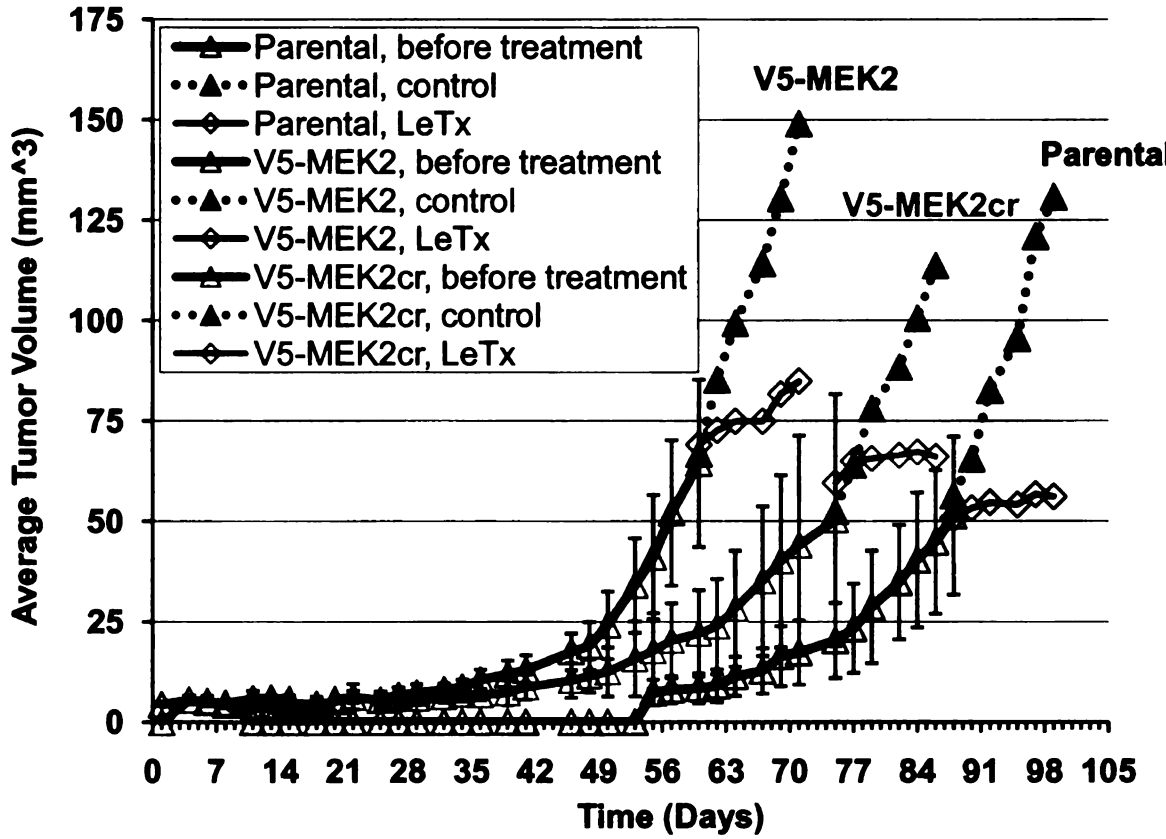

Figure 25. Does-dependent effect of LeTx on SK-MEL-28 xenograft tumor growth.

SK-MEL-28 parental xenograft tumors (black lines) and tumors expressing V5-MEK2 (green lines) or V5-MEK2cr (red lines) were established in 20 athymic nude mice as described in Material and methods and the legend of Figure 21. After the average volume of tumors in each group reached to 50-70 mm^3, mice were divided to four groups. Five mice in each group were intravenously injected with PA plus LF_E687C control (solid triangles) at a dosage of one standard dose, or LeTx (PA plus LF) at a dosage of 1 (open diamonds), 0.5 (open squares), or 0.25 (closed circles) standard dose every two days for a total of six injections. One standard dose equals 10 μg of PA plus 2 μg of LF or LF_E687C. Xenograft tumor growth is presented by average tumor volume (*y axis*) as a function of time (*x axis*). The thickest solid lines with open triangle data points represent the tumor growth before treatment. Error bars represent standard deviations of tumor volumes. Image in this figure is presented in color.

Figure 25. Does-dependent effect of LeTx on SK-MEL-28 xenograft tumor growth.

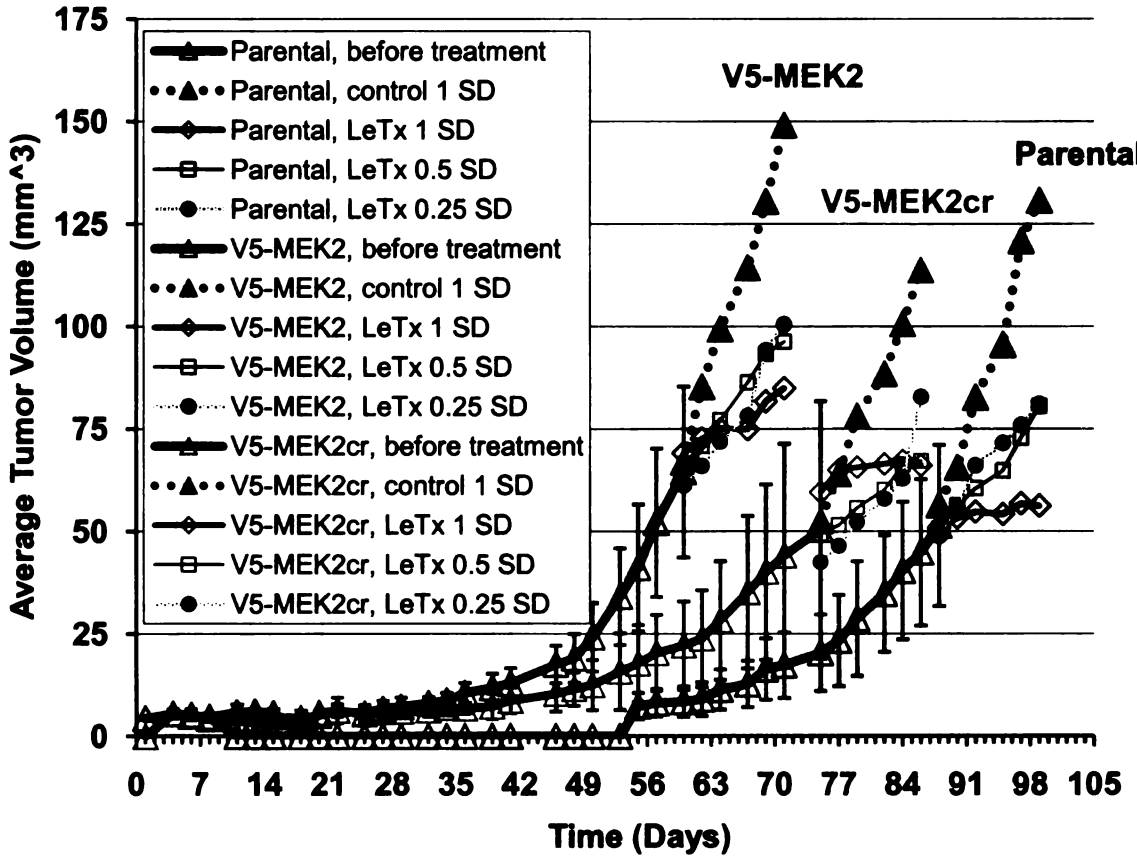

Figure 26. Loss of V5-MEKcr expression in SK-MEL-28 xenograft tumors.

Athymic nude mice bearing SK-MEL-28 xenograft tumors or tumors expressing V5-MEK1, V5-MEK1cr, V5-MEK2, or V5-MEK2cr were intravenously injected with control (PA plus LF_E687C) or LeTx (PA plus LF) as described. Tumors were dissected from mice after the end of the experiments. Tumor lysates were prepared and Selected tumor lysate samples (indicated by tumor identification numbers) were then immunoblotted with antibodies against V5 epitope (top panel), phospho-ERK1/2 (middle panel), and GAPDH (bottom panel).

Figure 26. Loss of V5-MEKcr expression in SK-MEL-28 xenograft tumors.

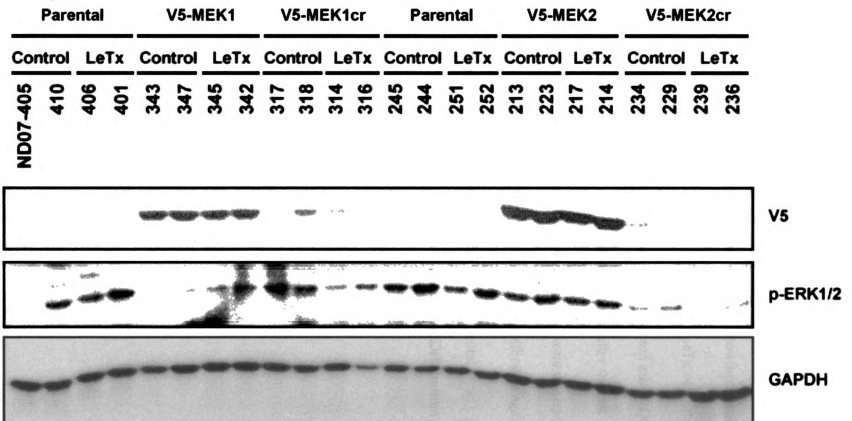

Figure 27. Systemic treatment of LeTx does not cause MEK cleavage in SK-MEL-28 xenograft tumor cells.

SK-MEL-28 parental xenograft tumors were established in athymic nude mice and LeTx was administrated intravenously as described with the following minor modification. Two days after the 5^{th} intravenous injection, the 6^{th} LeTx or control treatment (1 SD) was switched to intratumoral injection (it) on selected mice. Other mice still received the 6^{th} intravenous injection (iv). Twenty-four hours after the last administration, tumors (indicated by tumor identification numbers) were dissected for tumor lysates preparation. Immunoblotting was performed using antibodies against NH_2-terminus of MEK1 (top panel), carboxyl terminus of MEK1 (the second panel), phospho-ERK1/2 (the third panel), total ERK1/2 (the fourth panel), and GAPDH (bottom panel).

Figure 27. Systemic treatment of LeTx does not cause MEK cleavage in SK-MEL-28 xenograft tumor cells.

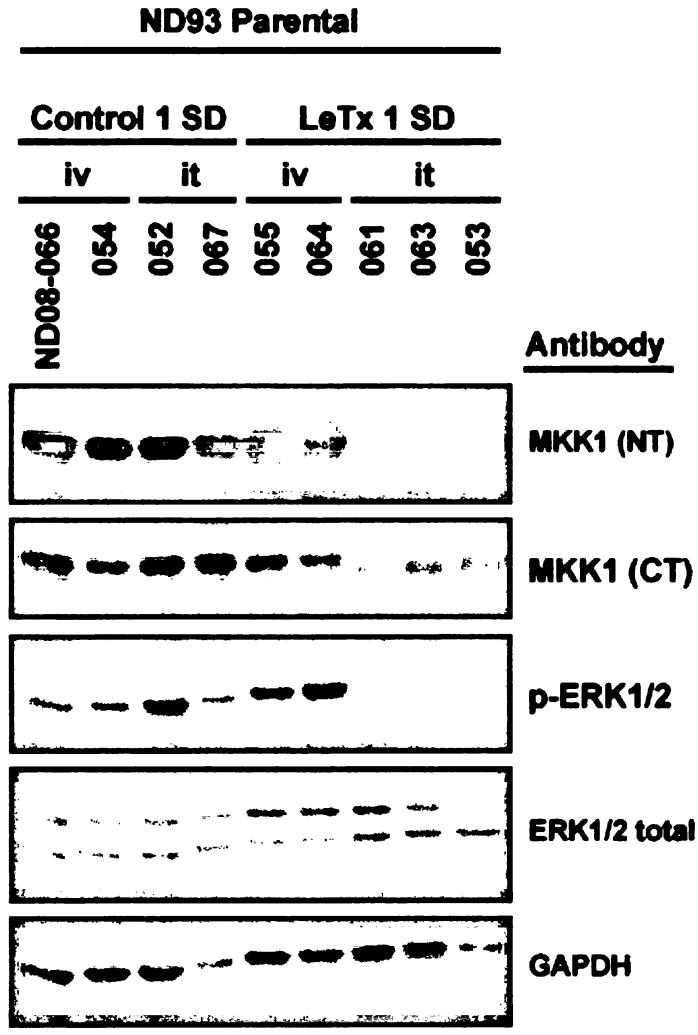

Figure 28. Unsupervised clustering of gene expression changes in LeTx-treated cells.

SK-MEL-28 parental cells and the cells stably expressing V5-*lac*Z, V5-MEK1, V5-MEK1cr, V5-MEK2, or V5-MEK2cr were treated with PA plus LF_E687C control (EC) or LeTx (LF) for 24h as described in Material and methods. Total RNA samples were collected and subjected to cDNA microarray hybridization and data processing as described in Material and methods. Three independent experiments (indicated by _A, _B, and _C) were performed to generate statistical significance. Total RNA isolated from control V5-*lac*Z-expressing cells (treated with PA plus LF_E687C) were used as a gene expression reference control to normalize the changes in LeTx-treated V5-*lac*Z-, V5-MEK1cr-, and V5-MEK2cr-expressing cells. Normalized gene expression changes were organized by hierarchical clustering.

Figure 28. Unsupervised clustering of gene expression changes in LeTx-treated cells.

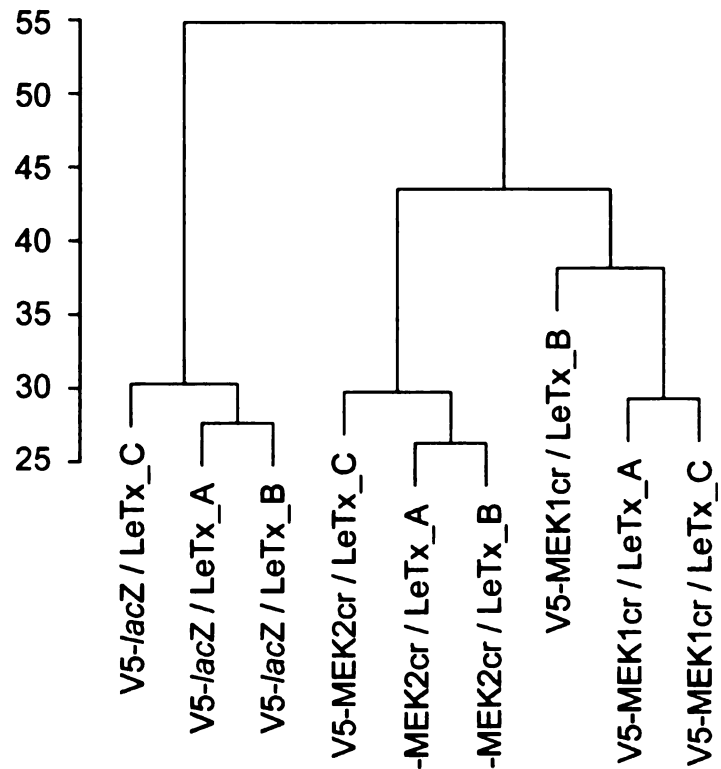

1.5. Materials and methods

1.5.1. Cell lines and stable cell line establishment.

SK-MEL-28 cells were obtained from CeeTox Inc. and grown in RPMI 1640 medium supplemented with 5% FBS and 50 units/ml penicillin/streptomycin. Cells were cultured at 37°C in a humidified 5% CO_2 incubator. To establish stable cell lines, SK-MEL-28 cells were transfected with V5-MEK, V5-MEKcr or V5-*lac*Z control expression vectors by using Lipofectamine 2000™ (Invitrogen) according to the manufacturer's instructions. Clonal stable transfectants were selected against 1 mg/ml Geneticin®. Expression levels of V5-fusion proteins in each stable clone were determined by immunoblotting. After stable cell lines were isolated, cells were maintained in medium containing 0.5 mg/ml Geneticin®. One day before subsequent assays, stable cells were subcultured once, and cultured in culture medium without Geneticin®.

1.5.2. Chemicals and LeTx

U0126 (Calbiochem) and PD 184352 (USBiological) were dissolved in dimethyl sulfoxide (DMSO) (Sigma) at a stock concentration of 100 mg/ml. PA and LF were expressed in an attenuated strain of Bacillus anthracis (BH445) and purified by fast pressure liquid chromatography as described (Bromberg-White & Duesbery, 2008).

1.5.3. siRNA-mediated MEK knock down.

Multiple siRNAs specifically against human MEK1 or MEK2 and AllStars non-silencing control siRNA were purchased from Qiagen. To deliver siRNA into SK-MEL-28 cells, the siLentFect™ Lipid (Bio-Rad) was used as the transfection reagent. To do this, SK-MEL-28 cells (3×10^5 cells) were seeded and cultured in 60-mm dishes. The next day, cells were washed three times with PBS and covered with 1.6 ml of OPTI-MEM®I (Invitrogen), to which siRNA:Lipid complexes (prepared as described below) were then added. To prepare siRNA:Lipid complexes, 10 µl of lipid was added into 30 µl of OPTI-MEM®I and incubate at room temperature for five minutes. The prepared lipid was then added into 360 µl of OPTI-MEM®I containing 100 pmole of each control or MEK siRNAs plus 100 pmole of AlexaFluor488-conjugated non-silencing siRNA, and incubated at room temperature for 20 minutes to allow siRNA:Lipid complexes form. Eight hours after addition of siRNA:Lipid complexes, cells were then trypsinized and split to two 60-mm dishes and culture in DMEM containing 10 % FBS and 50 units/ml penicillin/streptomycin for 72 hours. At this time point, AlexaFluor488 fluorescence could be observed in greater than 95% of cells under a fluorescence microscope (data not shown), indicating a high efficiency of siRNA transfection. Cells were then harvested for immunoblotting and cell cycle analysis.

1.5.4. In-cell MEK cleavage assay in SK-MEL-28 cells.

SK-MEL-28 parental cells and cells stably expressing V5-fusion proteins were treated with LeTx in a LF concentration-dependent manner (1 µg/ml PA plus 0, 1, 10, 100 ng/ml LF) for 24h. Total cell lysates were collected on ice in RIPA lysis buffer [50

mM Tris-HCl pH 7.5, 150 mM NaCl, 1 mM EDTA, 1 mM EGTA, 2 mM Na_3VO_4, 20 mM sodium pyrophosphate, 1% sodium deoxycholate, 1% Triton X-100, 0.1% SDS, and 1 × EDTA-free protease inhibitor cocktail (Roche)] and homogenized by sonication in ice bath. Protein concentrations were determined by BCA™ Protein Assay Kit (Pierce) according to the manufacturer's instructions. Lysates were then prepared in SDS sample buffer [47.5% Laemmli Sample Buffer (Bio-Rad) and 2.5% β-mercaptoethanol (Sigma)]. Five micrograms of total cell lysates were subjected to immunoblotting to detect LF-mediated cleavage and ERK activation as described in the results.

1.5.5. Immunoblotting.

Five micrograms of total cell lysates were separated in 10% Novex® Pre-Cast Tris-Glycine Gels (Invitrogen) and then electro-transferred onto polyvinylidene fluoride (PVDF) membranes (Millipore) according to the manufacturers' instructions. Membranes were then soaked in 5% non-fat milk for 1 hour and hybridized with primary antibodies against V5 epitope (Bethyl Laboratories), NH_2-terminus of MEK1 (Upstate, #07-641), COOH-terminus of MEK1 (Santa Cruz Biotechnology, SC-219), NH_2-terminus of MEK2 (Santa Cruz Biotechnology, SC-524), COOH-terminus of MEK2 Santa Cruz Biotechnology, SC-525), phospho-ERK (Cell Signaling, #9106), ERK (Cell Signaling, #9102), phospho-p38 MAPK (Cell Signaling #4631), phospho-JNK (Cell Signaling #9255), α-tubulin (Sigma, T9026), β-tubulin (Sigma, T5201), β-actin (Sigma, A1978), or GAPDH (Cell Signaling, #2118) at 4°C for overnight. Conditions for primary antibody hybridizations were followed according to the antibody datasheets.

After primary antibody hybridization, membranes were washed three times in TBST buffer (50 mM Tris, 150 mM NaCl, and 0.1% Tween-20), hybridized with HRP-conjugated secondary antibodies according to the instructions of the antibodies, and then washed three times in TBST buffer. Immunoblotting signals were then detected by LumiGLO™ Reagent and Peroxide (Cell Signaling).

1.5.6. Toxicity assay.

For LeTx toxicity assay, SK-MEL-28 cells (1,500 cells) were cultured in 96-well plates for 24 hours, and then treated with control (1 μg/ml PA) or LeTx (1 μg/ml PA plus 0.01-10,000 ng/ml LF) for 72h. For U0126 toxicity assay, cells were treated with DMSO control or 1-100,000 nM U0126 for 72h. For PD 184352 toxicity assay, cells were treated with DMSO control or 0.01-10,000 nM PD 184352 for 72h. Cell viability was determined by using CellTiter 96® Aqueous Non-Radioactive Cell Proliferation Assay (Promega) according to the manufacturer's instructions. LeTx toxicity was presented by plotting the relative viability (normalized by no LF control) against LF concentrations. IC_{50} values were determined by SigmaPlot software.

1.5.7. SK-MEL-28 tumor xenograft and LeTx systemic treatment

SK-MEL-28 parental cells or cells stably expressing V5-MEK or V5-MEKcr were cultured in exponential growth phase and then collected in Hanks' balanced salt solution (HBSS) (Invitrogen) at a density of 10^8 cells/ml. Cells were then subcutaneously injected at a number of 10^7 cells (in 100 μl of HBSS) into the right side

of the dorsalateral area of groups of ten athymic nude mice (Charles River Laboratories). Tumor volumes were measured every two days by using a caliper. Animal health and tumor volume were monitored till the end of the experiment. After the average volume of tumors in the group reached to 50 mm^3, mice were divided to two groups. Five mice in each group were intravenously injected with either LeTx (PA plus LF) or control (PA plus LF_E687C, an inactive form of LF) prepared in 50 μl of HBSS at a dosage of one standard dose (1×SD) every two days for a total of six injections (6×SD total). One standard dose equals 10 μg of PA plus 2 μg of LF or LF_E687C. Two hours after the last injection, mice were euthanized and tumors were dissected for subsequent analysis. To prepare tumor lysates for immunoblotting, tumors were homogenized in RIPA lysis buffer on ice, and clear tumor lysates were harvested by centrifugation.

To treat tumors in a LeTx does-dependent manner (Figure 25), cells were inoculated in 20 mice. After tumors established, mice were divided into four groups, and mice in each group were intravenously injected with 1×SD control (PA plus LF_E687C) or 1, 0.5, or 0.25×SD LeTx (PA plus LF) for a total of six injections.

To test if MEK in xenograft tumor cells was still cleavable by LF (Figure 27), two days after the 5^{th} intravenous injection, the 6^{th} control and LeTx treatment were switched to intratumoral injection on selected mice. Other mice still received the 6^{th} intravenous injection. Twenty-four hours after the 6^{th} injection, mice were euthanized and tumors were dissected for subsequent analysis.

1.5.8. Anchorage-independent growth assay.

Anchorage-independent growth assays were performed as previously described (Ding *et al.*, 2008). Briefly, 10,000 cells were prepared as single cell suspensions in 0.35% agar prepared in a volume of 1 ml of culture media, and then seeded onto 1 ml of hard agar (1% agar prepared in culture media) in 12-well plate. One day after cell seeding, 1 ml of culture media containing PA along control (1 μg/ml PA) or LeTx (1 μg/ml PA and 0.01 μg/ml LF) were added on the top of cell-containing agar layer. Cells were then incubated at 37°C in a humidified 5% CO_2 incubator. The PA- or LeTx-containing culture media was replaced every 2-3 days for a total of 21 days. Colonies were then fixed and stained with 1% crystal violet prepared in 10% ethanol for observation. Images were then taken under a dissecting microscope. Colonies were quantified using Imagine software (Ding *et al.*, 2008). Unsaturated area was selected, and colonies larger than 50 μm in the area were counted by the software. Colony density was determined by normalizing colony numbers by area size.

1.5.9. Human cDNA microarray and transcriptional signature analysis.

Two sets of SK-MEL-28 parental cells and cells stably expressing V5-*lac*Z, V5-MEK1, V5-MEK1cr, V5-MEK2, or V5-MEK2cr were treated with LeTx (1 μg/ml PA plus 10 ng/ml LF) or control (1 μg/ml PA plus 10 ng/ml LF_E687C) for 24 h. Totally cell lysates were collected from one of the two sets and subjected to immunoblotting to confirm MEK status and LeTx treatment. Total RNA samples were prepared from the other set of cells using a *mir*Vana™ RNA isolation kit (Ambion). Four RNA samples (control-treated V5-*lac*Z-expressing cells, LeTx-treated V5-*lac*Z-, V5-MEK1cr, and V5-

MEK2cr-expressing cells) were submitted to the Microarray Core Laboratory at the Van Andel Research Institute for microarray hybridization. A total of three independent experiments were performed. Gene expression profiles (n=12) were generated using the Agilent 60-mer Whole Human Genome 44k Microarray platform (Agilent) according to the manufacturer's instructions. All subsequent analysis was performed using the Bioconductor software environment. Microarray data was processed and normalized using the *limma* Bioconductor package (Gentleman *et al.*, 2004; Patterson *et al.*, 2006).

Gene set enrichment analysis was then performed using the PGSEA Bioconductor package (Furge *et al.*, 2007a) with only the most significant results shown. A signature was determined to be uniquely rescued by V5-MEK1cr or V5-MEK2cr when it satisfied two criteria. First, the signature in V5-*lac*Z-expressing cells had to have a highly significant ($p < 0.005$) positive or negative response to LeTx treatment while in cells expressing V5-MEK1cr or V5-MEK2cr showed a highly significant ($p < 0.005$) response to LeTx treatment in the opposite direction. Second, the signature in cells expressing the other V5-MEKcr isoform did not demonstrate a highly significant ($p < 0.005$) to LeTx treatment. Differentially expressed genes were identified using a moderated t-statistic as implemented in the *limma* Bioconductor package. Significance values were adjusted using the false discovery rate (FDR) method to compensate for multiple testing.

1.5.10. Examination of p38 MAPK and JNK activations in SK-MEL-28 cells.

Two sets of SK-MEL-28 parental cells were cultured and treated with PA alone (1 μg/ml PA) or LeTx (1 μg/ml PA plus 0.1 μg/ml LF) for 24h as described. One set of the cells were then subjected to UV treatment as positive controls for detecting p38 MAPK

and JNK activation using immunoblotting. The other set of the cells were used to detect basal activities of p38 MAPK and JNK. To treat cells with UV, the toxin-containing culture media were collected into a sterile tube. Culture dishes were placed in a UV Stratalinker (Stratagene) with the lid removed. Cells were then exposed to UV for 1 min (time mode). Control cells were exposed to air for 1 min as the non-UV-treated control. After UV or control treatment, the toxin-containing media were added back to the culture dishes, and cells were cultured for 2h. Total cell lysates were then harvested, and immunoblotting was performed to detect p38 MAPK and JNK activities.

Chapter IV. General discussion

To better understand the critical role of MEK signaling pathways in melanoma biology, it is important to determine both necessity and sufficiency of MEK signaling pathways for melanoma cell proliferation. For this purpose, two complementary approaches were used. First, MEK-specific siRNA was used to specifically knock down either MEK1 or MEK2 in human melanoma SK-MEL-28 cells and to determine the necessity of MEK1 and MEK2 signaling pathways for melanoma cell proliferation. Second, a novel experimental system was developed for determining the sufficiency of MEK1 and MEK2 signaling pathways for SK-MEL-28 cell proliferation. This experimental system utilizes the proteolytic activity of anthrax lethal toxin to inhibit multiple MEK/MKK signaling pathways in SK-MEL-28 cells. Simultaneously, either MEK1 or MEK2 was rescued by expressing a mutant MEK1 or MEK2 which is resistant to LF-mediated cleavage. Combining the siRNA technology and the novel experimental system, I determined both necessity and sufficiency of MEK1 and MEK2 signaling pathways for SK-MEL-28 melanoma cell proliferation, and made the following conclusions. First, neither MEK1 nor MEK2 signaling pathway is necessary for SK-MEL-28 cell proliferation as loss of one of the MEKs can be compensated by the other isoform. Second, the MEK2 signaling pathway alone is sufficient to drive SK-MEL-28 cell proliferation, but MEK1 is not. Third, while MEK2 can compensate for loss of MEK1, MEK1 can compensate for loss of MEK2 only when an as yet identified factor is present. From this work, several interesting observations and valuable information were obtained. These will be discussed in this Chapter.

1.1.Experimental tools to study MEK and MKK functions

I have used three distinct experimental tools to study MEK/MKK functions; small-molecule inhibitors, RNA interference, and LeTx. Each of these has its strengths and weaknesses depending on the needs of a study. This will be discussed as follows.

Small-molecule inhibitors are easy handled and delivered. Treating cultured cells with small-molecule inhibitors does not require transfection, and animals can often be treated with these inhibitors simply by oral gavage. In addition, small-molecule inhibitors directly target the proteins as opposed to the mRNAs. This generally gives a better efficiency compared to using siRNAs because expression of relatively stable proteins cannot be completely inhibited by targeting their coding mRNAs. The specificities of small-molecule inhibitors is always a cause for concern (Cohen, 1999). If the MEK1/2-ERK pathways need to be targeted, the non–ATP-competitive MEK inhibitors, such as PD 184352 and its derivatives, are the best agents because of their high selectivity. However, highly selective non–ATP-competitive inhibitors targeting MKK3/6 or MKK4/7 have not been identified, and ATP-competitive inhibitors have broad off-target effects as the ATP binding site is conserved in other protein kinases. On the other hand, due to the high homology shared between MEK1 and MEK2, the non–ATP-competitive MEK inhibitors do not discriminate one from the other, so that they are not suitable for dissecting the necessity of a single isoform.

If evaluating the necessity of a specific single MEK or MKK is the goal of a study, RNA interference is the best choice as it has the highest isoform specificity. For this

purpose, siRNA may be used to knockdown the expression of only one of the family proteins in cultured cells. In addition, RNA interference also has a great advantage of being amenable to rescue experiments. A targeted mRNA can be rescued by expressing an mRNA with one or more wobble mutations introduced into the targeting site. This strategy makes the rescuing mRNA resistant to RNA interference without changing the primary protein sequence. However, delivering interfering RNA can be a challenging task. Although reagents giving high transfection efficiency of siRNA are commercially available, they are best suited for transient transfection in cell culture. If knocking down a specific gene in xenotransplanted tumors is desired, cell lines stably expressing small hairpin RNA (shRNA) need to be established first. If the targeted gene product is required for cell proliferation, an inducible system will have to be included for stable cell line establishment. In this case, leakiness of shRNA expression is another technical problem that needs to be overcome. In addition, as mentioned above, interfering RNA targets expression at the mRNA level. If the targeted gene product is relatively stable, residual protein may be a concern especially for signaling molecules that are generally very sensitive to their activators. Finally, if multiple MEK/MKK family proteins need to be simultaneously knocked down, RNA interference is not suitable. Transfecting many siRNA molecules into cell culture to target multiple MEK/MKK proteins is not expected to be an efficient method because it may decrease the efficiency of RNA interference and increase off-target effects.

LeTx is a highly selective biological inhibitor targeting MEK1/2 and most other members in the MKK protein family. As a pan MEK/MKK protease, LeTx

proteolytically inhibits multiple MEK/MKK proteins in mammalian cells, and in turn, blocks the three canonical MAPK pathways. Compared to small-molecule inhibitors and siRNA, LeTx has both advantages and disadvantages depending on the purpose of a study. Delivering LeTx is relatively easy and efficient. It does not require transfection because LeTx mediates its own entry into cells, and the toxin receptors are ubiquitously expressed in many different types of cells (Bradley *et al.*, 2001; Scobie *et al.*, 2003). In addition, the proteolytic inactivation of MEK/MKK proteins by LF is an irreversible reaction in cells, yielding an efficient durable effect. In terms of experimental design, if studying the sufficiency of a single MEK/MKK signaling pathway is the goal, LeTx plus the MEKcr/MKKcr is the only available approach. Because of these strengths, LeTx has become a powerful tool for studying the involvement of MEK/MKK signaling pathways, not only in cancers but also in other MAPK pathway-involved diseases such as inflammatory diseases (Pellizzari *et al.*, 1999; Park *et al.*, 2002; Agrawal *et al.*, 2003) and eye diseases (Bromberg-White *et al.*, 2009). On the other hand, however, LeTx does not give an objective evaluation for necessity of individual MEK/MKK signaling as LeTx targets multiple MEK/MKK. For this purpose, RNA interference technology may be included as complementary approach, as presented in this dissertation.

1.2.Non-redundant roles of MEK1 and MEK2

MEK1 and MEK2 are generally assumed to be functionally redundant as they share the same upstream activators and downstream substrates. However, a few previous studies as well as the results presented in Chapter III indicate MEK1 and MEK2 have distinct and non-overlapping biological functions. During mouse embryonic

development, loss of MEK1 expression is lethal due to placental deficiency, which is a result of reduced blood vessels in the labyrinthine layer of the placenta (Giroux *et al.*, 1999). In contrast, MEK2 is dispensable as MEK2 deficient mice are viable and fertile (Belanger *et al.*, 2003). These knock-out studies indicate that MEK1 is required for blood vessel formation during mouse embryo development, and MEK2 is not required for this process. However, they do not indicate whether MEK2 can compensate for MEK1 as the developmental patterns of expression of these kinases may be different. Scholl *et al* (2009b) recently demonstrated that MEK1 is required for DMBA/TPA-induced benign epidermal papilloma formation, but MEK2 is not required. On the other hand, Voisin *et al* (2008) have shown that shRNA-mediated MEK2 knockdown has much stronger inhibitory effect on colon cancer cell proliferation than MEK1 knockdown does, leading to the conclusion that MEK2 is more important for colon cancer cell proliferation than MEK1. Finally, I demonstrate here that MEK2 signaling is sufficient for melanoma cell proliferation, but MEK1 signaling is not. Collectively these results lead to the conclusion that MEK1 and MEK2 are functionally distinct and that their relative importance varies by cell type and activity. MEK1 signaling seems to be more critical at early stages of embryo development and the initiation step of cancer cell transformation, while MEK2 signaling is more important to maintain cell proliferation and survival after the initiation steps. Further study is needed in order to fully understand the differential roles of MEK1 and MEK2.

1.3.Complexity of the MEK/MKK signaling network

For historic reasons MEK/MKK pathways have been artificially separated into modules of three tiered kinase cascades, each of which comprises an MKK kinase (MKKK), a MEK or MKK, and a MAP kinase. However, it is becoming apparent that substantial cross-talk between these pathways may coordinately regulate cellular responses to stimuli. For example, Xia *et al.* (1995) have suggested that apoptosis in NGF-differentiated PC-12 cells is regulated by opposing activities of ERK and p38 MAPK/JNK. Similar results also have been reported by MacKeigan *et al.* (2000) showing that enhanced apoptosis in paclitaxel (Taxol)-treated cells is regulated by opposing activities of ERK and JNK. More recently, Estrada *et al.* (2009) reported the cross talk between ERK and p38 MAPK for melanoma proliferation.

In Chapter III, I used two complementary approaches to test the hypothesis that the functions of MEK1 and MEK2 are critical and interchangeable for melanoma cell proliferation. In the first series of experiments MEK-directed siRNAs were used to selectively knock-down either MEK1 or MEK2, or both, in human melanoma SK-MEL-28 cells to determine the necessity of MEK signaling pathways for melanoma cell proliferation. In these experiments I found that only simultaneous knock-down of both MEK1 and MEK2 was capable of inhibiting ERK activation and blocking cell cycle progression. This indicates that neither MEK1 nor MEK2 is necessary for these activities in melanoma cells and supports the initial hypothesis that MEK1 and MEK2 are interchangeable for melanoma cell proliferation. In the second series of experiments, the novel experimental system utilizing the specific proteolytic activity of anthrax lethal

toxin and a rescue by MEK1cr or MEK2cr was used to evaluate the sufficiency of MEK/MKK signaling pathways for SK-MEL-28 cell proliferation. Using this approach I found the MEK2 signaling pathway, but not MEK1, was sufficient to drive proliferation of SK-MEL-28 cells. This indicates that MEK1 and MEK2 are not functionally redundant. Results from these two complementary approaches lead me to formulate a new hypothesis: while MEK2 is sufficient for SK-MEL28 melanoma cell proliferation, MEK1 can compensate for loss of MEK2 only in the presence of an as yet unidentified factor. Although it is not known what this critical factor is, it compensates for the loss of MEK2 by cooperating with MEK1 to drive cell proliferation. Since activity of this factor is repressed by LeTx, this factor is likely to be another MKK or is regulated by another MKK. This finding not only supports the previous findings that cross-talk between MEK and other MKK pathways may coordinately regulate cellular functions, but also provides a better appreciation of the complexity of the MEK/MKK network and the alternative mechanisms by which cancer cells maintain their survival.

A related observation arose when we analyzed gene expression profiles in LeTx-treated V5-MEK1cr- or V5-MEK2cr-expressing cells (Chapter III section 1.2.2.2). First, we observed that not all the genes that were affected by LeTx treatment can be rescued by wither MEK1cr or MEK2cr (Figure 14 the gray area that is not covered by the solid circle and the dashed circle). Using gene set enrichment analysis we noted that the signatures in this non-rescued area are not associated with cell proliferation or cell survival (see Appendix III for the full list of the signatures). It is very likely that other MKKs are responsible for the activities of these signatures. Further analysis using other

V5-MKKcr-expressing cells should be performed to address this question. Second, we observed that in addition to the non-overlapping rescue by V5-MEK1cr and V5-MEK2cr, this analysis also revealed that MEK2- and, to a less degree, MEK1-induced transcriptional activities that were not wholly contained within the LeTx-transcriptional footprint (Figure 14, the clear areas in the V5-MEKcr rescue circles but not overlapped with the LeTx effect circle. See Appendix IV, Appendix V, and Appendix VI for the full lists of the signatures). Since LeTx is a pan MEK/MKK inhibitor, I expected that the result of MEKcr expression would relieve a sub-set of LeTx-induced transcriptional changes. However, I found that MEK2cr, and to a lesser extent MEK1cr altered the expression of genes that were unaffected by LeTx. Although it is possible that the change in expression of this group of genes is a result of forced expression of exogenous V5-MEKcr, I cannot exclude the explanation that this group of genes is subject to antagonistic regulation by MEK and at least one of the other MKKs. Changes in expression of these genes are revealed when this dynamic balance is disturbed. This observation suggests an underlying complexity of the MEK/MKK signaling that has previously not been widely appreciated. There are examples of MKK-related antagonistic co-regulation in the literature. It has been demonstrated that the survival of differentiated rat PC-12 pheochromocytoma cells in culture is dependent on the presence of nerve growth factor (NGF), and removal of NGF from the medium causes an increase in p38 MAPK and JNK activities and a decrease in ERK activity, indicating that these changes are necessary and sufficient to induce apoptosis. Interestingly, expressing constitutively activated MEK1 prevents apoptosis induced by NGF withdrawal (Xia *et al.*, 1995). These results indicate that apoptosis in NGF-differentiated PC-12 cells is

regulated by opposing activities of ERK and p38 MAPK/JNK. Similar results also have been obtained by MacKeigan *et al.* (2000) showing that enhanced apoptosis in paclitaxel (Taxol)-treated cells is regulated by opposing activities of ERK and JNK. Collectively, these results demonstrate that there is cross-talk between MEK/MKK pathways. Thus, the true function of the pathways cannot be fully appreciated if they are only considered in isolation.

1.4.Therapeutic implications

Since Ray and Sturgill's (1987; 1988a) initial discovery, the regulators of ERK activity have been recognized as playing a key role in a variety of cellular processes including tumorigenesis and cancer survival, and inhibiting the Raf-MEK-ERK pathway has become a viable therapeutic strategy against cancers. Despite their pre-clinical successes, MEK small-molecule inhibitors have not performed well in cancer clinical trials because of issues such as a lack of clinical response, insufficient efficacy, and safety concerns. As discussed earlier in Chapter I, (section 1.3.4, page 24), several facts may explain why these MEK inhibitors work well on xenograft tumors in nude mice but fail to generate clinical responses in human patients. Nevertheless I believe targeting MEK remains a viable strategy against cancers, as the Raf-MEK-ERK signaling pathway plays a pivotal role in cancer cell survival. Designing novel inhibitors with the desired selectivity for MEK may increase their potency. Alternatively, new approaches may be required in order to increase clinical response. My research and other studies have suggested that targeting multiple MEK/MKK pathways may be a better strategy for treating cancers as LeTx, a pan MEK/MKK inhibitor, inhibits not only tumor cell

proliferation, but also tumor-associated endothelial functions. This is discussed as follows.

Friedlander *et al.* (1998) provided the first evidence of the anti-tumor activity of LeTx. Following this, Duesbery *et al.* (2001) then reported its anti-cancer effects not only on cancer cell proliferation and anchorage-independent growth, but also on the growth of xenograft tumors *in vivo*. This anti-cancer effect was also observed on other types of human cancer cell xenografts (Koo *et al.*, 2002; Depeille *et al.*, 2007; Ding *et al.*, 2008; Huang *et al.*, 2008; Rouleau *et al.*, 2008). Moreover, LeTx also has been modified to selectively target cancer cells that have potential for metastasis (Abi-Habib *et al.*, 2006b; Liu *et al.*, 2008), demonstrating the potential of using LeTx to treat late-stage cancers. In addition to cancers, LeTx has been used in other disease models (Pellizzari *et al.*, 1999; Park *et al.*, 2002; Agrawal *et al.*, 2003; Bromberg-White *et al.*, 2009). However, LeTx indeed has toxicity for animals, and PA and LF may cause an immune response as they are proteins. These obstacles make it difficult to advance LeTx to clinical trials. Nevertheless, LeTx has been successfully used as a powerful tool to study the involvement of MEK/MKK pathways in human diseases.

LeTx has been shown to possess anti-cancer activities by inhibiting not only tumor cell proliferation but also tumor angiogenic processes. The first evidence was provided by Duesbery *et al.* (2001) showing that LeTx-treated tumors have a pale appearance when compared to untreated tumors. Evidence supporting this anti-angiogenic activity of LeTx includes that the mean vascular density for LeTx-treated

tumors is dramatically reduced (Duesbery *et al.*, 2001; Depeille *et al.*, 2007; Ding *et al.*, 2008; Huang *et al.*, 2008). Furthermore, a recent study demonstrated the rapid inhibitory effect of LeTx on the perfusion of fibrosarcoma xenograft tumors but not in non-tumor host tissues (Ding *et al.*, 2008), suggesting that the inhibitory effect of LeTx on endothelial function is highly selective for tumor-associated blood vessels. However, the mechanism by which LeTx selectively targets tumor-associated blood vessels is uncertain. Initially it was hypothesized that systemic LeTx treatment *via* tail vein injection delivered LeTx into tumor cells and LeTx blocked MEK/MKK signaling pathways, as a result of which the release of pro-angiogenic factors from tumor cells was suppressed. This was supported by *in vitro* studies demonstrating that LeTx suppressed release of angiogenic cytokines such as vasculár endothelial growth factor (VEGF), interleukin-6 (IL-6) and basic fibroblast growth factor (bFGF) (Depeille *et al.*, 2007; Ding *et al.*, 2008). However, this hypothesis is challenged by the surprising observation from the SK-MEL-28 xenograft study (presented in Chapter III of this dissertation) showing that systemic administration did not deliver LeTx into tumor cells and the endogenous MEK in the tumor cells was still intact. Similarly, Liu *et al.* (2008) reported that the growth of xenograft tumors derived from CHO cells lacking anthrax toxin receptors (*i.e.*, these cells are resistant to LeTx) was still inhibited by LeTx.

This leads me to propose an alternative hypothesis. Systemic treatment with LeTx inhibits xenograft tumor growth by targeting a non-tumor compartment, which is critical for melanoma-associated endothelial function, such as endothelial cells. This is supported by several lines of evidence. First, endothelial cells are a potential target of

LeTx (Kirby, 2004; Warfel *et al.*, 2005; Alfano *et al.*, 2009). As discussed earlier in this section, LeTx systemic treatment reduces microvessel density in xenograft tumors, and also inhibits acute fibrosarcoma xenograft tumor perfusion within 24h. These studies have shown that LeTx reduces endothelial cell viability and endothelial function. Second, tumor-associated endothelial cells express elevated levels of the tumor endothelial marker 8 (TEM8), one of the identified anthrax toxin receptors (St Croix *et al.*, 2000), potentially making the cells more susceptible to LeTx. Finally, Mavria *et al.* (2006) have reported that expression of dominant-negative MEK1 specifically in tumor-associated endothelium inhibited tumor growth, indicating the MEK signaling pathway is required for tumor-associated endothelial function. Alternatively, LeTx may target another non-tumor compartment that is essential for vascular function such as macrophages or pericytes.

Regardless of which cell type LeTx is targeting, it is clear that inhibition of more than one MEK/MKK pathway is an effective strategy for inhibiting tumor growth and vascularization. Based on my study, I have proposed that MEK1 cooperates with a not-yet-identified factor to compensate for MEK2 function and to drive cell proliferation. This factor is very likely to be another MKK protein or an MKK-regulated protein. However, since the basal activities of p38 MAPK and JNK are very low in SK-MEL-28 cells (Figure 18), one cannot exclude the possibility that this factor may be a not-yet-identified LF substrate. Initial attempts to identify this factor have proved unsuccessful. However, its identification should be a priority since its function may be critical for melanoma survival.

Appendix I. Transcriptional signatures that are down-regulated by LeTx treatment and significantly rescued by MEK2cr

Appendix I. Transcriptional signatures that are down-regulated by LeTx treatment and significantly rescued by MEK2cr

Signatures/Pathways/Gene sets	t-statistics [a]			Reference [b]
	V5-*lacZ*	V5-MEK1cr	V5-MEK2cr	
Myc	-7.14	0.32	4.53	Ref. (Bild *et al.*, 2006)
Myc and Myc-associated factor X	-4.41	0.70	3.00	MSigDB Gene Set: V$MYCMAX_01
E2F1 transcription factor	-7.33	1.01	3.94	MSigDB Gene Set: V$E2F1_Q6_01
E2F3 transcription factor	-5.73	0.69	3.84	Ref. (Bild *et al.*, 2006)
E2F1, TFDP1, RB1 transcription factors	-6.28	1.07	3.29	MSigDB Gene Set: SGCGSSAAA_V$E2F1DP2_01
E2F transcription factors	-4.18	1.52	2.69	MSigDB Gene Set: V$E2F_01
USF transcription factors	-3.92	0.55	2.99	MSigDB Gene Set: V$USF_C
Genes with basally hypomethylated promoters upregulated by the combination of methylation and deacetylation inhibitors in ovarian carcinoma (CP70) cells	-3.09	1.38	2.58	MSigDB Gene Set: TSADAC_HYPOMETH_OVCA_UP
c-fos serum response transcription factors	-3.35	0.98	3.22	MSigDB Gene Set: CCAWWNAAGG_V$SRF_Q4
ncRNA processing	-6.11	0.90	3.48	GO: 0034470
mRNA splicing	-3.24	0.39	3.03	MSigDB Gene Set: MRNA_SPLICING
mRNA splicing complex	-2.55	0.34	2.66	GO:0005681; MSigDB Gene Set: SPLICEOSOME

Signatures/Pathways/Gene sets	t-statistics [a] V5-*lacZ*	V5-MEK1cr	V5-MEK2cr	Reference [b]
rRNA processing	-5.44	0.33	2.74	GO: 0006364
rRNA metabolic process	-5.40	0.32	2.77	GO: 0016072
Ribosome biogenesis	-6.46	0.67	3.80	GO: 0042254
Ribonucleoprotein complex	-4.20	0.59	3.10	Ref. (Ashburner *et al.*, 2000); MSigDB Gene Set: RIBONUCLEOPROTEIN_COMPLEX
Nucleolus	-5.54	1.54	3.65	GO: 0005730
Nucleolus	-4.30	1.47	3.46	GO: 0005730; MSigDB Gene Set: NUCLEOLUS
DNA recombination	-5.00	1.39	3.30	GO: 0006310
DNA recombination	-3.66	1.60	2.79	Ref. (Ashburner *et al.*, 2000); MSigDB Gene Set: DNA_RECOMBINATION
DNA damage	-3.99	1.69	3.38	MSigDB Gene Set: DNA_DAMAGE_SIGNALING
DNA repair	-2.98	1.01	2.76	GO:0003684
Pyrimidine metabolism	-4.56	1.56	3.12	MSigDB Gene Set: PYRIMIDINE_METABOLISM
Pyrimidine metabolism	-4.27	0.77	2.60	Ref. (Kanehisa *et al.*, 2008); MSigDB Gene Set: HSA00240_PYRIMIDINE_METABOLISM
Nucleotidyl-transfer reaction	-3.63	1.39	2.93	Ref. (Ashburner *et al.*, 2000); MSigDB Gene Set: NUCLEOTIDYLTRANSFERASE_ACTIVITY
Single-stranded DNA binding	-3.13	1.91	2.60	GO:0003697

Signatures/Pathways/Gene sets	t-statistics [a] V5-*lacZ*	V5-MEK1cr	V5-MEK2cr	Reference [b]
G1/S cell cycle transition	-3.67	1.49	2.77	MSigDB Gene Set: G1PATHWAY
Apoptosis	-3.16	1.69	2.43	GO:0008632
Genes that are upregulated in undifferentiated human embryonic stem cells	-3.01	1.13	2.55	MSigDB Gene Set: BHATTACHARYA_ESC_UP
Rapamycin starvation-responsive genes	-5.01	1.06	4.27	Ref. (Peng *et al.*, 2002); MSigDB Gene Set: PENG_RAPAMYCIN_DN
Genes that are down-regulated upon LPS stimulation in RAW 264.7 macrophages	-3.16	1.11	2.52	MSigDB Gene Set: NEMETH_TNF_DN
Top genes down-regulated in MLL T-ALL	-4.95	1.49	3.43	Ref. (Ferrando *et al.*, 2003); MSigDB Gene Set: FERRANDO_MLL_T_ALL_DN
Adhesion-related genes	-4.25	0.80	2.38	Ref. (Astier *et al.*, 2003); MSigDB Gene Set: ASTIER_FN_DIFF
Cancer gene module 61	-3.49	1.71	3.25	Ref. (Segal *et al.*, 2004); Cancer gene module 61
Cancer gene module 165	-4.07	1.52	3.47	Ref. (Segal *et al.*, 2004); Cancer gene module 165
Cancer gene module 485	-4.06	1.30	3.21	Ref. (Segal *et al.*, 2004); Cancer gene module 485
Genes that are up-regulated upon catechin treatment in MCF7 cells	-3.31	0.50	2.34	Ref. (Lamb *et al.*, 2006; Lamb, 2007)

Signatures/Pathways/Gene sets	t-statistics [a] V5-*lacZ*	V5-MEK1cr	V5-MEK2cr	Reference [b]
Genes that are down-regulated upon sodium phenylbutyrate treatment in MCF7 cells	-3.29	1.18	2.37	Ref. (Lamb *et al.*, 2006; Lamb, 2007)
Genes that are up-regulated upon oxamic acid treatment in MCF7 cells	-2.87	1.08	2.97	Ref. (Lamb *et al.*, 2006; Lamb, 2007)
TNF-alpha-upregulated genes	-2.93	0.85	2.59	MSigDB Gene Set: TNFALPHA_30MIN_UP
Neighborhood of protein tyrosine phosphatase, receptor type C (PTPRC)	2.49	-0.89	-2.63	MSigDB Gene Set: GNF2_PTPRC
Neighborhood of RAN, member RAS oncogene family	2.60	-0.88	-3.12	MSigDB Gene Set: GCM_RAN
Genes that are down-regulated by serum stimulation	5.46	-1.27	-4.30	Ref. (Chang *et al.*, 2004); MSigDB Gene Set: SERUM_FIBROBLAST_CORE_DN
Phosphoinositide binding	2.40	-0.38	-2.77	GO:0035091
Homeobox A9 (HOXA9) and myeloid ecotropic viral integration site 1 (MEIS1)	2.63	-0.43	-3.14	MSigDB Gene Set: V$MEIS1AHOXA9_01
Targets of microRNA miR-512-3P	2.92	-0.93	-2.90	MSigDB Gene Set: CAGCACT,MIR-512-3P
Genes that are up-regulated in the pubertal mouse mammary gland	3.38	0.87	-2.97	MSigDB Gene Set: MAMMARY_DEV_UP

Signatures/Pathways/Gene sets	t-statistics [a] V5-*lac*Z	V5-MEK1cr	V5-MEK2cr	Reference [b]
NRAS	3.46	-1.29	-2.40	Ref. (Whitwam *et al.*, 2007)
TNF.2 down	4.85	-0.66	-2.96	Ref. (Tian *et al.*, 2005)

[a] t-statistics were obtained from three independent microarray experiments, and the scores in V5-MEK1cr-expressing cells have *p* values greater than 0.005.

[b] MSigDB Gene Sets: http://www.broadinstitute.org/gsea/msigdb/search.jsp; GO (Gene Ontology): http://www.geneontology.org/; Cancer gene modules: http://robotics.stanford.edu/~erans/cancer/browse_by_modules.html.

Appendix II. Transcriptional signatures that are affected by LeTx treatment and significantly rescued by both MEK1cr and MEK2cr

Appendix II. Transcriptional signatures that are affected by LeTx treatment and significantly rescued by both MEK1cr and MEK2cr

Signatures/Pathways/Gene sets	t-statistics [a] V5-*lacZ*	V5-MEK1cr	V5-MEK2cr	Reference [b]
Cancer gene module 54	-13.97	8.12	12.20	Cancer gene module 54
SERUM_FIBROBLAST_CELLCYCLE	-10.58	6.70	8.79	MSigDB Gene Set: SERUM_FIBROBLAST_CELLCYCLE
Ras UP	-10.40	3.65	8.46	PubMed ID: 16273092
P53 repressed genes	-10.34	5.81	8.78	
VERNELL_PRB_CLSTR1	-9.70	3.73	6.80	MSigDB Gene Set: VERNELL_PRB_CLSTR1
IDX_TSA_UP_CLUSTER3	-9.50	6.71	9.19	MSigDB Gene Set: IDX_TSA_UP_CLUSTER3
MANALO_HYPOXIA_DN	-9.39	3.80	7.06	MSigDB Gene Set: MANALO_HYPOXIA_DN
Cancer gene module 18	-9.32	6.23	9.27	Cancer gene module 18
GNF2_RRM1	-9.21	5.10	7.35	MSigDB Gene Set: GNF2_RRM1
GNF2_PCNA	-9.16	5.43	7.43	MSigDB Gene Set: GNF2_PCNA
GNF2_SMC4L1	-9.05	4.78	6.40	MSigDB Gene Set: GNF2_SMC4L1
Cancer gene module 53	-9.03	3.76	6.86	Cancer gene module 53
Cancer gene module 3	-8.83	6.64	10.21	Cancer gene module 3
BAF57_BT549_DN	-8.77	5.72	8.13	MSigDB Gene Set: BAF57_BT549_DN

Signatures/Pathways/Gene sets	t-statistics [a] V5-*lacZ*	V5-MEK1cr	V5-MEK2cr	Reference [b]
Cancer gene module 16	-8.76	4.03	6.91	Cancer gene module 16
CHANG_SERUM_RESPONSE_UP	-8.58	3.57	7.77	MSigDB Gene Set: CHANG_SERUM_RESPONSE_UP
GNF2_FEN1	-8.55	4.89	6.57	MSigDB Gene Set: GNF2_FEN1
Cancer gene module 118	-8.45	6.64	9.85	Cancer gene module 118
RAS_ONCOGENIC_SIGNATURE	-8.44	4.08	7.01	MSigDB Gene Set: RAS_ONCOGENIC_SIGNATURE
Cancer gene module 98	-8.40	3.19	5.57	Cancer gene module 98
GNF2_MCM4	-8.35	4.63	6.90	MSigDB Gene Set: GNF2_MCM4
GNF2_RFC4	-8.24	4.13	6.01	MSigDB Gene Set: GNF2_RFC4
Cancer gene module 57	-8.06	4.26	6.59	Cancer gene module 57
Cancer gene module 8	-8.04	4.64	7.49	Cancer gene module 8
Cancer gene module 125	-8.04	3.50	5.29	Cancer gene module 125
V$E2F_Q6_01	-8.01	2.76	5.16	MSigDB Gene Set: V$E2F_Q6_01
HGF-VEGF UP	-8.01	4.43	5.61	PubMed ID: 14504135
vegf.hgf.1 UP	-7.92	4.52	5.88	PubMed ID: 14504135
Cancer gene module 158	-7.90	3.91	5.36	Cancer gene module 158

Signatures/Pathways/Gene sets	t-statistics [a]			Reference [b]
	V5-*lacZ*	V5-MEK1cr	V5-MEK2cr	
Cancer gene module 52	-7.89	7.13	10.39	Cancer gene module 52
ADIP_DIFF_CLUSTER4	-7.86	2.92	5.66	MSigDB Gene Set: ADIP_DIFF_CLUSTER4
Cancer gene module 252	-7.78	3.72	5.75	Cancer gene module 252
HOFFMANN_BIVSBII_BI_TABLE2	-7.76	5.40	6.74	MSigDB Gene Set: HOFFMANN_BIVSBII_BI_TABLE2
TFA.1 change	-7.75	5.57	7.22	PubMed ID: 16921376
LEE_TCELLS3_UP	-7.70	5.67	6.74	MSigDB Gene Set: LEE_TCELLS3_UP
GNF2_MCM5	-7.68	3.49	5.26	MSigDB Gene Set: GNF2_MCM5
NFKB1.1 up	-7.51	2.93	6.43	PubMed ID: 15722350
HYPOXIA.1 DOWN	-7.50	3.13	4.37	PubMed ID: 16417408
DNA_REPLICATION_REACTOME	-7.44	3.41	6.13	MSigDB Gene Set: DNA_REPLICATION_REACTOME
GNF2_CCNA2	-7.42	5.39	6.76	MSigDB Gene Set: GNF2_CCNA2
Cancer gene module 357	-7.32	6.76	6.75	Cancer gene module 357
Cancer gene module 297	-7.32	6.90	6.75	Cancer gene module 297
GNF2_CENPF	-7.20	4.59	6.11	MSigDB Gene Set: GNF2_CENPF
V$E2F1_Q4	-7.18	3.77	5.61	MSigDB Gene Set: V$E2F1_Q4

Signatures/Pathways/Gene sets	t-statistics [a] V5-*lacZ*	V5-MEK1cr	V5-MEK2cr	Reference [b]
DNA-dependent DNA replication	-7.16	2.82	4.56	GO: 0006261
Cancer gene module 126	-7.10	3.14	5.82	Cancer gene module 126
Cancer gene module 337	-7.07	3.61	4.45	Cancer gene module 337
CELL_CYCLE	-7.02	3.19	5.25	MSigDB Gene Set: CELL_CYCLE
CMV_IE86_UP	-6.91	2.92	4.62	MSigDB Gene Set: CMV_IE86_UP
HSA04110_CELL_CYCLE	-6.82	3.87	5.59	MSigDB Gene Set: HSA04110_CELL_CYCLE
Cancer gene module 154	-6.81	5.38	4.81	Cancer gene module 154
LI_FETAL_VS_WT_KIDNEY_DN	-6.79	3.50	5.47	MSigDB Gene Set: LI_FETAL_VS_WT_KIDNEY_DN
CELL_CYCLE_KEGG	-6.61	2.92	5.09	MSigDB Gene Set: CELL_CYCLE_KEGG
V$E2F_Q3	-6.53	2.86	4.17	MSigDB Gene Set: V$E2F_Q3
GNF2_BUB1B	-6.33	3.79	5.37	MSigDB Gene Set: GNF2_BUB1B
Proliferation_Node1618 NA	-6.33	4.35	5.33	PubMed ID: 16623765
DOX_RESIST_GASTRIC_UP	-6.32	4.21	5.74	MSigDB Gene Set: DOX_RESIST_GASTRIC_UP
SANSOM_APC_LOSS4_UP	-6.24	2.71	5.17	MSigDB Gene Set: SANSOM_APC_LOSS4_UP
GNF2_CDC2	-6.24	4.09	5.23	MSigDB Gene Set: GNF2_CDC2
GNF2_CKS2	-6.22	3.85	4.50	MSigDB Gene Set: GNF2_CKS2

Signatures/Pathways/Gene sets	t-statistics [a] V5-*lacZ*	V5-MEK1cr	V5-MEK2cr	Reference [b]
GNF2_HMMR	-6.00	4.59	5.23	MSigDB Gene Set: GNF2_HMMR
CROONQUIST_IL6_STARVE_UP	-5.91	3.98	5.14	MSigDB Gene Set: CROONQUIST_IL6_STARVE_UP
colchicine 1 uM UP	-5.86	7.88	8.87	PubMed ID: 17008526
LE_MYELIN_UP	-5.84	5.13	5.91	MSigDB Gene Set: LE_MYELIN_UP
RESPONSE_TO_STRESS	-5.82	4.01	5.78	MSigDB Gene Set: RESPONSE_TO_STRESS
DEFENSE_RESPONSE	-5.75	4.56	4.14	MSigDB Gene Set: DEFENSE_RESPONSE
Symporter activity	-5.72	3.81	4.70	GO: 0015293
P21_P53_ANY_DN	-5.71	4.58	6.28	MSigDB Gene Set: P21_P53_ANY_DN
deferoxamine [INN] 100 uM UP	-5.70	2.95	4.57	PubMed ID: 17008526
Cancer gene module 403	-5.65	2.80	4.20	Cancer gene module 403
YYCATTCAWW_UNKNOWN	-5.63	3.46	5.99	MSigDB Gene Set: YYCATTCAWW_UNKNOWN
Replication fork	-5.62	2.88	3.86	GO: 0005657
GNF2_TTK	-5.60	3.73	4.59	MSigDB Gene Set: GNF2_TTK
GNF2_CCNB2	-5.55	4.28	4.93	MSigDB Gene Set: GNF2_CCNB2
GNF2_CDC20	-5.44	4.43	5.14	MSigDB Gene Set: GNF2_CDC20

Signatures/Pathways/Gene sets	t-statistics [a]			Reference [b]
	V5-*lacZ*	V5-MEK1cr	V5-MEK2cr	
CANCER_UNDIFFERENTIATED_META_UP	-5.43	3.55	5.39	MSigDB Gene Set: CANCER_UNDIFFERENTIATED_META_UP
Tcell_PIind_CalciumDefPtdown4x NA	-5.25	3.53	4.18	PubMed ID: 16623765
CELL_CYCLE_GO_0007049	-5.25	3.40	4.78	MSigDB Gene Set: CELL_CYCLE_GO_0007049
GNF2_RRM2	-5.22	3.79	4.53	MSigDB Gene Set: GNF2_RRM2
RESPONSE_TO_EXTERNAL_STIMULUS	-5.19	2.95	4.38	MSigDB Gene Set: RESPONSE_TO_EXTERNAL_STIMULUS
CHROMOSOME	-5.15	2.86	3.38	MSigDB Gene Set: CHROMOSOME
CIS_XPC_UP	-4.99	3.45	3.55	MSigDB Gene Set: CIS_XPC_UP
GNF2_CENPE	-4.98	3.95	4.82	MSigDB Gene Set: GNF2_CENPE
BRAFV.vs.C3 up	-4.98	3.83	5.21	PubMed ID: 17297468
REN_E2F1_TARGETS	-4.89	2.63	3.94	MSigDB Gene Set: REN_E2F1_TARGETS
GOLDRATH_CELLCYCLE	-4.81	3.44	4.32	MSigDB Gene Set: GOLDRATH_CELLCYCLE
GNF2_CKS1B	-4.80	2.76	4.38	MSigDB Gene Set: GNF2_CKS1B
dimethyloxalylglycine 1 mM UP	-4.79	2.36	3.88	PubMed ID: 17008526
Cancer gene module 312	-4.79	3.62	4.62	Cancer gene module 312
STRESS_TPA_SPECIFIC_UP	-4.77	4.14	5.46	MSigDB Gene Set: STRESS_TPA_SPECIFIC_UP

Signatures/Pathways/Gene sets	t-statistics [a]			Reference [b]
	V5-*lacZ*	V5-MEK1cr	V5-MEK2cr	
HYPOXIA_REVIEW	-4.71	3.86	4.55	MSigDB Gene Set: HYPOXIA_REVIEW
RESPONSE_TO_WOUNDING	-4.70	3.01	4.61	MSigDB Gene Set: RESPONSE_TO_WOUNDING
GNF2_SMC2L1	-4.69	3.21	3.78	MSigDB Gene Set: GNF2_SMC2L1
CELL_PROLIFERATION_GO_0008283	-4.67	3.28	3.71	MSigDB Gene Set: CELL_PROLIFERATION_GO_0008283
CHROMOSOMAL_PART	-4.63	2.67	3.05	MSigDB Gene Set: CHROMOSOMAL_PART
HSA04060_CYTOKINE_CYTOKINE_RECEPTOR_INTERACTION	-4.51	3.56	4.14	MSigDB Gene Set: HSA04060_CYTOKINE_CYTOKINE_RECEPTOR_INTERACTION
nocodazole [INN] 1 uM UP	-4.49	3.53	5.08	PubMed ID: 17008526
P21_ANY_DN	-4.48	3.95	5.22	MSigDB Gene Set: P21_ANY_DN
GALINDO_ACT_UP	-4.47	2.70	4.05	MSigDB Gene Set: GALINDO_ACT_UP
GNF2_BUB1	-4.45	2.86	3.95	MSigDB Gene Set: GNF2_BUB1
LEI_MYB_REGULATED_GENES	-4.44	5.38	7.25	MSigDB Gene Set: LEI_MYB_REGULATED_GENES
CELL_CYCLE_PROCESS	-4.39	3.39	4.04	MSigDB Gene Set: CELL_CYCLE_PROCESS
GNF2_ESPL1	-4.38	3.35	4.47	MSigDB Gene Set: GNF2_ESPL1
Cancer gene module 254	-4.37	2.92	3.62	Cancer gene module 254

Signatures/Pathways/Gene sets	t-statistics [a] V5-*lacZ*	V5-MEK1cr	V5-MEK2cr	Reference [b]
Meiotic cell cycle	-4.31	2.67	4.28	GO: 0051321
IRITANI_ADPROX_VASC	-4.22	6.80	9.57	MSigDB Gene Set: IRITANI_ADPROX_VASC
CARIES_PULP_HIGH_UP	-4.21	3.49	3.52	MSigDB Gene Set: CARIES_PULP_HIGH_UP
REGULATION_OF_PROTEIN_KINASE_ACTIVITY	-4.20	2.91	3.02	MSigDB Gene Set: REGULATION_OF_PROTEIN_KINASE_ACTIVITY
REGULATION_OF_KINASE_ACTIVITY	-4.20	2.89	3.00	MSigDB Gene Set: REGULATION_OF_KINASE_ACTIVITY
GNF2_H2AFX	-4.20	3.46	4.17	MSigDB Gene Set: GNF2_H2AFX
Growth factor activity	-4.19	5.70	7.27	GO: 0008083
M phase of meiotic cell cycle	-4.18	2.67	4.14	GO: 0051327
Meiosis	-4.18	2.67	4.14	GO: 0007126
VERHAAK_AML_NPM1_MUT_VS_WT_UP	-4.16	3.08	3.14	MSigDB Gene Set: VERHAAK_AML_NPM1_MUT_VS_WT_UP
Nuclease activity	-4.14	2.88	4.99	GO: 0004518
MET up	-4.12	3.19	4.76	PubMed ID: 16710476
REGULATION_OF_TRANSFERASE_ACTIVITY	-4.06	2.68	2.85	MSigDB Gene Set: REGULATION_OF_TRANSFERASE_ACTIVITY
fisetin 50 uM DOWN	-4.05	3.39	4.32	PubMed ID: 17008526

Signatures/Pathways/Gene sets	t-statistics [a] V5-*lacZ*	V5-MEK1cr	V5-MEK2cr	Reference [b]
ELONGINA_KO_DN	-4.03	3.12	4.31	MSigDB Gene Set: ELONGINA_KO_DN
CELL_CYCLE_PHASE	-4.01	3.09	3.87	MSigDB Gene Set: CELL_CYCLE_PHASE
ADIP_DIFF_CLUSTER3	-4.01	3.19	4.33	MSigDB Gene Set: ADIP_DIFF_CLUSTER3
INOS_ALL_UP	-3.95	2.67	3.09	MSigDB Gene Set: INOS_ALL_UP
MITOTIC_CELL_CYCLE	-3.95	2.91	3.41	MSigDB Gene Set: MITOTIC_CELL_CYCLE
RUIZ_TENASCIN_TARGETS	-3.93	3.71	5.85	MSigDB Gene Set: RUIZ_TENASCIN_TARGETS
Cell cycle checkpoint	-3.90	2.51	3.39	GO: 0000075
IRITANI_ADPROX_LYMPH	-3.76	2.62	3.01	MSigDB Gene Set: IRITANI_ADPROX_LYMPH
M_PHASE	-3.76	3.29	3.85	MSigDB Gene Set: M_PHASE
Tube morphogenesis	-3.71	3.86	4.67	GO: 0035239
HTERT_DN	-3.71	4.46	4.89	MSigDB Gene Set: HTERT_DN
Regulation of cell motility	-3.70	5.32	4.41	GO: 0051270
HOFMANN_MDS_CD34_LOW_RISK	-3.70	3.97	4.58	MSigDB Gene Set: HOFMANN_MDS_CD34_LOW_RISK
CROONQUIST_IL6_STROMA_UP	-3.66	4.13	5.76	MSigDB Gene Set: CROONQUIST_IL6_STROMA_UP
staurosporine 10 nM DOWN	-3.62	2.60	3.93	PubMed ID: 17008526

Signatures/Pathways/Gene sets	t-statistics [a] V5-*lacZ*	V5-MEK1cr	V5-MEK2cr	Reference [b]
IDX_TSA_UP_CLUSTER2	-3.51	2.51	4.65	MSigDB Gene Set: IDX_TSA_UP_CLUSTER2
ALCALAY_AML_NPMC_DN	-3.50	4.79	5.32	MSigDB Gene Set: ALCALAY_AML_NPMC_DN
MATSUDA_VALPHAINKT_DIFF	-3.49	4.14	5.58	MSigDB Gene Set: MATSUDA_VALPHAINKT_DIFF
OXSTRESS_RPE_H2O2HNE_DN	-3.48	2.79	3.77	MSigDB Gene Set: OXSTRESS_RPE_H2O2HNE_DN
IGF1_NIH3T3_UP	-3.40	3.38	4.35	MSigDB Gene Set: IGF1_NIH3T3_UP
353451.3 Mitozolamide; Azolastone; Akylating agent	-3.33	3.99	4.82	Signature gernated from NCI DTP screen - http://dtp.nci.nih.gov/
Tube development	-3.28	3.98	4.21	GO: 0035295
staurosporine 100 nM DOWN	-3.21	3.08	4.36	PubMed ID: 17008526
Blood vessel development	-3.16	4.52	4.24	GO: 0001568
Vasculature development	-3.14	4.47	4.26	GO: 0001944
ADIP_DIFF_CLUSTER2	-3.08	3.23	4.61	MSigDB Gene Set: ADIP_DIFF_CLUSTER2
GERY_CEBP_TARGETS	-3.06	3.06	3.90	MSigDB Gene Set: GERY_CEBP_TARGETS
NUCLEASE_ACTIVITY	-3.00	2.50	3.74	MSigDB Gene Set: NUCLEASE_ACTIVITY
BRENTANI_CELL_ADHESION	-2.99	4.69	3.95	MSigDB Gene Set: BRENTANI_CELL_ADHESION

Signatures/Pathways/Gene sets	t-statistics [a] V5-*lacZ*	V5-MEK1cr	V5-MEK2cr	Reference [b]
DAC_PANC_UP	-2.93	3.72	5.80	MSigDB Gene Set: DAC_PANC_UP
Regulation of cell migration	-2.90	5.25	3.88	GO: 0030334
IFN_BETA_UP	-2.87	3.21	2.56	MSigDB Gene Set: IFN_BETA_UP
Protein polymerization	-2.81	3.34	4.07	GO: 0051258
IFNA_HCMV_6HRS_UP	-2.81	3.52	3.19	MSigDB Gene Set: IFNA_HCMV_6HRS_UP
IRITANI_ADPROX_DN	-2.80	4.60	6.47	MSigDB Gene Set: IRITANI_ADPROX_DN
Cancer gene module 321	-2.79	3.12	4.46	Cancer gene module 321
Cancer gene module 24	-2.79	3.16	4.69	Cancer gene module 24
IFN_BETA_GLIOMA_UP	-2.76	2.87	3.18	MSigDB Gene Set: IFN_BETA_GLIOMA_UP
Positive regulation of multicellular organismal process	-2.57	2.85	3.70	GO: 0051240
Chr. 7p15	-2.55	3.79	3.57	MSigDB Gene Set: chr7p15
Cancer gene module 5	-2.40	5.32	5.53	Cancer gene module 5
Regulation of protein modification process	-2.29	2.68	3.24	GO: 0031399
Clathrin-coated vesicle	2.58	-3.25	-3.25	GO: 0030136
HCC_SURVIVAL_GOOD_VS_POOR_UP	2.95	-4.59	-3.39	MSigDB Gene Set: HCC_SURVIVAL_GOOD_VS_POOR_UP

[a] t-statistics were obtained from three independent microarray experiments, and the scores in V5-MEK1cr-expressing cells have *p* values greater than 0.005.

[b] MSigDB Gene Sets: http://www.broadinstitute.org/gsea/msigdb/search.jsp; GO (Gene Ontology): http://www.geneontology.org/; Cancer gene modules: http://robotics.stanford.edu/~erans/cancer/browse_by_modules.html.

Appendix III. Transcriptional signatures that are not affected by LF treatment but cannot be rescued by either MEK1cr or MEK2cr

Appendix III. Transcriptional signatures that are not affected by LF treatment but cannot be rescued by either MEK1cr or MEK2cr

Signatures/Pathways/Gene sets	t-statistics [a] V5-*lacZ*	V5-MEK1cr	V5-MEK2cr	Reference [b]
Tcell_PIind4x NA	-5.39	0.06	1.83	PubMed ID: 16623765
Helicase activity	-3.96	0.05	1.16	GO: 0004386
Nucleobase, nucleoside, nucleotide and nucleic acid transport	-3.74	1.24	1.15	GO: 0015931
T cell activation	-3.66	0.36	-0.04	GO: 0042110
CANTHARIDIN_DN	-3.46	-0.67	1.60	MSigDB Gene Set: CANTHARIDIN_DN
Positive regulation of immune system process	-3.36	1.09	0.40	GO: 0002684
Nucleic acid transport	-3.26	1.00	0.96	GO: 0050657
RNA transport	-3.26	1.00	0.96	GO: 0050658
Establishment of RNA localization	-3.26	1.00	0.96	GO: 0051236
RNA localization	-3.22	1.02	0.97	GO: 0006403
mRNA transport	-3.15	0.56	0.85	GO: 0051028
GH_EXOGENOUS_LATE_DN	-3.13	0.44	1.20	MSigDB Gene Set: GH_EXOGENOUS_LATE_DN
DNA helicase activity	-3.04	0.40	1.55	GO: 0003678

Signatures/Pathways/Gene sets	t-statistics [a] V5-*lacZ*	V5-MEK1cr	V5-MEK2cr	Reference [b]
Positive regulation of T cell activation	-3.02	-0.11	0.05	GO: 0050870
Regulation of leukocyte activation	-3.02	0.24	1.23	GO: 0002694
Regulation of cell activation	-2.97	0.11	1.00	GO: 0050865
PURINE_METABOLISM	-2.96	-1.31	0.60	MSigDB Gene Set: PURINE_METABOLISM
Anion transmembrane transporter activity	-2.95	-0.24	-0.07	GO: 0008509
Thymic_SP_CD4+Tcell_gt_Blood_CD4+Tcell NA	-2.95	0.27	-0.09	PubMed ID: 16623765
Cancer gene module 183	-2.90	-0.71	0.77	Cancer gene module 183
HSC_EARLYPROGENITORS_ADULT	-2.89	-0.11	0.40	MSigDB Gene Set: HSC_EARLYPROGENITORS_ADULT
Positive regulation of leukocyte activation	-2.88	-0.73	-0.08	GO: 0002696
Positive regulation of cell activation	-2.88	-0.73	-0.08	GO: 0050867
HSC_EARLYPROGENITORS_SHARED	-2.88	-0.12	0.41	MSigDB Gene Set: HSC_EARLYPROGENITORS_SHARED
HSC_EARLYPROGENITORS_FETAL	-2.88	-0.12	0.41	MSigDB Gene Set: HSC_EARLYPROGENITORS_FETAL

Signatures/Pathways/Gene sets	t-statistics [a] V5-*lacZ*	V5-MEK1cr	V5-MEK2cr	Reference [b]
ATP-dependent helicase activity	-2.84	-0.01	0.78	GO: 0008026
MORF_UBE2N	-2.83	0.21	0.91	MSigDB Gene Set: MORF_UBE2N
S-adenosylmethionine-dependent methyltransferase activity	-2.83	0.41	0.63	GO: 0008757
MORF_GSPT1	-2.78	0.25	1.45	MSigDB Gene Set: MORF_GSPT1
MENSE_HYPOXIA_TRANSPORTER_GENES	-2.77	0.80	1.27	MSigDB Gene Set: MENSE_HYPOXIA_TRANSPORTER_GENES
RNA modification	-2.73	0.22	1.43	GO: 0009451
carbamazepine [INN] 100 nM DOWN	-2.73	0.32	1.12	PubMed ID: 17008526
Intracellular protein transport across a membrane	-2.73	0.51	1.54	GO: 0065002
NUCLEAR_ENVELOPE	-2.72	0.58	0.59	MSigDB Gene Set: NUCLEAR_ENVELOPE
Adaptive immune response based on somatic recombination of immune receptors built from immunoglobulin superfamily domains	-2.59	0.31	0.54	GO: 0002460
HDACI_COLON_CUR_DN	-2.55	-0.40	0.21	MSigDB Gene Set: HDACI_COLON_CUR_DN
CHAUVIN_ANDROGEN_REGULATED_GENES	-2.53	0.37	1.40	MSigDB Gene Set: CHAUVIN_ANDROGEN_REGULATED_GENES

Signatures/Pathways/Gene sets	t-statistics [a] V5-*lacZ*	V5-MEK1cr	V5-MEK2cr	Reference [b]
DNA-directed RNA polymerase activity	-2.51	0.29	1.15	GO: 0003899
RNA polymerase activity	-2.51	0.29	1.15	GO: 0034062
RIBONUCLEOPROTEIN_COMPLEX_BIOGENESIS_AND_ASSEMBLY	-2.46	-0.13	1.20	MSigDB Gene Set: RIBONUCLEOPROTEIN_COMPLEX_BIOGENESIS_AND_ASSEMBLY
N-methyltransferase activity	-2.44	-0.43	-0.16	GO: 0008170
Nucleotide-excision repair	-2.40	0.00	1.61	GO: 0006289
Regulation of lymphocyte activation	-2.38	-0.24	0.58	GO: 0051249
ENVELOPE	-2.36	-0.78	-0.18	MSigDB Gene Set: ENVELOPE
ORGANELLE_ENVELOPE	-2.36	-0.78	-0.18	MSigDB Gene Set: ORGANELLE_ENVELOPE
APOPTOTIC_PROGRAM	-2.31	1.13	1.62	MSigDB Gene Set: APOPTOTIC_PROGRAM
V$STAT1_02	-2.30	0.45	0.67	MSigDB Gene Set: V$STAT1_02
CELLULAR_COMPONENT_ASSEMBLY	-2.29	0.90	1.50	MSigDB Gene Set: CELLULAR_COMPONENT_ASSEMBLY
NUCLEAR_BODY	-2.23	-0.12	0.46	MSigDB Gene Set: NUCLEAR_BODY
BRAFV.vs.C3 down	2.15	0.32	-0.86	PubMed ID: 17297468
AGEING_BRAIN_UP	2.19	0.14	-0.19	MSigDB Gene Set: AGEING_BRAIN_UP

Signatures/Pathways/Gene sets	t-statistics [a] V5-*lacZ*	V5-MEK1cr	V5-MEK2cr	Reference [b]
V$VDR_Q6	2.27	-0.68	-1.52	MSigDB Gene Set: V$VDR_Q6
INNEREAR_UP	2.28	-0.41	0.07	MSigDB Gene Set: INNEREAR_UP
HSA04730_LONG_TERM_DEPRESSION	2.43	0.13	-0.23	MSigDB Gene Set: HSA04730_LONG_TERM_DEPRESSION
ROSS_MLL_FUSION	2.54	0.02	-1.95	MSigDB Gene Set: ROSS_MLL_FUSION
AP-type membrane coat adaptor complex	2.56	0.00	-0.71	GO: 0030119
Cancer gene module 221	2.62	-1.34	-1.52	Cancer gene module 221
KRAS.vs.C3 down	2.62	-0.41	-1.22	PubMed ID: 17297468
VESICLE_MEDIATED_TRANSPORT	2.65	-0.58	-1.07	MSigDB Gene Set: VESICLE_MEDIATED_TRANSPORT
Ensheathment of neurons	2.65	0.29	0.22	GO: 0007272
Axon ensheathment	2.65	0.29	0.22	GO: 0008366
Maintenance of location in cell	2.67	0.59	-0.25	GO: 0051651
V$SP1_Q2_01	2.69	-0.35	0.19	MSigDB Gene Set: V$SP1_Q2_01
ACCAATC,MIR-509	2.77	1.04	-0.62	MSigDB Gene Set: ACCAATC,MIR-509
VEGF.1 up	2.81	0.12	-1.37	PubMed ID: 16273092

Signatures/Pathways/Gene sets	t-statistics [a] V5-*lacZ*	V5-MEK1cr	V5-MEK2cr	Reference [b]
Regulation of action potential in neuron	2.82	-0.04	0.40	GO: 0019228
283162.5 Trimethyl TMM; Akylating agent	2.85	0.19	-0.69	Signature gernated from NCI DTP screen - http://dtp.nci.nih.gov/
YTAATTAA_V$LHX3_01	2.91	0.44	-1.03	MSigDB Gene Set: YTAATTAA_V$LHX3_01
Contractile fiber part	3.16	-0.93	0.09	GO: 0044449
Detection of stimulus	3.22	0.17	-1.21	GO: 0051606
Clathrin coat	3.37	-0.32	-0.95	GO: 0030118
CMYC.1 down	3.41	0.13	-1.01	PubMed ID: 16273092
Myc DOWN	3.41	0.13	-1.01	PubMed ID: 16273092
Contractile fiber	3.42	-0.96	-0.08	GO: 0043292
V$E47_02	3.46	-0.49	-0.57	MSigDB Gene Set: V$E47_02
HRAS.vs.C3 down	3.49	-0.18	-1.37	PubMed ID: 17297468
V$CP2_01	3.65	-0.70	-1.43	MSigDB Gene Set: V$CP2_01
Membrane coat	3.66	-0.57	-0.73	GO: 0030117
Coated membrane	3.66	-0.57	-0.73	GO: 0048475
V$OCT1_02	3.68	-0.10	-0.93	MSigDB Gene Set: V$OCT1_02

[a] t-statistics were obtained from three independent microarray experiments, and the scores in V5-MEK1cr-expressing cells have *p* values greater than 0.005.

[b] MSigDB Gene Sets: http://www.broadinstitute.org/gsea/msigdb/search.jsp; GO (Gene Ontology): http://www.geneontology.org/; Cancer gene modules: http://robotics.stanford.edu/~erans/cancer/browse_by_modules.html.

Appendix IV. Transcriptional signatures that are not affected by LF treatment but affected by V5-MEK1cr expression

Appendix IV. Transcriptional signatures that are not affected by LF treatment but affected by V5-MEK1cr expression

Signatures/Pathways/Gene sets	t-statistics [a] V5-*lacZ*	V5-MEK1cr	V5-MEK2cr	Reference [b]
NEGATIVE_REGULATION_OF_DEVELOPMENTAL_PROCESS	-1.07	2.40	1.82	MSigDB Gene Set: NEGATIVE_REGULATION_OF_DEVELOPMENTAL_PROCESS
DER_IFNG_UP	-0.64	2.57	1.45	MSigDB Gene Set: DER_IFNG_UP
DER_IF_UP	-0.54	3.13	1.71	MSigDB Gene Set: DER_IF_UP
CELL_MIGRATION	-0.53	2.54	1.69	MSigDB Gene Set: CELL_MIGRATION
SA_IFNG_ENDOTHELIAL_UP	-0.39	2.52	1.56	MSigDB Gene Set: SA_IFNG_ENDOTHELIAL_UP
Cancer gene module 43	-0.37	-2.45	-0.87	Cancer gene module 43
IFN_ALPHA_UP	0.00	2.98	1.55	MSigDB Gene Set: IFN_ALPHA_UP
TARTE_PC	0.20	2.78	1.00	MSigDB Gene Set: TARTE_PC
Negative regulation of signal transduction	0.31	2.81	0.95	GO: 0009968
Chr. Xq28	0.51	3.96	1.07	MSigDB Gene Set: chrxq28
CREB_BRAIN_8WKS_UP	0.67	2.65	1.28	MSigDB Gene Set: CREB_BRAIN_8WKS_UP
LEE_DE_DN	0.68	-2.57	-1.18	MSigDB Gene Set: LEE_DE_DN

[a] t-statistics were obtained from three independent microarray experiments, and the scores in V5-MEK1cr-expressing cells have *p* values greater than 0.005.

[b] MSigDB Gene Sets: http://www.broadinstitute.org/gsea/msigdb/search.jsp; GO (Gene Ontology): http://www.geneontology.org/; Cancer gene modules: http://robotics.stanford.edu/~erans/cancer/browse_by_modules.html.

Appendix V. Transcriptional signatures that are not affected by LF treatment but affected by V5-MEK2cr expression

Appendix V. Transcriptional signatures that are not affected by LF treatment but affected by V5-MEK2cr expression

Signatures/Pathways/Gene sets	t-statistics [a] V5-*lacZ*	V5-MEK1cr	V5-MEK2cr	Reference [b]
OXSTRESS_RPETHREE_DN	-1.61	1.55	2.61	MSigDB Gene Set: OXSTRESS_RPETHREE_DN
Carboxy-lyase activity	-1.39	1.31	3.08	GO: 0016831
Positive regulation of protein modification process	-1.38	1.34	2.30	GO: 0031401
Response to oxidative stress	-1.35	1.19	2.20	GO: 0006979
Chr. 18q12	-1.35	-0.27	3.34	MSigDB Gene Set: chr18q12
Oxygen and reactive oxygen species metabolic process	-1.32	1.82	2.76	GO: 0006800
Chr. 3q29	-1.30	0.42	2.69	MSigDB Gene Set: chr3q29
V$SRF_Q5_01	-1.14	1.33	3.39	MSigDB Gene Set: V$SRF_Q5_01
Heparin binding	-0.99	1.61	3.15	GO: 0008201
Chr. 1p34	-0.97	0.64	4.61	MSigDB Gene Set: chr1p34
Soluble fraction	-0.48	1.08	2.37	GO: 0005625
Cancer gene module 19	-0.46	1.32	2.64	Cancer gene module 19
V$AP1_Q6	-0.36	0.81	2.57	MSigDB Gene Set: V$AP1_Q6
Anion channel activity	-0.23	0.04	-2.49	GO: 0005253

Signatures/Pathways/Gene sets	t-statistics [a] V5-*lacZ*	V5-MEK1cr	V5-MEK2cr	Reference [b]
Vitamin binding	0.21	0.60	2.64	GO: 0019842
ATPase activity, coupled to transmembrane movement of ions, phosphorylative mechanism	0.35	-0.34	-2.85	GO: 0015662
V$FREAC7_01	0.51	0.53	2.24	MSigDB Gene Set: V$FREAC7_01
GACTGTT,MIR-212,MIR-132	0.53	-0.20	-2.71	MSigDB Gene Set: GACTGTT,MIR-212,MIR-132
Chr. 12q12	1.01	0.55	3.22	MSigDB Gene Set: chr12q12
Pigmentation	1.34	-0.62	-2.61	GO: 0043473
Cancer gene module 243	1.45	-1.09	-2.75	Cancer gene module 243
Ubiquitin ligase complex	1.61	-1.70	-2.19	GO: 0000151
Cancer gene module 226	NA	1.34	2.60	Cancer gene module 226

[a] t-statistics were obtained from three independent microarray experiments, and the scores in V5-MEK1cr-expressing cells have *p* values greater than 0.005.

[b] MSigDB Gene Sets: http://www.broadinstitute.org/gsea/msigdb/search.jsp; GO (Gene Ontology): http://www.geneontology.org/; Cancer gene modules: http://robotics.stanford.edu/~erans/cancer/browse_by_modules.html.

Appendix VI. Transcriptional signatures that are not affected by LF treatment but affected by both V5-MEK1cr and V5-MEK2cr expressions

Appendix VI. Transcriptional signatures that are not affected by LF treatment but affected by both V5-MEK1cr and V5-MEK2cr expressions

Signatures/Pathways/Gene sets	t-statistics [a]			Reference [b]
	V5-*lacZ*	V5-MEK1cr	V5-MEK2cr	
LEE_MYC_UP	-1.69	2.79	3.23	MSigDB Gene Set: LEE_MYC_UP
HSA04810_REGULATION_OF_ACTIN_CYTOSKELETON	-1.46	3.11	3.78	MSigDB Gene Set: HSA04810_REGULATION_OF_ACTIN_CYTOSKELETON
HEARTFAILURE_VENTRICLE_DN	-1.26	3.18	3.54	MSigDB Gene Set: HEARTFAILURE_VENTRICLE_DN
BLEO_HUMAN_LYMPH_HIGH_24HRS_UP	-1.26	2.56	2.90	MSigDB Gene Set: BLEO_HUMAN_LYMPH_HIGH_24HRS_UP
Basement membrane	-1.22	4.90	3.33	GO: 0005604
BRCA1_OVEREXP_PROSTATE_UP	-1.19	6.42	5.58	MSigDB Gene Set: BRCA1_OVEREXP_PROSTATE_UP
RYAAAKNNNNNNTTGW_UNKNOWN	-1.15	3.41	3.29	MSigDB Gene Set: RYAAAKNNNNNNTTGW_UNKNOWN
IDX_TSA_DN_CLUSTER1	-1.15	2.91	2.52	MSigDB Gene Set: IDX_TSA_DN_CLUSTER1
AGEING_KIDNEY_UP	-1.09	4.11	4.25	MSigDB Gene Set: AGEING_KIDNEY_UP
TAKEDA_NUP8_HOXA9_8D_UP	-1.05	6.16	4.86	MSigDB Gene Set: TAKEDA_NUP8_HOXA9_8D_UP

Signatures/Pathways/Gene sets	t-statistics [a] V5-*lacZ*	V5-MEK1cr	V5-MEK2cr	Reference [b]
TAKEDA_NUP8_HOXA9_3D_UP	-1.04	4.75	4.00	MSigDB Gene Set: TAKEDA_NUP8_HOXA9_3D_UP
V$RP58_01	-1.00	2.91	2.96	MSigDB Gene Set: V$RP58_01
CMV_HCMV_TIMECOURSE_ALL_DN	-0.90	4.71	5.41	MSigDB Gene Set: CMV_HCMV_TIMECOURSE_ALL_DN
chr1q42	-0.90	-3.05	-4.11	MSigDB Gene Set: chr1q42
IGLESIAS_E2FMINUS_UP	-0.89	3.31	3.39	MSigDB Gene Set: IGLESIAS_E2FMINUS_UP
EPIDERMIS_DEVELOPMENT	-0.80	3.21	4.03	MSigDB Gene Set: EPIDERMIS_DEVELOPMENT
GNF2_PTX3	-0.80	6.03	6.34	MSigDB Gene Set: GNF2_PTX3
METASTASIS_ADENOCARC_DN	-0.78	3.18	2.84	MSigDB Gene Set: METASTASIS_ADENOCARC_DN
HSA01430_CELL_COMMUNICATION	-0.77	4.13	4.21	MSigDB Gene Set: HSA01430_CELL_COMMUNICATION
MANALO_HYPOXIA_UP	-0.74	3.40	3.08	MSigDB Gene Set: MANALO_HYPOXIA_UP
Cancer gene module 99	-0.71	3.27	3.73	Cancer gene module 99
Cancer gene module 1	-0.62	4.03	4.39	Cancer gene module 1
FH.1 DOWN	-0.54	4.02	3.90	PubMed ID: 16319128
CMV_HCMV_TIMECOURSE_24HRS_DN	-0.51	4.23	4.82	MSigDB Gene Set: CMV_HCMV_TIMECOURSE_24HRS_DN

Signatures/Pathways/Gene sets	t-statistics [a] V5-*lacZ*	V5-MEK1cr	V5-MEK2cr	Reference [b]
Cancer gene module 33	-0.49	4.06	4.81	Cancer gene module 33
JECHLINGER_EMT_UP	-0.42	3.49	3.87	MSigDB Gene Set: JECHLINGER_EMT_UP
AGEING_KIDNEY_SPECIFIC_UP	-0.39	4.17	3.97	MSigDB Gene Set: AGEING_KIDNEY_SPECIFIC_UP
71261.3 Thioguanine deoxyriboside; Guanine analog	-0.28	3.87	3.99	Signature gernated from NCI DTP screen - http://dtp.nci.nih.gov/
HSA04514_CELL_ADHESION_MOLECULES	-0.27	4.85	2.87	MSigDB Gene Set: HSA04514_CELL_ADHESION_MOLECULES
EXTRACELLULAR_REGION	-0.20	4.02	3.44	MSigDB Gene Set: EXTRACELLULAR_REGION
DFOSB_BRAIN_2WKS_UP	-0.18	3.35	3.01	MSigDB Gene Set: DFOSB_BRAIN_2WKS_UP
EMT_UP	-0.11	3.64	3.41	MSigDB Gene Set: EMT_UP
Cancer gene module 292	0.03	4.42	3.62	Cancer gene module 292
Cancer gene module 324	0.05	3.41	4.28	Cancer gene module 324
Extracellular matrix organization and biogenesis	0.05	3.76	2.60	GO: 0030198
Cancer gene module 171	0.05	5.04	3.96	Cancer gene module 171
TGFBETA_LATE_UP	0.22	3.53	3.66	MSigDB Gene Set: TGFBETA_LATE_UP
Cancer gene module 208	0.26	5.53	3.84	Cancer gene module 208

Signatures/Pathways/Gene sets	t-statistics [a] V5-*lacZ*	V5-MEK1cr	V5-MEK2cr	Reference [b]
Cancer gene module 12	0.36	4.20	4.47	Cancer gene module 12
HSA04510_FOCAL_ADHESION	0.39	4.86	3.51	MSigDB Gene Set: HSA04510_FOCAL_ADHESION
chr1q22	0.66	-4.54	-3.72	MSigDB Gene Set: chr1q22
Cancer gene module 129	0.77	2.72	2.39	Cancer gene module 129
Growth factor binding	0.80	4.77	2.86	GO: 0019838
chr1q21	0.81	-5.37	-4.11	MSigDB Gene Set: chr1q21
Cancer gene module 436	0.91	4.16	2.86	Cancer gene module 436
BAF57_BT549_UP	0.98	4.54	2.82	MSigDB Gene Set: BAF57_BT549_UP
Microbody part	0.98	-3.00	-2.81	GO: 0044438
Peroxisomal part	0.98	-3.00	-2.81	GO: 0044439
Cancer gene module 345	1.42	3.94	2.44	Cancer gene module 345

[a] t-statistics were obtained from three independent microarray experiments, and the scores in V5-MEK1cr-expressing cells have *p* values greater than 0.005.

[b] MSigDB Gene Sets: http://www.broadinstitute.org/gsea/msigdb/search.jsp; GO (Gene Ontology): http://www.geneontology.org/; Cancer gene modules: http://robotics.stanford.edu/~erans/cancer/browse_by_modules.html.

Literature Cited

Literature Cited

Abi-Habib RJ, Singh R, Leppla SH, Greene JJ, Ding Y, Berghuis B, Duesbery NS , Frankel AE (2006a). Systemic Anthrax Lethal Toxin Therapy Produces Regressions of Subcutaneous Human Melanoma Tumors in Athymic Nude Mice. *Clin Cancer Res.* **12**, 7437-7443.

Abi-Habib RJ, Singh R, Liu S, Bugge TH, Leppla SH , Frankel AE (2006b). A urokinase-activated recombinant anthrax toxin is selectively cytotoxic to many human tumor cell types. *Mol Cancer Ther.* **5**, 2556-2562.

Abi-Habib RJ, Urieto JO, Liu S, Leppla SH, Duesbery NS , Frankel AE (2005). BRAF status and mitogen-activated protein/extracellular signal-regulated kinase kinase 1/2 activity indicate sensitivity of melanoma cells to anthrax lethal toxin. *Mol Cancer Ther.* **4**, 1303-1310.

Adjei AA, Cohen RB, Franklin W, Morris C, Wilson D, Molina JR, Hanson LJ, Gore L, Chow L, Leong S, Maloney L, Gordon G, Simmons H, Marlow A, Litwiler K, Brown S, Poch G, Kane K, Haney J , Eckhardt SG (2008). Phase I Pharmacokinetic and Pharmacodynamic Study of the Oral, Small-Molecule Mitogen-Activated Protein Kinase Kinase 1/2 Inhibitor AZD6244 (ARRY-142886) in Patients With Advanced Cancers. *J Clin Oncol.* **26**, 2139-2146.

Agrawal A, Lingappa J, Leppla SH, Agrawal S, Jabbar A, Quinn C , Pulendran B (2003). Impairment of dendritic cells and adaptive immunity by anthrax lethal toxin. *Nature.* **424**, 329-334.

Ahn NG, Seger R, Bratlien RL, Diltz CD, Tonks NK , Krebs EG (1991). Multiple components in an epidermal growth factor-stimulated protein kinase cascade. In vitro activation of a myelin basic protein/microtubule-associated protein 2 kinase. *Journal of Biological Chemistry.* **266**, 4220-4227.

Ahn NG, Stines Nahreini T, Tolwinski NS, Resing KA , W.E. Balch CJDaAH (2001). Pharmacologic Inhibitors of MKK1 and MKK2. In *Methods in Enzymology*): Academic Press, pp. 417-431.

Aitken J, Welch J, Duffy D, Milligan A, Green A, Martin N , Hayward N (1999). CDKN2A variants in a population-based sample of Queensland families with melanoma. *J Natl Cancer Inst.* **91**, 446-452.

Alessi DR, Cuenda A, Cohen P, Dudley DT , Saltiel AR (1995). PD 098059 Is a Specific Inhibitor of the Activation of Mitogen-activated Protein Kinase Kinase in Vitro and in Vivo. *J. Biol. Chem.* **270**, 27489-27494.

Alessi DR, Saito Y, Campbell DG, Cohen P, Sithanandam G, Rapp U, Ashworth A, Marshall CJ , Cowley S (1994). Identification of the sites in MAP kinase kinase-1 phosphorylated by p74raf-1. *EMBO J.* **13**, 1610-1619.

Alfano RW, Leppla SH, Liu S, Bugge TH, Meininger CJ, Lairmore TC, Mulne AF, Davis SH, Duesbery NS , Frankel AE (2009). Matrix metalloproteinase-activated anthrax lethal toxin inhibits endothelial invasion and neovasculature formation during in vitro morphogenesis. *Mol Cancer Res.* **7**, 452-461.

Allen LF, Sebolt-Leopold J , Meyer MB (2003). CI-1040 (PD184352), a targeted signal transduction inhibitor of MEK (MAPKK). *Seminars in Oncology.* **30**, 105-116.

Altekruse SF, Kosary CL, Krapcho M, Neyman N, Aminou R, Waldron W, Ruhl J, Howlader N, Tatalovich Z, Cho H, Mariotto A, Eisner MP, Lewis DR, Cronin K, Chen HS, Feuer EJ, Stinchcomb DG , Edwards BK: SEER Cancer Statistics Review, 1975-2007, based on November 2009 SEER data submission, posted to the SEER web site, 2010. (Accessed June 19, 2010)

American Cancer Society (2010). Cancer Facts & Figures 2010ed^eds). Atlanta: American Cancer Society.

Anderson NG, Maller JL, Tonks NK , Sturgill TW (1990). Requirement for integration of signals from two distinct phosphorylation pathways for activation of MAP kinase. *Nature.* **343**, 651-653.

Ashburner M, Ball CA, Blake JA, Botstein D, Butler H, Cherry JM, Davis AP, Dolinski K, Dwight SS, Eppig JT, Harris MA, Hill DP, Issel-Tarver L, Kasarskis A, Lewis S, Matese JC, Richardson JE, Ringwald M, Rubin GM , Sherlock G (2000). Gene ontology: tool for the unification of biology. The Gene Ontology Consortium. *Nat Genet.* **25**, 25-29.

Astier AL, Xu R, Svoboda M, Hinds E, Munoz O, de Beaumont R, Crean CD, Gabig T , Freedman AS (2003). Temporal gene expression profile of human precursor B leukemia cells induced by adhesion receptor: identification of pathways regulating B-cell survival. *Blood.* **101**, 1118-1127.

Balch CM, Gershenwald JE, Soong SJ, Thompson JF, Atkins MB, Byrd DR, Buzaid AC, Cochran AJ, Coit DG, Ding S, Eggermont AM, Flaherty KT, Gimotty PA, Kirkwood JM, McMasters KM, Mihm MC, Jr., Morton DL, Ross MI, Sober AJ , Sondak VK (2009). Final version of 2009 AJCC melanoma staging and classification. *J Clin Oncol.* **27**, 6199-6206.

Ball NJ, Yohn JJ, Morelli JG, Norris DA, Golitz LE , Hoeffler JP (1994). Ras mutations in human melanoma: a marker of malignant progression. *J Invest Dermatol.* **102**, 285-290.

Bardwell AJ, Abdollahi M , Bardwell L (2004). Anthrax lethal factor-cleavage products of MAPK (mitogen-activated protein kinase) kinases exhibit reduced binding to their cognate MAPKs. *Biochem. J.* **378**, 569-577.

Belanger L-F, Roy S, Tremblay M, Brott B, Steff A-M, Mourad W, Hugo P, Erikson R , Charron J (2003). Mek2 Is Dispensable for Mouse Growth and Development. *Mol. Cell. Biol.* **23**, 4778-4787.

Bild AH, Yao G, Chang JT, Wang Q, Potti A, Chasse D, Joshi MB, Harpole D, Lancaster JM, Berchuck A, Olson JA, Jr., Marks JR, Dressman HK, West M , Nevins JR (2006). Oncogenic pathway signatures in human cancers as a guide to targeted therapies. *Nature.* **439**, 353-357.

Birck A, Ahrenkiel V, Zeuthen J, Hou-Jensen K , Guldberg P (2000). Mutation and allelic loss of the PTEN/MMAC1 gene in primary and metastatic melanoma biopsies. *J Invest Dermatol.* **114**, 277-280.

Borg A, Johannsson U, Johannsson O, Hakansson S, Westerdahl J, Masback A, Olsson H , Ingvar C (1996). Novel germline p16 mutation in familial malignant melanoma in southern Sweden. *Cancer Res.* **56**, 2497-2500.

Bosenberg M, Muthusamy V, Curley DP, Wang Z, Hobbs C, Nelson B, Nogueira C, Horner JW, 2nd, Depinho R , Chin L (2006). Characterization of melanocyte-specific inducible Cre recombinase transgenic mice. *genesis.* **44**, 262-267.

Boulton TG, Yancopoulos GD, Gregory JS, Slaughter C, Moomaw C, Hsu J , Cobb MH (1990). An insulin-stimulated protein kinase similar to yeast kinases involved in cell cycle control. *Science.* **249**, 64-67.

Bradley KA, Mogridge J, Mourez M, Collier RJ , Young JA (2001). Identification of the cellular receptor for anthrax toxin. *Nature.* **414**, 225-229.

Braig M , Schmitt CA (2006). Oncogene-induced senescence: putting the brakes on tumor development. *Cancer Res.* **66**, 2881-2884.

Bromberg-White JL, Boguslawski E , Duesbery NS (2009). Perturbation of Mouse Retinal Vascular Morphogenesis by Anthrax Lethal Toxin. *PLoS ONE.* **4**, e6956.

Bromberg-White JL , Duesbery NS (2008). Biological and biochemical characterization of anthrax lethal factor, a proteolytic inhibitor of MEK signaling pathways. *Methods Enzymol.* **438**, 355-365.

Cannon-Albright LA, Goldgar DE, Meyer LJ, Lewis CM, Anderson DE, Fountain JW, Hegi ME, Wiseman RW, Petty EM, Bale AE , et al. (1992). Assignment of a locus for familial melanoma, MLM, to chromosome 9p13-p22. *Science.* **258**, 1148-1152.

Catalanotti F, Reyes G, Jesenberger V, Galabova-Kovacs G, de Matos Simoes R, Carugo O , Baccarini M (2009). A Mek1-Mek2 heterodimer determines the strength and duration of the Erk signal. *Nat Struct Mol Biol.* **16**, 294-303.

Chang HY, Sneddon JB, Alizadeh AA, Sood R, West RB, Montgomery K, Chi JT, van de Rijn M, Botstein D , Brown PO (2004). Gene expression signature of fibroblast serum response predicts human cancer progression: similarities between tumors and wounds. *PLoS Biol.* **2**, E7.

Chen Z, Gibson TB, Robinson F, Silvestro L, Pearson G, Xu B-e, Wright A, Vanderbilt C , Cobb MH (2001). MAP Kinases. *Chemical Reviews.* **101**, 2449-2476.

Chin L, Pomerantz J, Polsky D, Jacobson M, Cohen C, Cordon-Cardo C, Horner JW, 2nd , DePinho RA (1997). Cooperative effects of INK4a and ras in melanoma susceptibility in vivo. *Genes Dev.* **11**, 2822-2834.

Chin L, Tam A, Pomerantz J, Wong M, Holash J, Bardeesy N, Shen Q, O'Hagan R, Pantginis J, Zhou H, Horner JW, 2nd, Cordon-Cardo C, Yancopoulos GD , DePinho RA (1999). Essential role for oncogenic Ras in tumour maintenance. *Nature.* **400**, 468-472.

Chong H, Vikis HG , Guan KL (2003). Mechanisms of regulating the Raf kinase family. *Cell Signal.* **15**, 463-469.

Chopra AP, Boone SA, Liang X , Duesbery NS (2003). Anthrax Lethal Factor Proteolysis and Inactivation of MAPK Kinase. *J. Biol. Chem.* **278**, 9402-9406.

Clark WH, Jr., Elder DE, Guerry Dt, Epstein MN, Greene MH , Van Horn M (1984). A study of tumor progression: the precursor lesions of superficial spreading and nodular melanoma. *Hum Pathol.* **15**, 1147-1165.

ClinicalTrials.gov Identifier: NCT00147550 , U.S. National Institutes of Health. A service of the U.S. National Institutes of Health: ClinicalTrials.gov Identifier: NCT00147550. MEK Inhibitor PD-325901 To Treat Advanced Breast Cancer, Colon Cancer, And Melanoma. http://clinicaltrials.gov/ct2/show/NCT00147550 (Accessed August 12, 2009)

Cohen C, Zavala-Pompa A, Sequeira JH, Shoji M, Sexton DG, Cotsonis G, Cerimele F, Govindarajan B, Macaron N , Arbiser JL (2002). Mitogen-actived Protein Kinase Activation Is an Early Event in Melanoma Progression. *Clin Cancer Res.* **8**, 3728-3733.

Cohen P (1999). The development and therapeutic potential of protein kinase inhibitors. *Current Opinion in Chemical Biology.* **3**, 459-465.

Collisson EA, De A, Suzuki H, Gambhir SS , Kolodney MS (2003). Treatment of Metastatic Melanoma with an Orally Available Inhibitor of the Ras-Raf-MAPK Cascade. *Cancer Res.* **63**, 5669-5673.

Cowan JM, Halaban R , Francke U (1988). Cytogenetic analysis of melanocytes from premalignant nevi and melanomas. *J Natl Cancer Inst.* **80**, 1159-1164.

Crews CM , Erikson RL (1992). Purification of a murine protein-tyrosine/threonine kinase that phosphorylates and activates the Erk-1 gene product: relationship to the fission yeast byr1 gene product. *Proc Natl Acad Sci U S A.* **89**, 8205-8209.

Dankort D, Curley DP, Cartlidge RA, Nelson B, Karnezis AN, Damsky Jr WE, You MJ, DePinho RA, McMahon M , Bosenberg M (2009a). BrafV600E cooperates with Pten loss to induce metastatic melanoma. *Nat Genet.* **41**, 544-552.

Dankort D, Curley DP, Cartlidge RA, Nelson B, Karnezis AN, Damsky WE, Jr., You MJ, DePinho RA, McMahon M , Bosenberg M (2009b). Braf(V600E) cooperates with Pten loss to induce metastatic melanoma. *Nat Genet.* **41**, 544-552.

Dankort D, Filenova E, Collado M, Serrano M, Jones K , McMahon M (2007). A new mouse model to explore the initiation, progression, and therapy of BRAFV600E-induced lung tumors. *Genes & Development.* **21**, 379-384.

Davies H, Bignell GR, Cox C, Stephens P, Edkins S, Clegg S, Teague J, Woffendin H, Garnett MJ, Bottomley W, Davis N, Dicks E, Ewing R, Floyd Y, Gray K, Hall S, Hawes R, Hughes J, Kosmidou V, Menzies A, Mould C, Parker A, Stevens C, Watt S, Hooper S, Wilson R, Jayatilake H, Gusterson BA, Cooper C, Shipley J, Hargrave D, Pritchard-Jones K, Maitland N, Chenevix-Trench G, Riggins GJ, Bigner DD, Palmieri G, Cossu A, Flanagan A, Nicholson A, Ho JWC, Leung SY, Yuen ST, Weber BL, Seigler HF, Darrow TL, Paterson H, Marais R, Marshall CJ, Wooster R, Stratton MR , Futreal PA (2002). Mutations of the BRAF gene in human cancer. *Nature.* **417**, 949-954.

Davies SP, Reddy H, Caivano M , Cohen P (2000). Specificity and mechanism of action of some commonly used protein kinase inhibitors. *Biochem. J.* **351**, 95-105.

Dent P, Haser W, Haystead TA, Vincent LA, Roberts TM , Sturgill TW (1992). Activation of mitogen-activated protein kinase kinase by v-Raf in NIH 3T3 cells and in vitro. *Science.* **257**, 1404-1407.

Depeille P, Young JJ, Boguslawski EA, Berghuis BD, Kort EJ, Resau JH, Frankel AE , Duesbery NS (2007). Anthrax Lethal Toxin Inhibits Growth of and Vascular Endothelial Growth Factor Release from Endothelial Cells Expressing the Human Herpes Virus 8 Viral G Protein Coupled Receptor. *Clin Cancer Res.* **13**, 5926-5934.

Ding Y, Boguslawski EA, Berghuis BD, Young JJ, Zhang Z, Hardy K, Furge K, Kort E, Frankel AE, Hay RV, Resau JH , Duesbery NS (2008). Mitogen-activated protein kinase kinase signaling promotes growth and vascularization of fibrosarcoma. *Mol Cancer Ther.* **7**, 648-658.

Dudley DT, Pang L, Decker SJ, Bridges AJ , Saltiel AR (1995). A synthetic inhibitor of the mitogen-activated protein kinase cascade. *Proceedings of the National Academy of Sciences of the United States of America.* **92**, 7686-7689.

Duesbery NS, Resau J, Webb CP, Koochekpour S, Koo HM, Leppla SH , Vande Woude GF (2001). Suppression of ras-mediated transformation and inhibition of tumor growth and angiogenesis by anthrax lethal factor, a proteolytic inhibitor of multiple MEK pathways. *Proceedings of the National Academy of Sciences of the United States of America.* **98**, 4089-4094.

Duesbery NS, Webb CP, Leppla SH, Gordon VM, Klimpel KR, Copeland TD, Ahn NG, Oskarsson MK, Fukasawa K, Paull KD , Vande Woude GF (1998). Proteolytic Inactivation of MAP-Kinase-Kinase by Anthrax Lethal Factor. *Science.* **280**, 734-737.

Eisen T, Ahmad T, Flaherty KT, Gore M, Kaye S, Marais R, Gibbens I, Hackett S, James M, Schuchter LM, Nathanson KL, Xia C, Simantov R, Schwartz B, Poulin-Costello M, O'Dwyer PJ , Ratain MJ (2006). Sorafenib in advanced melanoma: a Phase II randomised discontinuation trial analysis. *Br J Cancer.* **95**, 581-586.

English J, Pearson G, Wilsbacher J, Swantek J, Karandikar M, Xu S , Cobb MH (1999). New Insights into the Control of MAP Kinase Pathways. *Experimental Cell Research.* **253**, 255-270.

Erickson AK, Ray LB , Sturgill TW (1990). Microtubule-associated protein 1A is the fibroblast HMW MAP undergoing mitogen-stimulated serine phosphorylation. *Biochem Biophys Res Commun.* **166**, 827-832.

Estrada Y, Dong J , Ossowski L (2009). Positive crosstalk between ERK and p38 in melanoma stimulates migration and in vivo proliferation. *Pigment Cell Melanoma Res.* **22**, 66-76.

Favata MF, Horiuchi KY, Manos EJ, Daulerio AJ, Stradley DA, Feeser WS, Van Dyk DE, Pitts WJ, Earl RA, Hobbs F, Copeland RA, Magolda RL, Scherle PA , Trzaskos JM (1998). Identification of a Novel Inhibitor of Mitogen-activated Protein Kinase Kinase. *J. Biol. Chem.* **273**, 18623-18632.

Ferrando AA, Armstrong SA, Neuberg DS, Sallan SE, Silverman LB, Korsmeyer SJ , Look AT (2003). Gene expression signatures in MLL-rearranged T-lineage and B-precursor acute leukemias: dominance of HOX dysregulation. *Blood.* **102**, 262-268.

Fischmann TO, Smith CK, Mayhood TW, Myers JE, Reichert P, Mannarino A, Carr D, Zhu H, Wong J, Yang R-S, Le HV , Madison VS (2009). Crystal Structures of MEK1 Binary and Ternary Complexes with Nucleotides and Inhibitors. *Biochemistry.* **48**, 2661-2674.

FitzGerald MG, Harkin DP, Silva-Arrieta S, MacDonald DJ, Lucchina LC, Unsal H, O'Neill E, Koh J, Finkelstein DM, Isselbacher KJ, Sober AJ , Haber DA (1996). Prevalence of germ-line mutations in p16, p19ARF, and CDK4 in familial melanoma: analysis of a clinic-based population. *Proc Natl Acad Sci U S A.* **93**, 8541-8545.

Flores JF, Pollock PM, Walker GJ, Glendening JM, Lin AH, Palmer JM, Walters MK, Hayward NK , Fountain JW (1997). Analysis of the CDKN2A, CDKN2B and CDK4 genes in 48 Australian melanoma kindreds. *Oncogene.* **15**, 2999-3005.

Fountain JW, Karayiorgou M, Ernstoff MS, Kirkwood JM, Vlock DR, Titus-Ernstoff L, Bouchard B, Vijayasaradhi S, Houghton AN, Lahti J , et al. (1992). Homozygous deletions within human chromosome band 9p21 in melanoma. *Proc Natl Acad Sci U S A.* **89**, 10557-10561.

Friday BB, Yu C, Dy GK, Smith PD, Wang L, Thibodeau SN , Adjei AA (2008). BRAF V600E Disrupts AZD6244-Induced Abrogation of Negative Feedback Pathways between Extracellular Signal-Regulated Kinase and Raf Proteins. *Cancer Res.* **68**, 6145-6153.

Friedlander AM (1998). Antitumor effects of anthrax lethal toxin. In *Third International Conference on Anthrax*ed^eds). University of Plymouth, pp. 104.

Furge KA, Chen J, Koeman J, Swiatek P, Dykema K, Lucin K, Kahnoski R, Yang XJ , Teh BT (2007a). Detection of DNA copy number changes and oncogenic signaling abnormalities from gene expression data reveals MYC activation in high-grade papillary renal cell carcinoma. *Cancer Res.* **67**, 3171-3176.

Furge KA, Tan MH, Dykema K, Kort E, Stadler W, Yao X, Zhou M , Teh BT (2007b). Identification of deregulated oncogenic pathways in renal cell carcinoma: an integrated oncogenomic approach based on gene expression profiling. *Oncogene.* **26**, 1346-1350.

Gentleman RC, Carey VJ, Bates DM, Bolstad B, Dettling M, Dudoit S, Ellis B, Gautier L, Ge Y, Gentry J, Hornik K, Hothorn T, Huber W, Iacus S, Irizarry R, Leisch F, Li C, Maechler M, Rossini AJ, Sawitzki G, Smith C, Smyth G, Tierney L, Yang JY , Zhang J (2004). Bioconductor: open software development for computational biology and bioinformatics. *Genome Biol.* **5**, R80.

Gershenwald JE, Soong SJ , Balch CM (2010). 2010 TNM staging system for cutaneous melanoma...and beyond. *Ann Surg Oncol.* **17**, 1475-1477.

Ghosh P (2004). Process of Protein Transport by the Type III Secretion System. *Microbiol. Mol. Biol. Rev.* **68**, 771-795.

Giroux S, Tremblay M, Bernard D, Cardin-Girard JF, Aubry S, Larouche L, Rousseau S, Huot J, Landry J, Jeannotte L , Charron J (1999). Embryonic death of Mek1-deficient mice reveals a role for this kinase in angiogenesis in the labyrinthine region of the placenta. *Current Biology.* **9**, 369.

Gomez N , Cohen P (1991). Dissection of the protein kinase cascade by which nerve growth factor activates MAP kinases. *Nature.* **353**, 170-173.

Govindarajan B, Bai X, Cohen C, Zhong H, Kilroy S, Louis G, Moses M , Arbiser JL (2003). Malignant Transformation of Melanocytes to Melanoma by Constitutive Activation of Mitogen-activated Protein Kinase Kinase (MAPKK) Signaling. *J. Biol. Chem.* **278**, 9790-9795.

Gray-Schopfer V, Wellbrock C , Marais R (2007). Melanoma biology and new targeted therapy. *Nature.* **445**, 851-857.

Guldberg P, thor Straten P, Birck A, Ahrenkiel V, Kirkin AF , Zeuthen J (1997). Disruption of the MMAC1/PTEN gene by deletion or mutation is a frequent event in malignant melanoma. *Cancer Res.* **57**, 3660-3663.

Haass NK, Sproesser K, Nguyen TK, Contractor R, Medina CA, Nathanson KL, Herlyn M , Smalley KSM (2008). The Mitogen-Activated Protein/Extracellular Signal-Regulated Kinase Kinase Inhibitor AZD6244 (ARRY-142886) Induces Growth Arrest in Melanoma Cells and Tumor Regression When Combined with Docetaxel. *Clin Cancer Res.* **14**, 230-239.

Hao Y-H, Wang Y, Burdette D, Mukherjee S, Keitany G, Goldsmith E , Orth K (2008). Structural requirements for Yersinia YopJ inhibition of MAP kinase pathways. *PLoS ONE.* **3**, e1375.

Harland M, Meloni R, Gruis N, Pinney E, Brookes S, Spurr NK, Frischauf AM, Bataille V, Peters G, Cuzick J, Selby P, Bishop DT , Bishop JN (1997). Germline mutations of the CDKN2 gene in UK melanoma families. *Hum Mol Genet.* **6**, 2061-2067.

Hatzivassiliou G, Song K, Yen I, Brandhuber BJ, Anderson DJ, Alvarado R, Ludlam MJ, Stokoe D, Gloor SL, Vigers G, Morales T, Aliagas I, Liu B, Sideris S, Hoeflich KP, Jaiswal BS, Seshagiri S, Koeppen H, Belvin M, Friedman LS , Malek S (2010). RAF inhibitors prime wild-type RAF to activate the MAPK pathway and enhance growth. *Nature.* **464**, 431-435.

Heidorn SJ, Milagre C, Whittaker S, Nourry A, Niculescu-Duvas I, Dhomen N, Hussain J, Reis-Filho JS, Springer CJ, Pritchard C , Marais R (2010). Kinase-dead BRAF and oncogenic RAS cooperate to drive tumor progression through CRAF. *Cell.* **140**, 209-221.

Herbst RA, Weiss J, Ehnis A, Cavenee WK , Arden KC (1994). Loss of heterozygosity for 10q22-10qter in malignant melanoma progression. *Cancer Res.* **54**, 3111-3114.

Huang CY , Ferrell JE, Jr. (1996). Ultrasensitivity in the mitogen-activated protein kinase cascade. *Proc Natl Acad Sci U S A.* **93**, 10078-10083.

Huang D, Ding Y, Luo W-M, Bender S, Qian C-N, Kort E, Zhang Z-F, VandenBeldt K, Duesbery NS, Resau JH , Teh BT (2008). Inhibition of MAPK Kinase Signaling Pathways Suppressed Renal Cell Carcinoma Growth and Angiogenesis In vivo. *Cancer Res.* **68**, 81-88.

Hussussian CJ, Struewing JP, Goldstein AM, Higgins PA, Ally DS, Sheahan MD, Clark WH, Jr., Tucker MA , Dracopoli NC (1994). Germline p16 mutations in familial melanoma. *Nat Genet.* **8**, 15-21.

Hwang PH, Yi HK, Kim DS, Nam SY, Kim JS , Lee DY (2001). Suppression of tumorigenicity and metastasis in B16F10 cells by PTEN/MMAC1/TEP1 gene. *Cancer Lett.* **172**, 83-91.

Johnson GL , Lapadat R (2002). Mitogen-Activated Protein Kinase Pathways Mediated by ERK, JNK, and p38 Protein Kinases. *Science.* **298**, 1911-1912.

Kamakura S, Moriguchi T , Nishida E (1999). Activation of the Protein Kinase ERK5/BMK1 by Receptor Tyrosine Kinases. IDENTIFICATION AND CHARACTERIZATION OF A SIGNALING PATHWAY TO THE NUCLEUS. *J. Biol. Chem.* **274**, 26563-26571.

Kamb A, Gruis NA, Weaver-Feldhaus J, Liu Q, Harshman K, Tavtigian SV, Stockert E, Day RS, 3rd, Johnson BE , Skolnick MH (1994). A cell cycle regulator potentially involved in genesis of many tumor types. *Science.* **264**, 436-440.

Kanehisa M, Araki M, Goto S, Hattori M, Hirakawa M, Itoh M, Katayama T, Kawashima S, Okuda S, Tokimatsu T , Yamanishi Y (2008). KEGG for linking genomes to life and the environment. *Nucleic Acids Res.* **36**, D480-484.

Kannan K, Sharpless NE, Xu J, O'Hagan RC, Bosenberg M , Chin L (2003). Components of the Rb pathway are critical targets of UV mutagenesis in a murine melanoma model. *Proc Natl Acad Sci U S A.* **100**, 1221-1225.

Kelsall SR , Mintz B (1998). Metastatic cutaneous melanoma promoted by ultraviolet radiation in mice with transgene-initiated low melanoma susceptibility. *Cancer Res.* **58**, 4061-4065.

Kirby JE (2004). Anthrax Lethal Toxin Induces Human Endothelial Cell Apoptosis. *Infect. Immun.* **72**, 430-439.

Knudson AG, Jr. (1971). Mutation and cancer: statistical study of retinoblastoma. *Proc Natl Acad Sci U S A.* **68**, 820-823.

Kohno M , Pouyssegur J (2003). Pharmacological inhibitors of the ERK signaling pathway: application as anticancer drugs. *Prog Cell Cycle Res.* **5**, 219-224.

Kohno M , Pouyssegur J (2006). Targeting the ERK signaling pathway in cancer therapy. *Ann Med.* **38**, 200-211.

Koo H-M, VanBrocklin M, McWilliams MJ, Leppla SH, Duesbery NS , Woude GFV (2002). Apoptosis and melanogenesis in human melanoma cells induced by anthrax lethal factor inactivation of mitogen-activated protein kinase kinase. *Proceedings of the National Academy of Sciences of the United States of America.* **99**, 3052-3057.

Kyriakis JM, App H, Zhang XF, Banerjee P, Brautigan DL, Rapp UR , Avruch J (1992). Raf-1 activates MAP kinase-kinase. *Nature.* **358**, 417-421.

Lamb J (2007). The Connectivity Map: a new tool for biomedical research. *Nat Rev Cancer.* **7**, 54-60.

Lamb J, Crawford ED, Peck D, Modell JW, Blat IC, Wrobel MJ, Lerner J, Brunet JP, Subramanian A, Ross KN, Reich M, Hieronymus H, Wei G, Armstrong SA, Haggarty SJ, Clemons PA, Wei R, Carr SA, Lander ES , Golub TR (2006). The Connectivity Map: using gene-expression signatures to connect small molecules, genes, and disease. *Science.* **313**, 1929-1935.

Lee CS , Duesbery NS (2010). Highly Selective MEK inhibitors. *Current Enzyme Inhibition (in press).*

Lee P, Wallace E, Yeh T, Poch G, Litwiler K, Pheneger T, Lyssikatos J , Winkler J (2004). ARRY-142886, a potent and selective MEK inhibitor: III) Efficacy in murine xenograft models correlates with decreased ERK phosphorylation. In *Annual Meeting of the American Association for Cancer Researched^eds), pp.* 897.

Levine AJ (2009). The common mechanisms of transformation by the small DNA tumor viruses: The inactivation of tumor suppressor gene products: p53. *Virology.* **384**, 285-293.

Li J, Yen C, Liaw D, Podsypanina K, Bose S, Wang SI, Puc J, Miliaresis C, Rodgers L, McCombie R, Bigner SH, Giovanella BC, Ittmann M, Tycko B, Hibshoosh H, Wigler MH , Parsons R (1997). PTEN, a putative protein tyrosine phosphatase gene mutated in human brain, breast, and prostate cancer. *Science.* **275**, 1943-1947.

Limon J, Dal Cin P, Sait SN, Karakousis C , Sandberg AA (1988). Chromosome changes in metastatic human melanoma. *Cancer Genet Cytogenet.* **30**, 201-211.

Liu S, Wang H, Currie BM, Molinolo A, Leung HJ, Moayeri M, Basile JR, Alfano RW, Gutkind JS, Frankel AE, Bugge TH , Leppla SH (2008). Matrix Metalloproteinase-activated Anthrax Lethal Toxin Demonstrates High Potency in Targeting Tumor Vasculature. *J. Biol. Chem.* **283**, 529-540.

LoRusso P, Krishnamurthi S, Rinehart JR, Nabell L, Croghan G, Varterasian M, Sadis SS, Menon SS, Leopold J , Meyer MB (2005a). A phase 1-2 clinical study of a second generation oral MEK inhibitor, PD 0325901 in patients with advanced cancer. In *American Society of Clinical Oncology Annual Meeting*ed^eds), pp. 3011.

LoRusso PM, Adjei AA, Varterasian M, Gadgeel S, Reid J, Mitchell DY, Hanson L, DeLuca P, Bruzek L, Piens J, Asbury P, Van Becelaere K, Herrera R, Sebolt-Leopold J , Meyer MB (2005b). Phase I and Pharmacodynamic Study of the Oral MEK Inhibitor CI-1040 in Patients With Advanced Malignancies. *J Clin Oncol.* **23**, 5281-5293.

Lowe SW , Sherr CJ (2003). Tumor suppression by Ink4a-Arf: progress and puzzles. *Curr Opin Genet Dev.* **13**, 77-83.

Lynch HT, Fusaro RM, Danes BS, Kimberling WJ , Lynch JF (1983). A review of hereditary malignant melanoma including biomarkers in familial atypical multiple mole melanoma syndrome. *Cancer Genet Cytogenet.* **8**, 325-358.

Lyssikatos J, Yeh T, Wallace E, Marsh V, Bernat B, Gross S, Evans R, Colwell H, Parry J, Baker S, Ballard J, Morales T, Smith D, Brandhuber B , Winkler J (2004). ARRY-142886, a potent and selective MEK inhibitor: I) ATP-independent inhibition results in high enzymatic and cellular selectivity. In *Annual Meeting of the American Association for Cancer Research*ed^eds), pp. 896-b.

MacKeigan JP, Collins TS , Ting JP (2000). MEK inhibition enhances paclitaxel-induced tumor apoptosis. *J Biol Chem.* **275**, 38953-38956.

Mansour SJ, Matten WT, Hermann AS, Candia JM, Rong S, Fukasawa K, Vande Woude GF , Ahn NG (1994a). Transformation of mammalian cells by constitutively active MAP kinase kinase. *Science.* **265**, 966-970.

Mansour SJ, Resing KA, Candi JM, Hermann AS, Gloor JW, Herskind KR, Wartmann M, Davis RJ , Ahn NG (1994b). Mitogen-activated protein (MAP) kinase phosphorylation of MAP kinase kinase: determination of phosphorylation sites by mass spectrometry and site-directed mutagenesis. *J Biochem.* **116**, 304-314.

Mao L, Merlo A, Bedi G, Shapiro GI, Edwards CD, Rollins BJ , Sidransky D (1995). A novel p16INK4A transcript. *Cancer Res.* **55**, 2995-2997.

Mavria G, Vercoulen Y, Yeo M, Paterson H, Karasarides M, Marais R, Bird D , Marshall CJ (2006). ERK-MAPK signaling opposes Rho-kinase to promote endothelial cell survival and sprouting during angiogenesis. *Cancer Cell.* **9**, 33-44.

Menon SS, Whitfield LR, Sadis S, Meyer MB, Leopold J, Lorusso PM, Krishnamurthi S, Rinehart JR, Nabell L , Croghan G (2005). Pharmacokinetics (PK) and pharmacodynamics (PD) of PD 0325901, a second generation MEK inhibitor after multiple oral doses of PD 0325901 to advanced cancer patients. In *American Society of Clinical Oncology Annual Meeting*ed^eds), pp. 3066.

Michaloglou C, Vredeveld LC, Soengas MS, Denoyelle C, Kuilman T, van der Horst CM, Majoor DM, Shay JW, Mooi WJ , Peeper DS (2005). BRAFE600-associated senescence-like cell cycle arrest of human naevi. *Nature.* **436**, 720-724.

Miller AJ , Mihm MC, Jr. (2006). Melanoma. *N Engl J Med.* **355**, 51-65.

Mittal R, Peak-Chew S-Y , McMahon HT (2006). Acetylation of MEK2 and IκB kinase (IKK) activation loop residues by YopJ inhibits signaling. *Proceedings of the National Academy of Sciences.* **103**, 18574-18579.

Mody N, Leitch J, Armstrong C, Dixon J , Cohen P (2001). Effects of MAP kinase cascade inhibitors on the MKK5/ERK5 pathway. *FEBS letters.* **502**, 21-24.

Mukherjee S, Keitany G, Li Y, Wang Y, Ball HL, Goldsmith EJ , Orth K (2006). Yersinia YopJ Acetylates and Inhibits Kinase Activation by Blocking Phosphorylation. *Science.* **312**, 1211-1214.

Nakielny S, Cohen P, Wu J , Sturgill T (1992). MAP kinase activator from insulin-stimulated skeletal muscle is a protein threonine/tyrosine kinase. *EMBO J.* **11**, 2123-2129.

Naumov GN, Akslen LA , Folkman J (2006). Role of angiogenesis in human tumor dormancy: animal models of the angiogenic switch. *Cell Cycle.* **5**, 1779-1787.

Nobori T, Miura K, Wu DJ, Lois A, Takabayashi K , Carson DA (1994). Deletions of the cyclin-dependent kinase-4 inhibitor gene in multiple human cancers. *Nature.* **368**, 753-756.

Ohren JF, Chen H, Pavlovsky A, Whitehead C, Zhang E, Kuffa P, Yan C, McConnell P, Spessard C, Banotai C, Mueller WT, Delaney A, Omer C, Sebolt-Leopold J, Dudley DT, Leung IK, Flamme C, Warmus J, Kaufman M, Barrett S, Tecle H , Hasemann CA (2004). Structures of human MAP kinase kinase 1 (MEK1) and MEK2 describe novel noncompetitive kinase inhibition. *Nat Struct Mol Biol.* **11**, 1192-1197.

Orth K, Palmer LE, Bao ZQ, Stewart S, Rudolph AE, Bliska JB , Dixon JE (1999). Inhibition of the Mitogen-Activated Protein Kinase Kinase Superfamily by a Yersinia Effector. *Science.* **285**, 1920-1923.

Orth K, Xu Z, Mudgett MB, Bao ZQ, Palmer LE, Bliska JB, Mangel WF, Staskawicz B , Dixon JE (2000). Disruption of Signaling by Yersinia Effector YopJ, a Ubiquitin-Like Protein Protease. *Science.* **290**, 1594-1597.

Palmer LE, Hobbie S, Galan JE , Bliska JB (1998). YopJ of Yersinia pseudotuberculosis is required for the inhibition of macrophage TNF-alpha production and downregulation of the MAP kinases p38 and JNK. *Mol Microbiol.* **27**, 953-965.

Palmer LE, Pancetti AR, Greenberg S , Bliska JB (1999). YopJ of Yersinia spp. Is Sufficient To Cause Downregulation of Multiple Mitogen-Activated Protein Kinases in Eukaryotic Cells. *Infect. Immun.* **67**, 708-716.

Pannifer AD, Wong TY, Schwarzenbacher R, Renatus M, Petosa C, Bienkowska J, Lacy DB, Collier RJ, Park S, Leppla SH, Hanna P , Liddington RC (2001). Crystal structure of the anthrax lethal factor. *Nature.* **414**, 229-233.

Park JM, Greten FR, Li Z-W , Karin M (2002). Macrophage Apoptosis by Anthrax Lethal Factor Through p38 MAP Kinase Inhibition. *Science.* **297**, 2048-2051.

Parmiter AH, Balaban G, Clark WH, Jr. , Nowell PC (1988). Possible involvement of the chromosome region 10q24----q26 in early stages of melanocytic neoplasia. *Cancer Genet Cytogenet.* **30**, 313-317.

Patterson TA, Lobenhofer EK, Fulmer-Smentek SB, Collins PJ, Chu TM, Bao W, Fang H, Kawasaki ES, Hager J, Tikhonova IR, Walker SJ, Zhang L, Hurban P, de Longueville F, Fuscoe JC, Tong W, Shi L , Wolfinger RD (2006). Performance comparison of one-color and two-color platforms within the MicroArray Quality Control (MAQC) project. *Nat Biotechnol.* **24**, 1140-1150.

Payne DM, Rossomando AJ, Martino P, Erickson AK, Her JH, Shabanowitz J, Hunt DF, Weber MJ , Sturgill TW (1991). Identification of the regulatory phosphorylation sites in pp42/mitogen-activated protein kinase (MAP kinase). *EMBO J.* **10**, 885-892.

Pearson G, Robinson F, Beers Gibson T, Xu BE, Karandikar M, Berman K , Cobb MH (2001). Mitogen-activated protein (MAP) kinase pathways: regulation and physiological functions. *Endocr Rev.* **22**, 153-183.

Pedersen MI, Bennett JW , Wang N (1986). Nonrandom chromosome structural aberrations and oncogene loci in human malignant melanoma. *Cancer Genet Cytogenet.* **20**, 11-27.

Pellizzari R, Guidi-Rontani C, Vitale G, Mock M , Montecucco C (1999). Anthrax lethal factor cleaves MKK3 in macrophages and inhibits the LPS/IFNgamma-induced release of NO and TNFalpha. *FEBS Lett.* **462**, 199-204.

Peng T, Golub TR , Sabatini DM (2002). The immunosuppressant rapamycin mimics a starvation-like signal distinct from amino acid and glucose deprivation. *Mol Cell Biol.* **22**, 5575-5584.

Petty EM, Gibson LH, Fountain JW, Bolognia JL, Yang-Feng TL, Housman DE , Bale AE (1993). Molecular definition of a chromosome 9p21 germ-line deletion in a woman with multiple melanomas and a plexiform neurofibroma: implications for 9p tumor-suppressor gene(s). *Am J Hum Genet.* **53**, 96-104.

Platz A, Hansson J, Mansson-Brahme E, Lagerlof B, Linder S, Lundqvist E, Sevigny P, Inganas M , Ringborg U (1997). Screening of germline mutations in the CDKN2A and CDKN2B genes in Swedish families with hereditary cutaneous melanoma. *J Natl Cancer Inst.* **89**, 697-702.

Polager S , Ginsberg D (2009). p53 and E2f: partners in life and death. *Nat Rev Cancer.* **9**, 738-748.

Pollock PM, Harper UL, Hansen KS, Yudt LM, Stark M, Robbins CM, Moses TY, Hostetter G, Wagner U, Kakareka J, Salem G, Pohida T, Heenan P, Duray P, Kallioniemi O, Hayward NK, Trent JM , Meltzer PS (2003). High frequency of BRAF mutations in nevi. *Nat Genet.* **33**, 19-20.

Poulikakos PI, Zhang C, Bollag G, Shokat KM , Rosen N (2010). RAF inhibitors transactivate RAF dimers and ERK signalling in cells with wild-type BRAF. *Nature.* **464**, 427-430.

Powell MB, Gause PR, Hyman P, Gregus J, Lluria-Prevatt M, Nagle R , Bowden GT (1999). Induction of melanoma in TPras transgenic mice. *Carcinogenesis.* **20**, 1747-1753.

Quelle DE, Zindy F, Ashmun RA , Sherr CJ (1995). Alternative reading frames of the INK4a tumor suppressor gene encode two unrelated proteins capable of inducing cell cycle arrest. *Cell.* **83**, 993-1000.

Rapp UR, Goldsborough MD, Mark GE, Bonner TI, Groffen J, Reynolds FH, Jr. , Stephenson JR (1983). Structure and biological activity of v-raf, a unique oncogene transduced by a retrovirus. *Proc Natl Acad Sci U S A.* **80**, 4218-4222.

Ray LB , Sturgill TW (1987). Rapid stimulation by insulin of a serine/threonine kinase in 3T3-L1 adipocytes that phosphorylates microtubule-associated protein 2 in vitro. *Proc Natl Acad Sci U S A.* **84**, 1502-1506.

Ray LB , Sturgill TW (1988a). Characterization of insulin-stimulated microtubule-associated protein kinase. Rapid isolation and stabilization of a novel serine/threonine kinase from 3T3-L1 cells. *J Biol Chem.* **263**, 12721-12727.

Ray LB , Sturgill TW (1988b). Insulin-stimulated microtubule-associated protein kinase is phosphorylated on tyrosine and threonine in vivo. *Proc Natl Acad Sci U S A.* **85**, 3753-3757.

Rinehart J, Adjei AA, LoRusso PM, Waterhouse D, Hecht JR, Natale RB, Hamid O, Varterasian M, Asbury P, Kaldjian EP, Gulyas S, Mitchell DY, Herrera R, Sebolt-Leopold JS , Meyer MB (2004). Multicenter Phase II Study of the Oral MEK Inhibitor, CI-1040, in Patients With Advanced Non-Small-Cell Lung, Breast, Colon, and Pancreatic Cancer. *J Clin Oncol.* **22**, 4456-4462.

Roberts PJ , Der CJ (2007). Targeting the Raf-MEK-ERK mitogen-activated protein kinase cascade for the treatment of cancer. *Oncogene.* **26**, 3291-3310.

Robertson GP, Furnari FB, Miele ME, Glendening MJ, Welch DR, Fountain JW, Lugo TG, Huang HJ , Cavenee WK (1998). In vitro loss of heterozygosity targets the PTEN/MMAC1 gene in melanoma. *Proc Natl Acad Sci U S A.* **95**, 9418-9423.

Rossomando AJ, Payne DM, Weber MJ , Sturgill TW (1989). Evidence that pp42, a major tyrosine kinase target protein, is a mitogen-activated serine/threonine protein kinase. *Proc Natl Acad Sci U S A.* **86**, 6940-6943.

Rouleau C, Menon K, Boutin P, Guyre C, Yoshida H, Kataoka S, Perricone M, Shankara S, Frankel AE, Duesbery NS, Vande Woude G, Biemann HP , Teicher BA (2008). The systemic administration of lethal toxin achieves a growth delay of human melanoma and neuroblastoma xenografts: assessment of receptor contribution. *Int J Oncol.* **32**, 739-748.

Roux PP , Blenis J (2004). ERK and p38 MAPK-Activated Protein Kinases: a Family of Protein Kinases with Diverse Biological Functions. *Microbiol. Mol. Biol. Rev.* **68**, 320-344.

Ruckdeschel K, Harb S, Roggenkamp A, Hornef M, Zumbihl R, Kohler S, Heesemann J , Rouot B (1998). Yersinia enterocolitica Impairs Activation of Transcription Factor NF-kappa B: Involvement in the Induction of Programmed Cell Death and

in the Suppression of the Macrophage Tumor Necrosis Factor alpha roduction. *J. Exp. Med.* **187**, 1069-1079.

Sagata N, Oskarsson M, Copeland T, Brumbaugh J , Vande Woude GF (1988). Function of c-mos proto-oncogene product in meiotic maturation in Xenopus oocytes. *Nature.* **335**, 519-525.

Sato C, Nishizawa K, Nakayama T , Kobayashi T (1985). Effect upon mitogenic stimulation of calcium-dependent phosphorylation of cytoskeleton-associated 350,000- and 80,000-mol-wt polypeptides in quiescent 3Y1 cells. *J. Cell Biol.* **100**, 748-753.

Sato C, Nishizawa K, Nakayama T, Nose K, Takasaki Y, Hirose S , Nakamura H (1986). Intranuclear appearance of the phosphorylated form of cytoskeleton-associated 350-kDa proteins in U1-ribonucleoprotein regions after growth stimulation of fibroblasts. *Proc Natl Acad Sci U S A.* **83**, 7287-7291.

Schechter I , Berger A (1967). On the size of the active site in proteases. I. Papain. *Biochem Biophys Res Commun.* **27**, 157-162.

Schesser K, Spiik A-K, Dukuzumuremyi J-M, Neurath MF, Pettersson S , Wolf-Watz H (1998). The yopJ locus is required for Yersinia-mediated inhibition of NF-kappaB activation and cytokine expression: YopJ contains a eukaryotic SH2-like domain that is essential for its repressive activity. *Molecular Microbiology.* **28**, 1067-1079.

Scholl FA, Dumesic PA, Barragan DI, Charron J , Khavari PA (2009a). Mek1/2 gene dosage determines tissue response to oncogenic Ras signaling in the skin. *Oncogene.* **28**, 1485-1495.

Scholl FA, Dumesic PA, Barragan DI, Harada K, Charron J , Khavari PA (2009b). Selective Role for Mek1 but not Mek2 in the Induction of Epidermal Neoplasia. *Cancer Res.* **69**, 3772-3778.

Scobie HM, Rainey GJ, Bradley KA , Young JA (2003). Human capillary morphogenesis protein 2 functions as an anthrax toxin receptor. *Proc Natl Acad Sci U S A.* **100**, 5170-5174.

Sebolt-Leopold JS, Dudley DT, Herrera R, Becelaere KV, Wiland A, Gowan RC, Tecle H, Barrett SD, Bridges A, Przybranowski S, Leopold WR , Saltiel AR (1999). Blockade of the MAP kinase pathway suppresses growth of colon tumors in vivo. *Nat Med.* **5**, 810-816.

Sebolt-Leopold JS , Herrera R (2004). Targeting the mitogen-activated protein kinase cascade to treat cancer. *Nat Rev Cancer.* **4**, 937-947.

Sebolt-Leopold JS, Merriman R, Omer C, Tecle H, Bridges A, Klohs W, Loi C-M, Valik H, Przybranowski S, Meyer M , Leopold WR (2004). The biological profile of PD 0325901: A second generation analog of CI-1040 with improved pharmaceutical potential. In *Annual Meeting of the American Association for Cancer Researched^eds)*, pp. 925.

Segal E, Friedman N, Koller D , Regev A (2004). A module map showing conditional activity of expression modules in cancer. *Nat Genet.* **36**, 1090-1098.

Seger R, Ahn NG, Posada J, Munar ES, Jensen AM, Cooper JA, Cobb MH , Krebs EG (1992). Purification and characterization of mitogen-activated protein kinase activator(s) from epidermal growth factor-stimulated A431 cells. *Journal of Biological Chemistry.* **267**, 14373-14381.

Serrano M, Hannon GJ , Beach D (1993). A new regulatory motif in cell-cycle control causing specific inhibition of cyclin D/CDK4. *Nature.* **366**, 704-707.

Singh Y, Liang X , Duesbery NS (2005). Pathogenesis of Bacillus anthracis: the role of Anthrax toxins. In *Microbial Toxins. Molecular and Cellular Biology.* (T Proft, ed). Norfolk, England: Horizon Bioscience, pp. 285-312.

Solit DB, Garraway LA, Pratilas CA, Sawai A, Getz G, Basso A, Ye Q, Lobo JM, She Y, Osman I, Golub TR, Sebolt-Leopold J, Sellers WR , Rosen N (2006). BRAF mutation predicts sensitivity to MEK inhibition. *Nature.* **439**, 358.

Soufir N, Avril MF, Chompret A, Demenais F, Bombled J, Spatz A, Stoppa-Lyonnet D, Benard J , Bressac-de Paillerets B (1998). Prevalence of p16 and CDK4 germline mutations in 48 melanoma-prone families in France. The French Familial Melanoma Study Group. *Hum Mol Genet.* **7**, 209-216.

St Croix B, Rago C, Velculescu V, Traverso G, Romans KE, Montgomery E, Lal A, Riggins GJ, Lengauer C, Vogelstein B , Kinzler KW (2000). Genes expressed in human tumor endothelium. *Science.* **289**, 1197-1202.

Stahl JM, Cheung M, Sharma A, Trivedi NR, Shanmugam S , Robertson GP (2003). Loss of PTEN promotes tumor development in malignant melanoma. *Cancer Res.* **63**, 2881-2890.

Steck PA, Pershouse MA, Jasser SA, Yung WK, Lin H, Ligon AH, Langford LA, Baumgard ML, Hattier T, Davis T, Frye C, Hu R, Swedlund B, Teng DH , Tavtigian SV (1997). Identification of a candidate tumour suppressor gene, MMAC1, at chromosome 10q23.3 that is mutated in multiple advanced cancers. *Nat Genet.* **15**, 356-362.

Stone S, Jiang P, Dayananth P, Tavtigian SV, Katcher H, Parry D, Peters G , Kamb A (1995). Complex structure and regulation of the P16 (MTS1) locus. *Cancer Res.* **55**, 2988-2994.

Sturgill TW , Ray LB (1986). Muscle proteins related to microtubule associated protein-2 are substrates for an insulin-stimulatable kinase. *Biochem Biophys Res Commun.* **134**, 565-571.

Tanami H, Imoto I, Hirasawa A, Yuki Y, Sonoda I, Inoue J, Yasui K, Misawa-Furihata A, Kawakami Y , Inazawa J (2004). Involvement of overexpressed wild-type BRAF in the growth of malignant melanoma cell lines. *Oncogene.* **23**, 8796.

Tanoue T, Adachi M, Moriguchi T , Nishida E (2000). A conserved docking motif in MAP kinases common to substrates, activators and regulators. *Nat Cell Biol.* **2**, 110-116.

Tarhini AA , Agarwala SS (2006). Cutaneous melanoma: available therapy for metastatic disease. *Dermatol Ther.* **19**, 19-25.

Teng DH, Hu R, Lin H, Davis T, Iliev D, Frye C, Swedlund B, Hansen KL, Vinson VL, Gumpper KL, Ellis L, El-Naggar A, Frazier M, Jasser S, Langford LA, Lee J, Mills GB, Pershouse MA, Pollack RE, Tornos C, Troncoso P, Yung WK, Fujii G, Berson A, Steck PA , et al. (1997). MMAC1/PTEN mutations in primary tumor specimens and tumor cell lines. *Cancer Res.* **57**, 5221-5225.

Tian B, Nowak DE, Jamaluddin M, Wang S , Brasier AR (2005). Identification of direct genomic targets downstream of the nuclear factor-kappaB transcription factor mediating tumor necrosis factor signaling. *J Biol Chem.* **280**, 17435-17448.

Trisciuoglio D, Iervolino A, Zupi G , Del Bufalo D (2005). Involvement of PI3K and MAPK Signaling in bcl-2-induced Vascular Endothelial Growth Factor Expression in Melanoma Cells. *Mol. Biol. Cell.* **16**, 4153-4162.

Tsao H, Zhang X, Benoit E , Haluska FG (1998). Identification of PTEN/MMAC1 alterations in uncultured melanomas and melanoma cell lines. *Oncogene.* **16**, 3397-3402.

Tsao H, Zhang X, Fowlkes K , Haluska FG (2000). Relative Reciprocity of NRAS and PTEN/MMAC1 Alterations in Cutaneous Melanoma Cell Lines. *Cancer Res.* **60**, 1800-1804.

van 't Veer LJ, Burgering BM, Versteeg R, Boot AJ, Ruiter DJ, Osanto S, Schrier PI , Bos JL (1989). N-ras mutations in human cutaneous melanoma from sun-exposed body sites. *Mol Cell Biol.* **9**, 3114-3116.

Vitale G, Bernardi L, Napolitani G, Mock M , Montecucco C (2000). Susceptibility of mitogen-activated protein kinase kinase family members to proteolysis by anthrax lethal factor. *Biochem. J.* **352**, 739-745.

Vitale G, Pellizzari R, Recchi C, Napolitani G, Mock M , Montecucco C (1998). Anthrax Lethal Factor Cleaves the N-Terminus of MAPKKs and Induces Tyrosine/Threonine Phosphorylation of MAPKs in Cultured Macrophages. *Biochemical and Biophysical Research Communications.* **248**, 706-711.

Voisin L, Julien C, Duhamel S, Gopalbhai K, Claveau I, Saba-El-Leil M, Rodrigue-Gervais I, Gaboury L, Lamarre D, Basik M , Meloche S (2008). Activation of MEK1 or MEK2 isoform is sufficient to fully transform intestinal epithelial cells and induce the formation of metastatic tumors. *BMC Cancer.* **8**, 337.

Wajapeyee N, Serra RW, Zhu X, Mahalingam M , Green MR (2008). Oncogenic BRAF induces senescence and apoptosis through pathways mediated by the secreted protein IGFBP7. *Cell.* **132**, 363-374.

Walker GJ, Hussussian CJ, Flores JF, Glendening JM, Haluska FG, Dracopoli NC, Hayward NK , Fountain JW (1995). Mutations of the CDKN2/p16INK4 gene in Australian melanoma kindreds. *Hum Mol Genet.* **4**, 1845-1852.

Wallace E, Yeh T, Lyssikatos J, Winkler J, Lee P, Marlow A, Hurley B, Marsh V, Bernat B, Evans R, Colwell H, Ballard J, Morales T, Smith D, Brandhuber B, Gross S, Poch G, Litwiler K, Hingorani G, Otten J, Sullivan F, Blake J, Pheneger T, Goyette M , Koch K (2004). Preclinical development of ARRY-142886, a potent and selective MEK inhibitor. In *Annual Meeting of the American Association for Cancer Researched^eds)*, pp. 897-a.

Warfel JM, Steele AD , D'Agnillo F (2005). Anthrax Lethal Toxin Induces Endothelial Barrier Dysfunction. *Am J Pathol.* **166**, 1871-1881.

Warmus JS, Flamme C, Zhang LY, Barrett S, Bridges A, Chen H, Gowan R, Kaufman M, Sebolt-Leopold J, Leopold W, Merriman R, Ohren J, Pavlovsky A, Przybranowski S, Tecle H, Valik H, Whitehead C , Zhang E (2008). 2-Alkylamino- and alkoxy-substituted 2-amino-1,3,4-oxadiazoles--O-Alkyl benzohydroxamate esters replacements retain the desired inhibition and selectivity against MEK (MAP ERK kinase). *Bioorganic & Medicinal Chemistry Letters.* **18**, 6171-6174.

Wellbrock C, Ogilvie L, Hedley D, Karasarides M, Martin J, Niculescu-Duvaz D, Springer CJ , Marais R (2004). V599EB-RAF is an Oncogene in Melanocytes. *Cancer Res.* **64**, 2338-2342.

Whitwam T, Vanbrocklin MW, Russo ME, Haak PT, Bilgili D, Resau JH, Koo HM , Holmen SL (2007). Differential oncogenic potential of activated RAS isoforms in melanocytes. *Oncogene.* **26**, 4563-4570.

Wu H, Goel V , Haluska FG (2003). PTEN signaling pathways in melanoma. *Oncogene.* **22**, 3113-3122.

Xia Z, Dickens M, Raingeaud J, Davis RJ , Greenberg ME (1995). Opposing effects of ERK and JNK-p38 MAP kinases on apoptosis. *Science.* **270**, 1326-1331.

Yeh T, Wallace E, Lyssikatos J , Winkler J (2004). ARRY-142886, a potent and selective MEK inhibitor: II) Potency against cellular MEK leads to inhibition of cellular proliferation and induction of apoptosis in cell lines with mutant Ras or B-Raf. In *Annual Meeting of the American Association for Cancer Researche*d^eds), pp. 896-c-897.

Yeh TC, Marsh V, Bernat BA, Ballard J, Colwell H, Evans RJ, Parry J, Smith D, Brandhuber BJ, Gross S, Marlow A, Hurley B, Lyssikatos J, Lee PA, Winkler JD, Koch K , Wallace E (2007). Biological Characterization of ARRY-142886 (AZD6244), a Potent, Highly Selective Mitogen-Activated Protein Kinase Kinase 1/2 Inhibitor. *Clin Cancer Res.* **13**, 1576-1583.

You MJ, Castrillon DH, Bastian BC, O'Hagan RC, Bosenberg MW, Parsons R, Chin L , DePinho RA (2002). Genetic analysis of Pten and Ink4a/Arf interactions in the suppression of tumorigenesis in mice. *Proc Natl Acad Sci U S A.* **99**, 1455-1460.

Zheng CF , Guan KL (1994). Activation of MEK family kinases requires phosphorylation of two conserved Ser/Thr residues. *EMBO J.* **13**, 1123-1131.

Zhou XP, Gimm O, Hampel H, Niemann T, Walker MJ , Eng C (2000). Epigenetic PTEN silencing in malignant melanomas without PTEN mutation. *Am J Pathol.* **157**, 1123-1128.